APATITE FISSION TRACK STUDY OF TECTONICS AND PROVENANCE OF SEDIMENTS IN THE SAWTOOTH RANGE, SVERDRUP BASIN, CANADIAN ARCTIC ARCHIPELAGO

Michael Collins

Distribution License

DalSpace requires agreement to this non-exclusive distribution license before your item can appear on DalSpace.

NON-EXCLUSIVE DISTRIBUTION LICENSE

You (the author(s) or copyright owner) grant to Dalhousie University the non-exclusive right to reproduce and distribute your submission worldwide in any medium.

You agree that Dalhousie University may, without changing the content, reformat the submission for the purpose of preservation.

You also agree that Dalhousie University may keep more than one copy of this submission for purposes of security, back-up and preservation.

You agree that the submission is your original work, and that you have the right to grant the rights contained in this license. You also agree that your submission does not, to the best of your knowledge, infringe upon anyone's copyright.

If the submission contains material for which you do not hold copyright, you agree that you have obtained the unrestricted permission of the copyright owner to grant Dalhousie University the rights required by this license, and that such third-party owned material is clearly identified and acknowledged within the text or content of the submission.

If the submission is based upon work that has been sponsored or supported by an agency or organization other than Dalhousie University, you assert that you have fulfilled any right of review or other obligations required by such contract or agreement.

Dalhousie University will clearly identify your name(s) as the author(s) or owner(s) of the submission, and will not make any alteration to the content of the files that you have submitted.

If you have questions regarding this license please contact the repository manager at dalspace@dal.ca.

Grant the distribution license by signing and dating below.

_____   _____

Name of signatory   Date

Dalhousie University

Department of Earth Sciences
Halifax, Nova Scotia
Canada B3H 3J5
(902) 494-2358
FAX (902) 494-6889

DATE   April 9, 1996

AUTHOR   John Michael William Collins

TITLE   APATITE FISSION TRACK STUDY OF TECTONICS AND PROVENANCE

OF SEDIMENTS IN THE SAWTOOTH RANGE SVERDRUP BASIN

CANADIAN ARCTIC ARCHIPELAGO

Degree   B Sc   Convocation   Spring, 1996   Year   1996

Permission is herewith granted to Dalhousie University to circulate and to have copied for non-commercial purposes, at its discretion, the above title upon the request of individuals or institutions.

ABSTRACT

The Sverdrup Basin in the Canadian Arctic is a large intracratonic rift basin initiated during the late Paleozoic. Its sediments were deposited in two sequences: Proterozoic to mid-Paleozoic deformed in the Ellesmerian Orogeny, and a late Paleozoic to early Cenozoic sequence, affected by the Eurekan Orogeny. The source of sediments is understood to be from the exhumed pre-Paleozoic basement along the cratonic margins, although a possible derivation from an Arctic Ocean rift margin in the northwest has been proposed, and there is some volcanic input. Detrital apatite samples have been obtained from two transects in the northern and southern Sawtooth Range. The first section traverses the Vesley Fiord Thrust, with Cretaceous-Tertiary rocks in the footwall and Permo-Triassic rocks in the hangingwall. The second transect combines two measured sections, with Triassic to Miocene rocks, in the footwall, and Permian to Triassic-Jurassic rocks in the hangingwall of the East Cape Thrust.

The apatite samples were analysed for fission track histories and for compositional variation. The analysis of fission tracks in apatite grains yields information on burial, cooling and exhumation events in sedimentary rocks. By contrasting fission track cooling histories of samples offset by the two thrusts it has been possible to constrain the timing of thrusting and exhumation in the central Sverdrup Basin. The study shows that oil generation from Mesozoic source rocks predated the formation of structural traps in the Sawtooth Range, thus explaining in part the lack of success of 30 years of oil exporation in the study area.

The major and trace element composition (e.g. F, Cl, OH, CO_2, Sr, La, Ce, Nd, Y) of detrital and igneous apatite used in the study was obtained with the microprobe. Fluoroapatite predominates in the strata from Permian to Miocene, and no major shifts in provenance can be discerned on the basis of trace elements. The use of radial plots allows for the identification of discrete populations of apatite based on their FT ages, and suggests there may have been several distinct source areas for sediments in this locality during the Tertiary.

Key Words: apatite fission track analysis, provenance, age of thrusting, Sverdrup Basin, Eurekan Orogeny, apatite, rare earth elements.

TABLE OF CONTENTS

TABLE OF FIGURES

TABLE OF TABLES

ACKNOWLEDGEMENTS

Chapter 1 Introduction

1.1   Opening Statement

The Sverdrup Basin is the largest sedimentary basin in the Canadian Arctic Archipelago (Fig. 1.1) , and stretches ~1300km from the northern end of Ellesmere Island to Melville Island in the south. Exploration of the Sverdrup Basin in the 1960s and 1970s delineated large hydrocarbon resources, significant coal deposits and economic base metal finds. This period of economic activity culminated with the successful development of the Bent Horn well on Cameron Island and the development of the Nanisivik and Polaris Lead-Zinc mines. In spite of promising structural traps and source rocks, hydrocarbon exploration in the north central basin was disappointing. This thesis attempts to explain the possible reasons for this lack of success.

The development of the Sverdrup Basin is central to the geological history of the whole arctic region and contains clues to the tectonic development of the present-day Arctic Basin. Field work was carried out in the summer of 1994 as a part of a larger regional thermal-tectonic project. The apatite separates used in this study are derived from that sample set. The author's project investigates the thermal tectonic history and the provenance of sediments in the north-central Sverdrup Basin in terms of 1) apatite fission track analysis, and 2) composition of apatite.

Fission track analysis is a novel application of fission track dating, which applied to detrital and igneous apatite, provides the basis for the formulation of thermal-tectonic histories. Computer modelling based on fission track ages and annealing characteristics of apatite provide cooling and uplift histories for individual samples. However the chemical composition of apatite exerts a significant influence on its thermal behaviour and it is important to constrain the compositional range of apatite samples. The interpretation of the thermal histories of samples, in terms of stratigraphic depth and structural relationships,

Fig. 1.1 Map of the Canadian Arctic Islands. indicating the different tectonic zones and delineating the Sverdrup Basin. The main study area is denoted by the box.
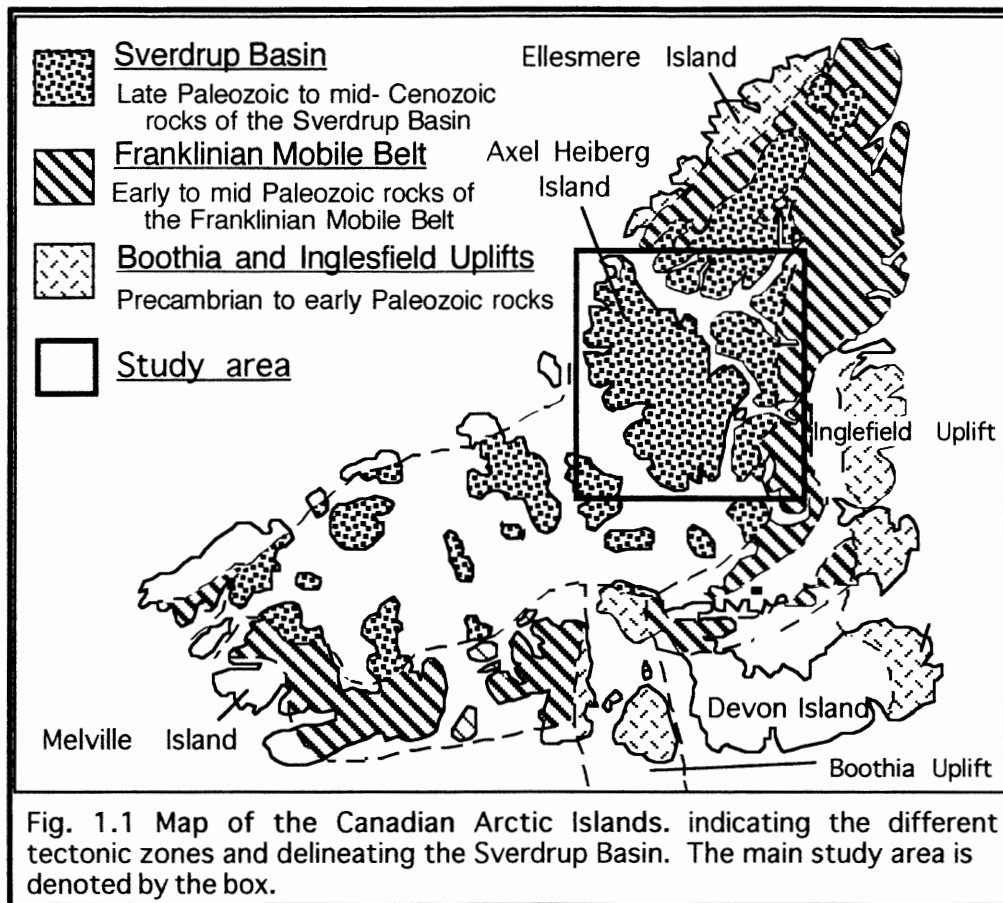
provides constraints on the tectonic history of north-central Sverdrup Basin during the

Eurekan orogeny. Specifically, the study constrains the timing of movement on an

Eurekan thrust fault in the central Sverdrup Basin. Compositional analysis of the apatite

separates was less conclusive due to homogeneity within the sample group.

1.2   Methods

This thesis derives data from field work and two related laboratory techniques; 1)

fission track analysis of apatite and 2) the physical and chemical analysis of apatite. The

volatile (F,Cl,OH) composition of apatite has been analysed because the time-temperature

fission-track models are sensitive to the variation in Cl content. The apatite trace element (REE) chemistry has been applied to problems of provenance.

1.2.1 Field Work

Field work was carried out over a four week period in July 1994. Field sites were accessed with air support from the Geological Survey of Canada (GSC) and Polar Continental Shelf Project. Four to five days were spent at each site, with three additional day trips. During this time the measurement of sections was performed by Dr. D. Arne who was assisted by the author. Sampling also was supervised by Dr. D. Arne. Work focused on Eurekan structures with significant lithological offsets and lithologies suitable for concentration of apatite. Samples chosen for this thesis are from Mt. Bridgeman and Vesley Fiord, at the north and south ends of the Sawtooth Range on the Fosheim Peninsula of Ellesmere Island, (Fig. 1.1).

1.2.2 Fission track analysis

Apatite fission track analysis (AFTA) is a dating technique that constrains the time of cooling of rocks as they pass through the 100°C isotherm. An AFTA age can represent the timing of initial rock formation in upper crustal igneous rocks or the timing of exhumation for rocks that where formed or heated at temperatures higher than the ca. 100°C isotherm. For sedimentary rocks the AFTA age can represent 1) the time of exhumation when the rock has been heated above the 100°C isotherm or, 2) if the rock has not passed through the 100°C isotherm, the age of the rock is a function of the inherited AFTA age of the source rock. AFTA is particularly useful in petroleum exploration because the 100°C isotherm lies within the liquid oil window.

Apatite fission track dating utilises the natural spontaneous decay of ^{238}U. Damage zones or tracks are produced in the crystal lattice structure by this natural fission. Tracks are made visible through the etching of a polished surface. The fission track age can

be determined if one knows the uranium content of the sample, the number of tracks that have spontaneously accumulated with time, and the decay constant of ^{238}U.

Fission tracks are known to anneal, or shorten, at rates that are proportional to time and temperature and follow the laws of diffusion (Ravenhurst and Donelick, 1992). More specifically, apatite is known to completely anneal at temperatures of 125° over a time period of >2 Ma. If an apatite sample has been reheated above the total annealing isotherm due to burial in a basin or due to igneous interaction, the age derived from the track density represents only the last cooling event the sample underwent. The distribution of the track lengths can be used to define the time and rate of cooling due to denudation and uplift. Where the detrital apatite fission track age result is greater than the stratigraphic age of the sample, the fission track age is considered to be an inherited age from the sediment source area and is due to incomplete annealing of the apatite. Conversely, the distribution of single grain ages in unannealed samples can indicate the number of source areas and their respective cooling FT ages.

Recent work has integrated AFTA with vitrinite reflectance techniques to create a wider base of information. Reflectance of vitrinite (R_o) is a proven technique used to determine the degree of thermal maturation in a basin and represents a useful complement to AFTA data. However, AFTA provides limits to the heating event, which can be applied even in the absence of organic matter (Arne and Zentilli, 1994)

1.2.3 Provenance analysis: the geochemistry of apatite

In the process of separating apatite from whole rocks the entire heavy mineral suite must be separated first. It was originally intended that the provenance component of the study would use ratios of heavy minerals, such as the rutile-zircon index (Morton, 1991; Morton and Hallsworth, 1994) to discriminate amongst the samples. Unfortunately, due to a lack of foresight, the samples were separated beyond the possible reconstruction of the

applicable ratios. Therefore, apatite was the only mineral analysed in the provenance study. Work on single mineral compositional variation (Morton, 1985), and more specifically apatite compositional variation (Dill, 1994), has shown that it is possible to identify shifts in provenance in relationship to unique compositional signatures in source areas. The apatite grains chosen for compositional work were also analysed in terms of grain shape. In addition, fission track data were plotted using radial plotting techniques (Galbraith, 1990). Radial plots are illustrative in showing fields of inherited ages in detrital apatite samples with source areas of different (exhumation or cooling) ages. It was expected that the integration of compositional variation with physical grain shape analysis, and the radial plots of inherited ages, would define discrete populations. These expectations have been fulfilled to some extent.

The geochemical aspect of defining populations is based on microprobe analysis using wave detection spectrometry (WDS) for trace elements, and energy dispersive spectrometry (EDS) for major element constituents. OH and CO_2 values are derived iteratively from excess oxygen assuming a 21 unit atom molecule. The primary geochemical constraint is the F-Cl-OH ternary relationship: solid solution exists between end-member apatite compositions, but populations derived from a unique igneous melt occupy discrete areas in the F-Cl-OH ternary field (see Chapter 4). The secondary identifier is the relationship of chondrite normalised LREE, (La, Ce, Nd) and Y. In apatite of igneous origin, these elements exhibit unique patterns based on the melt type from which they were derived (Taylor and McLennan, 1985).

An attempt was made to distinguish different populations based on roundness and corrosion of the detrital apatite grains. Grains of the different groups were probed and variation in composition within individual grains was evaluated and compared with variation between samples. The identification of discrete populations, chemically and

physically, was expected to provide a framework for the interpretation of shifting sediment sources or shifting source areas through time.

1.3 Geological Setting

The Sverdrup Basin covers most of the Canadian Arctic Archipelago (Fig. 1.1) and is one of the largest sedimentary basins in Canada. The development, sedimentation, and the inversion of the Sverdrup Basin occurred in two discrete cycles. The first cycle of sedimentation occurred during the late Proterozoic to the mid-Paleozoic. These sediments were subsequently folded and faulted during the mid-Paleozoic Ellesmerian Orogeny. The second period of sedimentation began in the late Paleozoic and ended in the mid-Cenozoic (Trettin, 1991b). The Early Cretaceous to Tertiary indentation of Greenland induced compressional subsidence and the eventual collapse and closure of the Sverdrup Basin by the Miocene. This collapse and inversion of the Sverdrup basin is known as the Eurekan Orogeny. The remnants of the basin are characterised by a horst-like feature to the Northwest which is know as the Sverdrup Rim and by an indentor, on the eastern basin, edge which is related to the collision with Greenland (Fig 1.1).

Upper Paleozoic strata are up to 3 km in thickness and Mesozoic strata reach a maximum of 9 km. Sedimentary deposition from the mid-Cretaceous to Miocene led to the accumulation of up to 3 km of syntectonic sediments (Davies and Nassichuk, 1991; Embry, 1991). Clastic sediments were primarily derived from the southern and eastern sides of the basin. A poorly quantified amount of sediments is also thought to be derived from the Sverdrup Rim in the northwestern part of the Sverdrup Basin during the Mesozoic (Embry, 1992). Late Paleozoic sedimentation was dominated by marine carbonates with minor evaporite and clastic input. Mesozoic and Tertiary sedimentation was primarily marine clastics with impure carbonates in the Triassic. Two periods of volcanic activity are recorded in basin sediments. An initial period of volcanism, related to the formation of the Sverdrup Basin occurred from the Middle Carboniferous to the Early Permian (Embry,

1991). The Early Cretaceous witnessed a second period of volcanic activity accompanied by the emplacement of dikes and sills throughout the northern basin (Embry, 1991). Bentonites, interpreted as volcanic ash layers were deposited in the Sverdrup Basin during the Cretaceous (Parsons, 1994).

This study takes advantage of samples located on measured sections across thrust faults in the Sawtooth Range, Fosheim Peninsula, Ellesmere Island (Fig. 1.1). Sedimentary units in the immediate study area range in age from middle Permian to Miocene. Igneous dikes and sills are commonplace in formations of Cretaceous or earlier ages. The footwalls of some of the thrust faults contain strata of Tertiary age and give some indication of the maximum timing of the last major fault movement.

1.4   Background

Historically, the first accounts of the Sverdrup Basin were compiled by arctic navigators in search of the elusive Northwest Passage. Although exploration started in the 1500s it wasn't until the 1800s that explorers broached the interior of the Arctic Archipelago. The first regional geological synthesis was compiled in 1858 by Haughton (1858 in Christie and Dawes, 1991). The Canadian government started supporting geography and geology studies in the high Arctic in the 1920s to reinforce sovereignty claims to the Arctic Islands.

Fortier et al. (1950) outlined the hydrocarbon potential of the Sverdrup Basin. Initial exploration was promoted by the government through the granting of large tax incentives. One hundred and eighty seven exploration wells were drilled in search of oil and gas and resulted in the delineation of significant reserves and resources, but most of the significant discoveries were made in the southern part of the Sverdrup Basin. The basic structure of the basin is relatively well known and the lithology and stratigraphic correlations are well defined and understood. In 1991, the Decade of North American Geology (DNAG) series, volume 3: was published (Trettin, 1991a). Entitled, Geology of

the Innuitian Orogen and Arctic Platform of Canada and Greenland, this book is a synthesis of all the information produced up to the late 1980s and this thesis draws heavily on this useful reference. The Sverdrup Basin has been completely mapped at a scale of $1:5x10^6$. Since the publication of DNAG volume 3, geological work has generally concentrated on the refinement and documentation of local variation in existing models. Two geological problems of particular note are: 1) the source of sediments prograding from the Sverdrup Rim (Embry, 1993) and 2) the timing and nature of the final closure and inversion of the basin (Ricketts, 1994).

This thesis is a subsidiary project that evolved out of a NSERC strategic grant to Dr. M Zentilli and Dr. D. Arne, "The thermal and tectonic history of the Sverdrup Basin". The NSERC project attempts to refine the understanding of thermal maturation and its relationship with the tectonic history of the basin. As a multi-year project, the NSERC project can been seen in terms of several sub-projects. The primary phase of the strategic project developed a thermal tectonic model for the southern portion of the Sverdrup Basin. This work was based on fission track analysis of apatite concentrates from well samples. The fission track analysis was performed by Dr. D. Arne and A.M. Grist (MSc) at the Fission Track Research Laboratory at Dalhousie University. The fission track data was integrated with vitrinite reflectance data produced by Dr. F. Goodarzi at the Institute of Sedimentary and Petroleum Geology.

When the author joined the project in the summer of 1994, fission track analysis work had been completed in the southern Sverdrup Basin and indicated post-Triassic cooling during post-Ellesmerian exhumation of the southern Franklinian Mobile Belt (Arne, 1994). The author was involved in sample preparation in the second phase of the project which applied fission track and vitrinite reflectance analysis to a group of well samples from the northern half of the Sverdrup Basin. Fission track analysis in this portion of the

project was carried out by Dr. D. Arne (Arne, 1995) and vitrinite reflectance analysis was performed by Dr. Prasanta Mukhopadhyay.

Sampling for the third and final phase of the project was carried out in the summer of 1994. Sampling focused on outcrops in measured sections that contained thrust faults with significant stratigraphic offset. The samples were prepared by the author, and the majority of samples were analysed for fission tracks by A.M. Grist (MSc) with a small number being analysed by the author. Again, Dr. Prasanta Mukhopadhyay performed the vitrinite reflectance analysis.

Fission track analysis has been developed over the last thirty years, (e.g. see summary by Andriessen, 1995). The underlying theory has been expanded from the simple relationship between track density and age, to the understanding of track annealing and its relationship with tectonic exhumation and heating by hydrothermal fluids. Experimental work (e.g. see summary by O'Sullivan, 1995) has also demonstrated the relationship between annealing rate and compositional variation in the apatite.

Detrital mineral composition and its relationship with provenance is a relatively new field (Dill, 1994). Previously, analysis of detrital grains in terms of provenance has focused on ratios of grain types, or ratios of specific heavy mineral suites (Hubert, 1962). The analysis of provenance with a single mineral reduces the chance that the provenance study could be affected by differential sorting processes.

Apatite is a mineral that is particularly well suited to single mineral provenance studies (Morton and Hallsworth, 1994). Apatite is known as a repository for rare earth elements (REE) in solidifying rockforming melts (Taylor and McLennan, 1985). The resulting REE patterns are representative of the parent melt and, in combination with major anion variation (F, Cl, OH), detrital grains can be matched with apatite samples from a specific source area (Dill, 1994).

1.5   Objectives

The primary objectives of this thesis were: 1) to constrain the timing of Eurekan thrust faults in relation to oil maturation and migration in the north-central Sverdrup basin; and 2) to analyse igneous and detrital apatite and examine their relationship to provenance. The compositional data also help to improve the constraints of annealing variables in the fission track analysis and the resulting thermal tectonic model, which is developed across a representative section of the basin.

1.6   Scope Of Study And Thesis Organisation

This thesis investigates the geochemical provenance and the thermal tectonic history, of a transect in the Sawtooth Range, Ellesmere Island, in the central Sverdrup Basin. Studies of apatite provenance attempt to identify discrete chemical populations of apatite and relate the populations to sediment sources. These compositional populations improve the resolution the fission track model. The apatite fission track analysis constrains the absolute timing of the thrusting and erosion in the Sawtooth Range in the north-central section of the Sverdrup Basin. The fission track model developed here does not have the breadth of data necessary to be extended to a basin-wide level.

Chapter 2 of this thesis focuses on the geology of the Sawtooth Range and presents several cross sections. Chapter 3 discusses the technique of apatite fission track analysis and its application. Chapter 4 presents the compositional variation of detrital apatite and its relevance as an indicator of provenance. Finally, chapter 5 summarises the results of the thesis and presents conclusions derived from these results.

CHAPTER 2: GEOLOGY OF THE SAWTOOTH RANGE

2.1   Introduction

Samples were taken on 3 measured sections in the Sawtooth Range, Ellesmere Island (Fig. 2.1). The first section(Fig. 2.2) runs north-west of Vesley Fiord into the Sawtooth Range and transects the Vesley Fiord Thrust. The second and third(Fig. 2.3) sections are located on the south-east and north-west sides of Mount Bridgeman in the northern end of the Sawtooth Range.   These two sections are in the footwall and hangingwall of the East Cape Thrust, respectively. Measuring chains, altimeters, and a Magellan® global positioning system (GPS) unit were used to collect data on these sections. Samples were taken on a regular basis with a bias towards rocks that were likely to contain apatite grains (e.g. lithic sandstone as opposed to coal or carbonates). The stratigraphic nomenclature used is defined in Embry (1991,1992) and Ricketts (1994). The age of stratigraphic boundaries are taken from the GSC geological time scale (Okulitch, 1995).

The rock formations in the Sawtooth Range vary in age from Permian to Tertiary. The Sawtooth Range itself is a result of the Eurekan orogenic compression and thrusting with more durable Paleozoic hangingwall rocks capping and protecting softer Mesozoic and Cenozoic footwall strata from erosion.

2.2   Regional Geology

The Sverdrup Basin records only a small part of the geological history of the Arctic Islands. The Phanerozoic Innuitian fold belt extends along the north-eastern margin of the North American continental margin and stretches from northern Greenland to the Parry Islands in the South. The fold belt can be devolved into two discrete mountain building events:

Figure. 2.1 Location map. Showing cross sections in the Sawtooth Range in the Fosheim Pennisula, Ellesmere Island and the location of the two isolated samples on the Kanguk Peninsula, Axel Heiberg Island. Appendix A includes the exact geographic locations of individual samples.   (modified from Parsons, 1994)
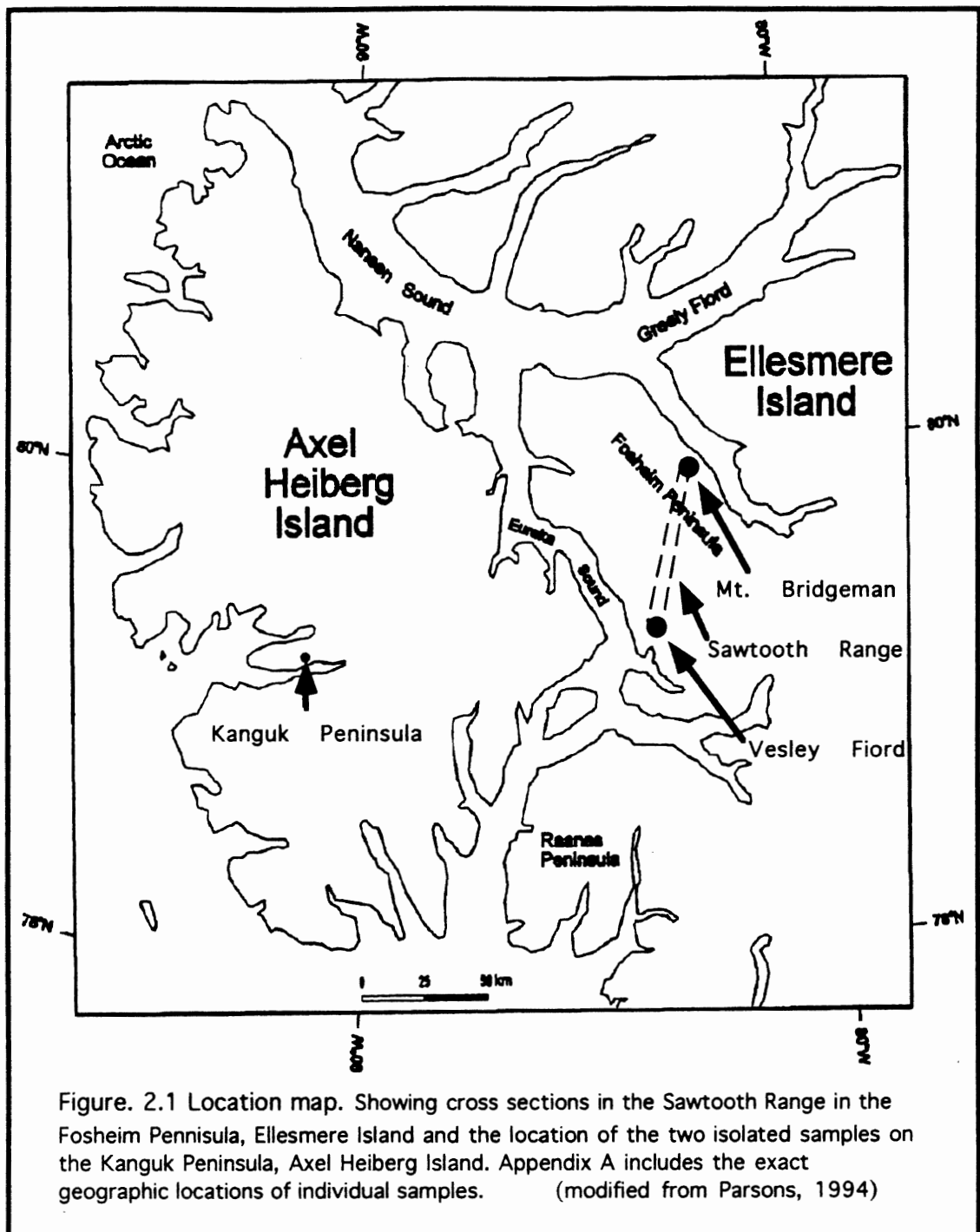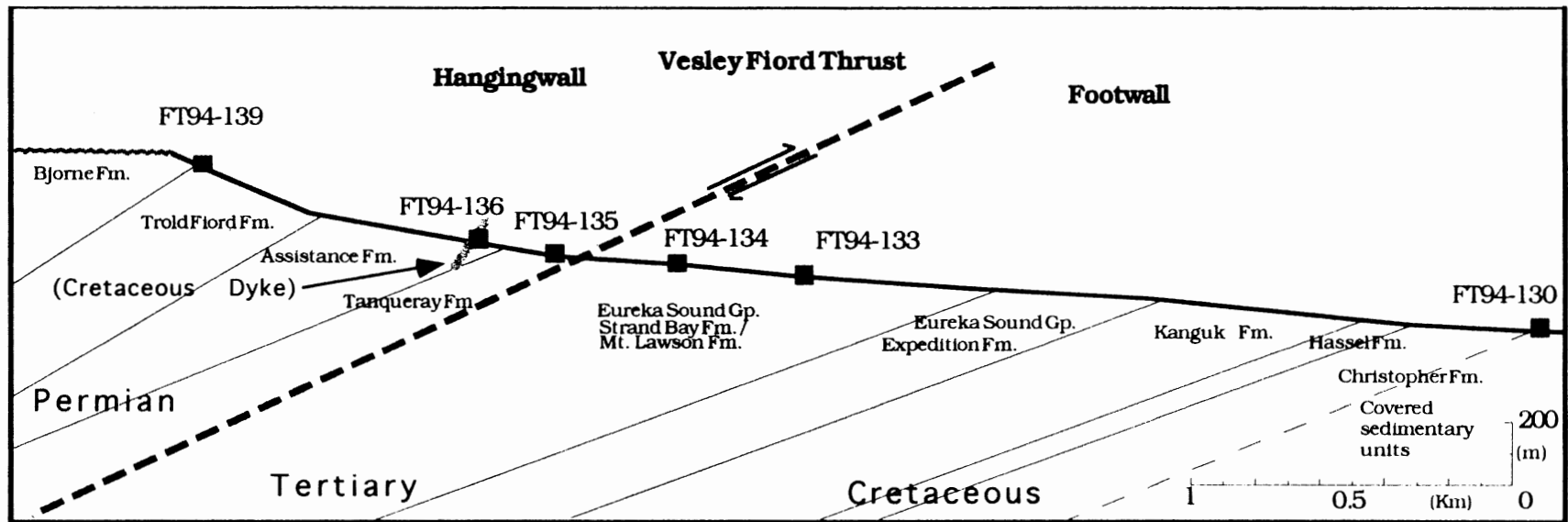
Figure 2.2. Measured section at Vesley Fiord, southern Sawtooth Range. Oriented perpendicular to the strike of the bedding in both the hangingwall and the footwall, this cross section shows the stratigraphic, and spatial relationships of the samples.

A)

FT94- 153
FT94-154

Trold
Fiord Fm.
Assistance Fm

Sabine Bay Fm

100

0

Bjorne Fm.

El.187 m Triassic

Permian

500   0

El. 500 m

Hangingwall

Footwall

B)
FT94-143
El.230

FT94-145
FT94-146

Heiberg Fm.

Awingak Fm.

FT94-147

syncline
axis

Bjorne Fm.

50

undifferentiated
Mesozoic and Tertiary

Eureka Sound Gp.

0

0   500

Triassic | Jurassic

Tertiary

El.116
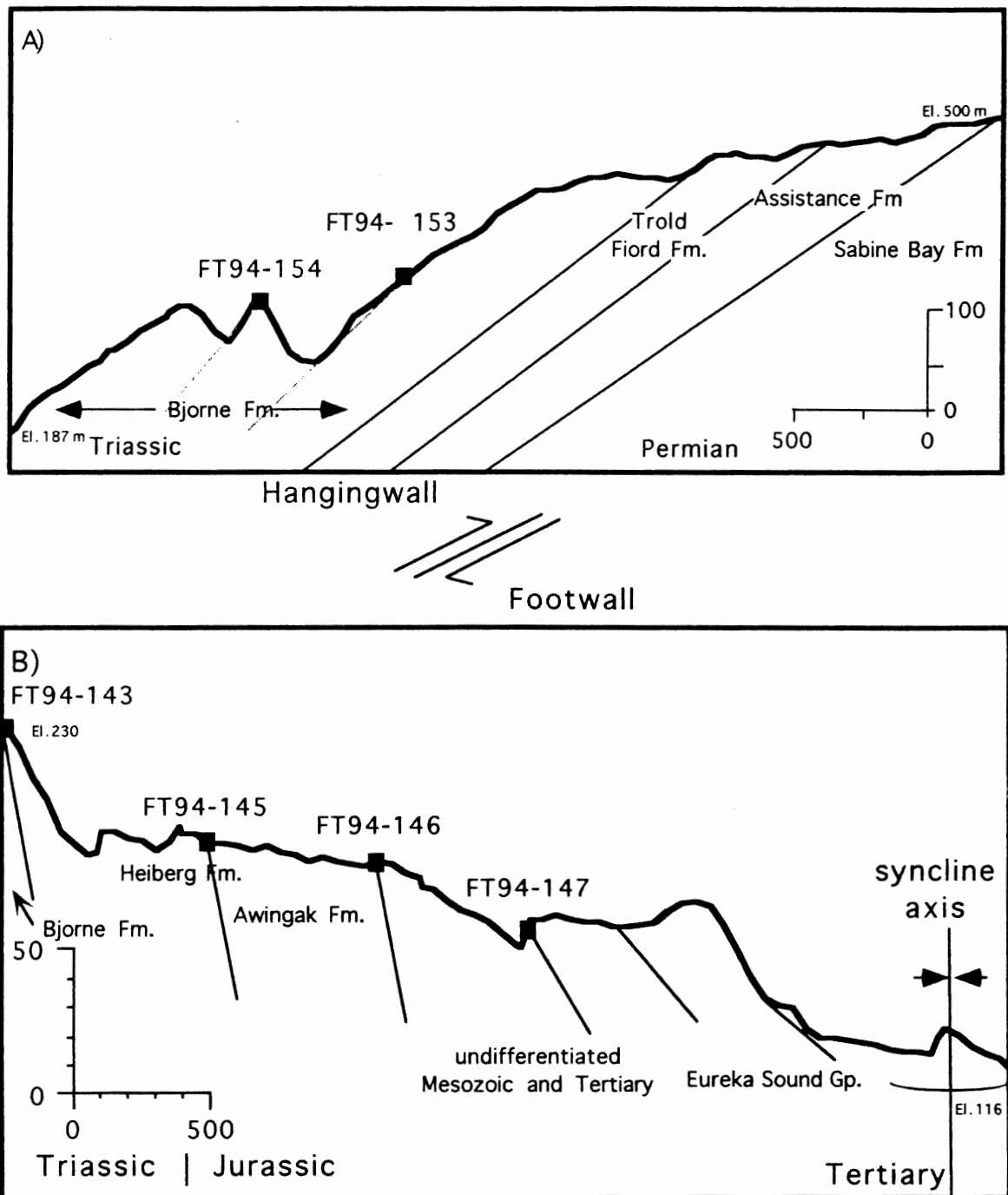
Figure 2.3 Cross sections of A) the Hangingwall, and B) the Footwall of the East Cape Thrust at Mount Bridgeman, Sawtooth Range. The offset between the two sections was not measured but is on the kilometre scale.

the Ellesmerian and Eurekan orogenies. Sedimentation preceded the two orogenies and formed the Franklinian and Sverdrup Basins, respectively.

The Proterozoic to Paleozoic strata of the Franklinian Basin were deposited on Precambrian crystalline basement rocks. The Franklinian Basin was subjected to deformation and faulting during the mid-Paleozoic Ellesmerian orogeny. Crustal thinning and extensional faulting in the late Paleozoic marks the start of sedimentation in the Sverdrup Basin (Embry, 1991).

Due to the Mesozoic northward drift and climatic cooling of the Sverdrup Basin, the sediments were primarily clastic in nature with (the exception of evaporite sequences found in the basal section of the basin) (Embry, 1991). Sedimentation continued contemporaneously with the onset of the Eurekan orogeny in the late Cretaceous (Fig. 2.4, Table 2.1). Caused by the indentation of the Greenland plate into the Laurasian plate, the Eurekan orogeny ended in the Miocene with the closure and inversion of the Sverdrup Basin (Ricketts, 1994). The structural style of the Eurekan orogen is heavily influenced by the reactivation of earlier Ellesmerian faults in Proterozoic to Devonian strata of the Franklinian Basin (De Paor et al., 1989).

2.3   Methods And Procedures

The basic tools for measuring sections were a 50 m chain, marked in one meter increments, and two Brunton compasses. The chain was placed along the section to be measured and the end positions were marked. Standing at either end of the section the author and Dr. D. Arne shot forward and backward bearings as well as dip angles. This information was recorded along with lithological information . Sample locations were also measured on the sections along with GPS and altimeter readings were taken for these locations. The measured section south-east of Mount Bridgeman, an unpublished

stratigraphic log, produced by Dr. Ashton Embry of the ISPG in July of 1982, was used to

ensure consistency with previous work in the designation of stratigraphic relationships.

Cross sections and stratigraphic offset of samples are derived from the measured sections

using basic trigonometry (Fig. 2.5). The COS of the chain dip multiplied by the chain

length (Eqn 2.1) resolves the horizontal distance. If the chain bearing is greater than 10°

from the dip direction of the bedding plane, then the horizontal distance must be multiplied

by the COS of the difference between the chain bearing and the plunge direction (Eqn.

2.2). The SIN of the chain angle multiplied by the chain length, (Eqn. 2.3) resolves the

change in elevation over a given section. Stratigraphic offsets between samples are derived
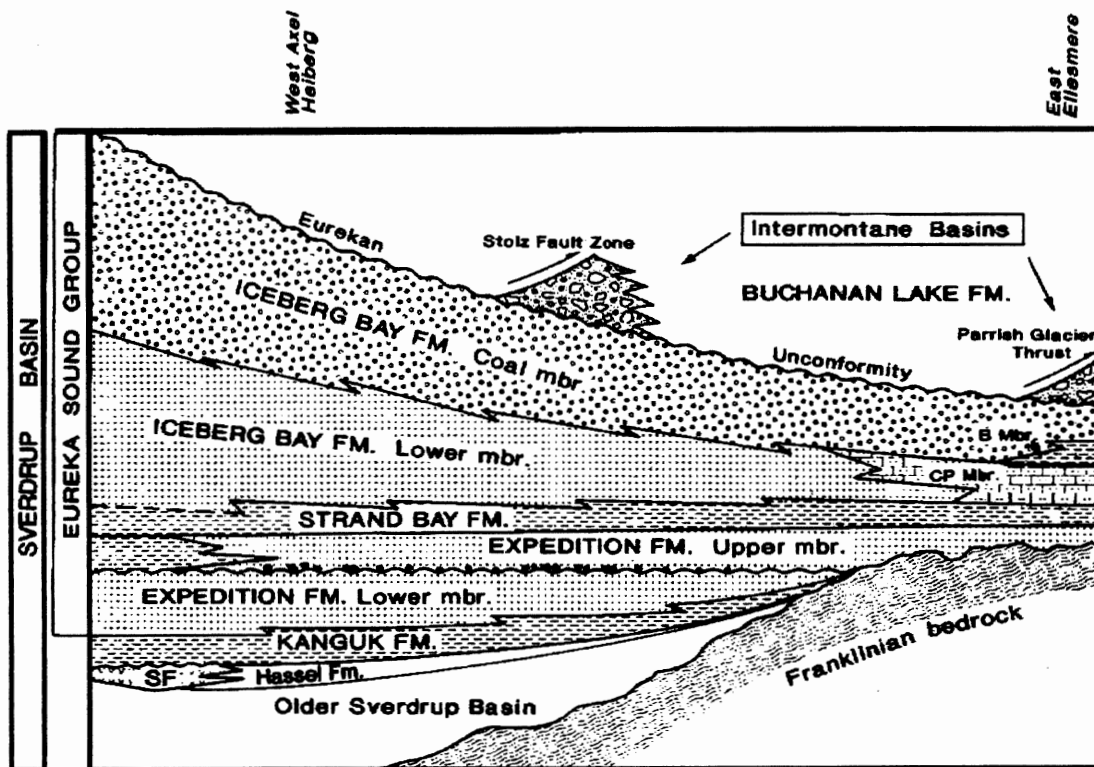
Figure 2.4a A schematic summary of Sverdrup Basin formations. The transect is oriented approximately east-west from western Axel Heiberg to eastern Ellesmere Island. B=Braskeruds Member; CP=Cape Pillsbury Member; SF=Strand Fiord Volcanics. (from Ricketts, 1994)
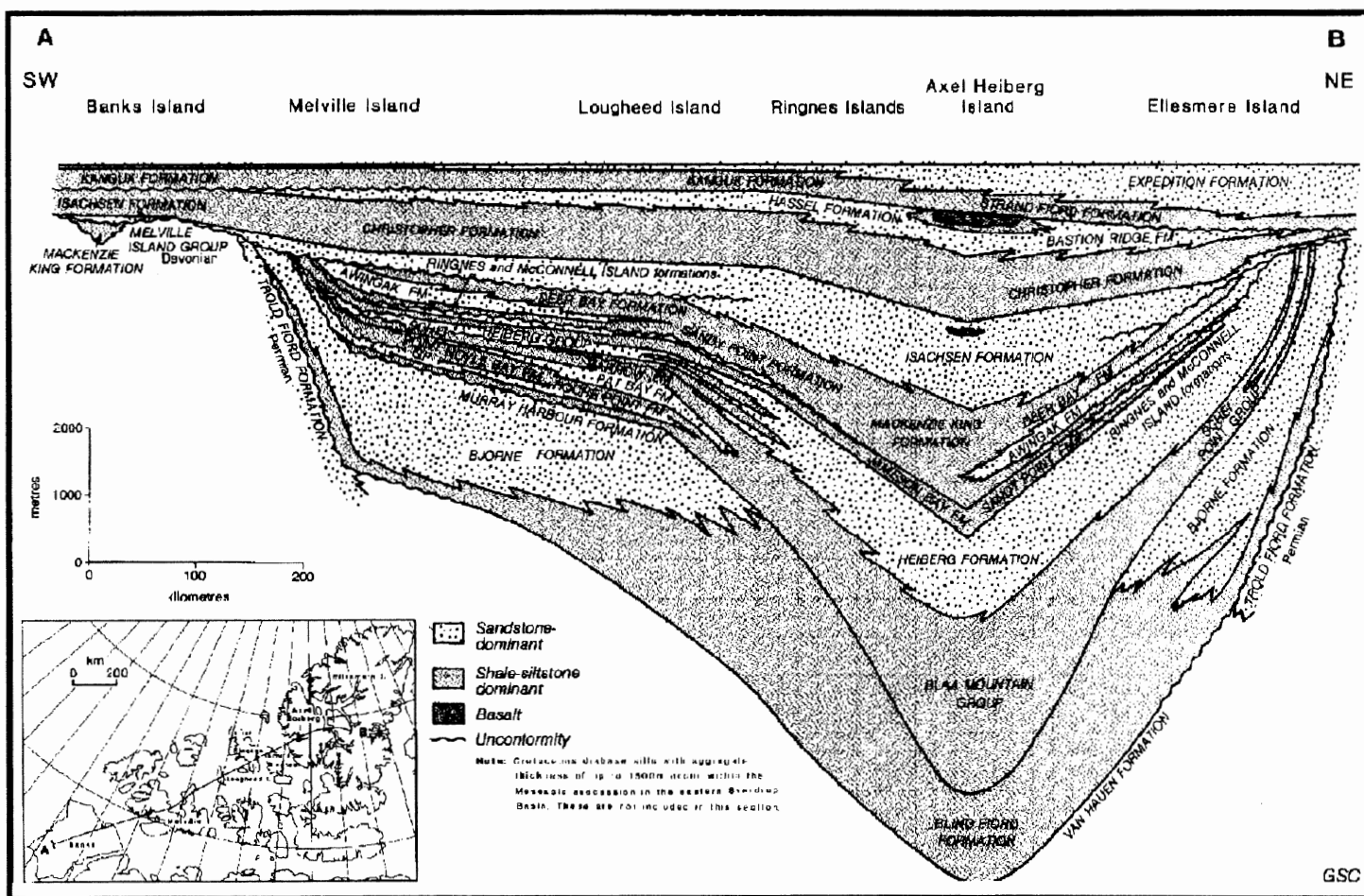
Figure 2.4b A schematic summary of Sverdrup Basin formations.
The Mesozoic and Tertiary Formation of Sverdrup Basin. (Embry, 1991)

Age	Formation	Vesley Fiord		Mt. Bridgeman	
		Footwall	Hangingwall	Footwall	Hangingwall
Tertiary	Eureka Sd. Gp.	Fault contact 600 m		Top of section 564 m	
Undivided Cretaceous-Tertiary				695 m	
Cretaceous	Kanguk Fm.	400 m			
	Hassel Fm.	110 m			
	Christopher Fm.	150 m			
	Isachsen			147 m	
Jurrasic	Awingak Fm.			148 m	
Triassic- Jurassic	Heiberg Fm.			281 m	
Triassic	Barrow Fm			50 m	
	Pat Bay Fm.			64 m	
	Hoyle Bay Fm.			100 m	
	Roche Point Fm.			25 m	(end of
	C. Caledonia Fm.			132 m	section)
	Bjorne Fm.		(ends at base)	start of section	1450 m
Permian	Trold Fiord Fm.		170 m		320 m
	Assistance Fm				400 m
	Tanqueray Fm.		+240 m		N/A
	Sabine Bay Fm.		(fault contact)		380 m
					(start of section)

Table 2.1   The stratigraphic relationships between units, and measured sections.   Thickness of strata measured in sections at Vesley Fiord and Mt. Bridgeman.   Dotted lines (--)indicate an unconformity. (mainly from Embry, 1991)

by multiplying the true horizontal distance by the COS of the dip of the bedding plane (Eqn. 2.4).

$$COS[\text{chain angle}] * \text{chain length} = \text{horizontal distance} \tag{2.1}$$

$$COS[|\text{chain bearing-plunge}|] * \text{horizontal distance} = \text{true horizontal distance} \tag{2.2}$$

$$SIN[\text{chain angle}] * \text{chain length} = D \text{ elevation} \tag{2.3}$$

$$COS[\text{dip of } S_o] * \text{true horizontal distance} = \text{Stratigraphic offset} \tag{2.4}$$

Cross-sections were produced (Figs. 2.3 and 2.4) using the derived changes in altitude and true horizontal offsets. The derived altitudes were double and triple checked
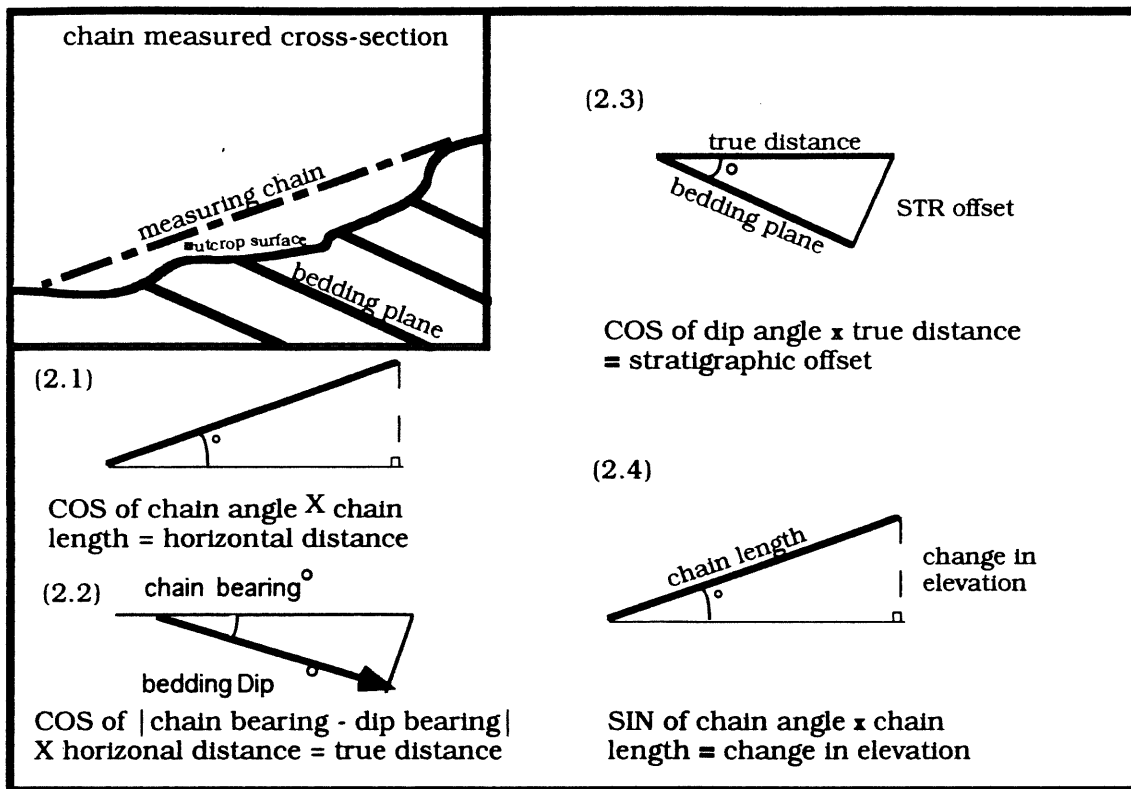
Fig. 2.5 A hypothetical measured section defining the trigonometric relationships of the chain length, chain angle and bedding plane. Equation (2.1) derives the horizontal distance. (2.2) This equation corrects for the deviation from strike. (2.3) Given the true distance,this equation derives the stratigraphic offset. (2.4) This equation gives a measure of the change in elevation.

using an altimeter and a Magellan 5-channel GPS. In all cases the derived altitudes are within ±100m of the GPS and altimeter readings (APPENDIX A, B, C,). This variation is acceptable when considered in terms of the time and distance as well as the finite resolution of the GPS, which is ±100m. This level of GPS accuracy may seem low to the reader but it must be noted that high-accuracy GPS systems rely on a local transponder to correct for designed signal degradation. Because of the nature of the geometric relationship of the signal satellites, GPS systems are also more sensitive to vertical drift than the more often reported horizontal drift.

The stratigraphic offset between samples, and, or lithological boundaries, was derived from the addition of the stratigraphic offset of individual chain sections.

2.4   Stratigraphy

2.4.1 Southern Sawtooth Range, Vesley Fiord

The Vesley Fiord cross-section (Fig. 2.2 and 2.6) is based on a measured section running from the northern edge of Quaternary sediments in Vesley Fiord and moved up-section through an unnamed creek bed for approximately 4 km (APPENDIX A). The section ends on a saddle at the top of the watershed of this creek.

The Cretaceous Christopher Formation is the first formation on the measured section. The Christopher Formation consists of finely laminated silty to coaly shale with yellow-brown sulphate staining and interbedded with more resistant hematite stained bands. The Christopher Formation extends up-section for approximately 150m and is conformably overlain by the Hassel Formation, 110 m thick. The Hassel Formation is composed of finely laminated siltstone and fine grained lithic sandstone which alternate on a meter to centimetre scale. Both the top and bottom of the Hassel Formation are denoted by more massive, fine sandstone units that are approximately 10 m in thickness. The Hassel Formation is conformably overlain by the Kanguk Formation, both being of Late Cretaceous age. The Kanguk Formation is easily identified by its finely laminated fissile shale units but is poorly exposed due to its low resistance to erosion. The Kanguk Formation is approximately 400 m thick. The contact with the Eureka Sound Group however, is not visible, therefore this estimate is tentative and should be considered a maximum thickness.

The Kanguk Formation is conformably overlain by the Eureka Sound Group encompassing formations of Late Cretaceous to Miocene age. In the Southern Sawtooth Range the Eureka Sound Group is tentatively divided into the Expedition Fiord Formation, and the conformably overlying Strand Bay Formation (Ricketts, 1994). The Expedition Fiord Formation is composed of tan to beige sandstone with minor siltstone. Bedding ranges from massive on a meter scale for medium to coarse grained sandstone, to finely
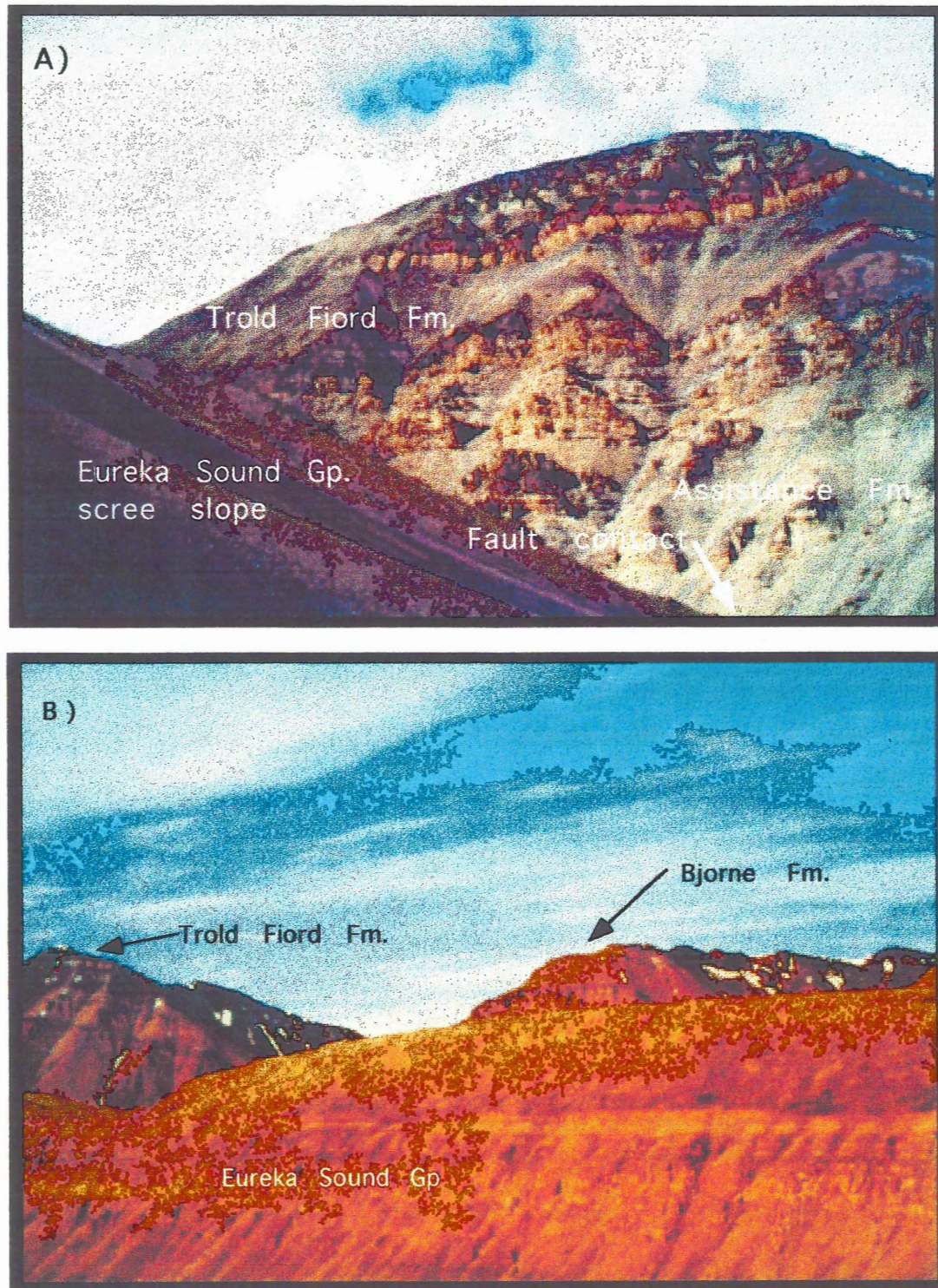
Figure 2.6 Photographs of the Vesley Fiord Thrust in the Sawtooth Range.
A) The hangingwall section. Note the distinctive banding in the Trold Fiord Fm. B) The top of the footwall section with hangingwall units in the background. Note the lack of structural deformation and planar nature of the units.

laminated and crossbedded in the fine sandstone and siltstone. The Expedition Fiord Formation has a stratigraphic thickness of at least 350 m, depending on the placement of the basal contact with the Kanguk Formation. The basal contact of the Strand Bay Formation is denoted by a thick shale that coarsens upward into interbedded shale and minor fine sandstone. The presence of coal beds and the predominance of shale suggest that the upper section of this unit may grade into the Cape Pillsbury Member of the Iceberg Bay Formation. In either case the upper age limit for the top section of the Eureka Sound Group is Upper Paleocene and the actual formation designation does not affect the outcome of this study. The whole Eureka Sound Group section is approximately 600 m thick and ends at an unconformity with the footwall of the Vesley Fiord Thrust.

The Vesley Fiord Thrust juxtaposed the Permian Tanqueray Formation in the hangingwall with the Tertiary Eureka Sound Group in the footwall. The fault plane is sub-parallel to bedding in both the footwall and hangingwall. Minor bedding-parallel faults with offsets on a centimetre scale are present in the footwall. The hangingwall side of the thrust is made of laminated calcareous siltstone and massive carbonate rock. Suprisingly it does not exhibit any deformation related to the thrust.

The Tanqueray Formation is approximately 240 m thick and the colour grades from grey to a creamy-pink at the contact with the Assistance Formation. The Assistance Formation (240 m) is composed of tabular greywacke. Thin layers containing brachiopods, bryozoans, and calcareous cementation are characteristic of this formation. A gabbroic dyke (5 m) intrudes the Assistance Formation at a sub-vertical angle and is assumed to be of Cretaceous age. The contact with the overlying Trold Fiord Formation is readily identified by a mottled green and purple basal unit. The Trold Fiord Formation is 170 m thick and its upper boundary is tentatively placed at the first definitive outcrop of the Triassic Bjorne Formation, a red, medium to coarse grained sandstone unit. The bottom contact of this unit also coincides with the end of the measured section.

2.4.2 Northern Sawtooth Range, East Cape

The Mt. Bridgeman cross-section (Fig. 2.5) is based on two measured sections. The first section runs south-east downstrean along an unnamed creek bed from the footwall of the East Cape Thrust to a syncline axis on the coastal plain (APPENDIX B). The second measured section is on the west of Mount Bridgeman and runs up-section from East Cape Fault (APPENDIX C). The geometry of this section is significantly different from the measured section at Vesley Fiord. At Vesley Fiord the bedding planes in both the footwall and hangingwall are sub-parallel to the fault plane, whereas at Mount Bridgeman the fault plane truncates the limb of a syncline and the hangingwall is sub-parallel to the fault plane. This indicates that the tectonic environment there is a footwall ramp, as opposed to the Vesley Fiord location, where the thrust contact is a ramp flat.

2.4.2.1 Section 1

The footwall section begins in the red sandstone at the top of the Triassic Bjorne Formation and moves up strata to the centre of the syncline where it ends in the Tertiary Eureka Sound Group. Overlying the Bjorne Formation is the Triassic Cape Caledonia Formation, a recessive shale unit 132 m thick. The overlying Roche Point Formation is a thin tan-buff sandstone package approximately 25 m thick and it is conformably overlain by the Hoyle Bay Formation, 100 m thick, which is distinctive in outcrop due to hard marine limestone packets at the top and middle of the formation. The Pat Bay Formation conformably overlies the Hoyle Bay Formation and consists of 64 m of grey to tan sandstone packages. The recessive Barrow Formation above, (covered in outcrop) is a shaly unit that fines upward into the Triassic Heiberg Formation. The Barrow Formation is estimated to be 50 m in thickness but that may include some of the lower Heiberg Formation.

The Heiberg Formation consists of three members in upwards conformable
succession: 1) the Romus Member consists of 93 m of marine sandstone, siltstone and
shale; 2) the Fosheim Member (168 m), a transitional marine to non-marine sandstone and
siltstone with shale and coal intercalations; and 3) the Remus Member, approximately 20
m thick, forming a durable outcrop due to cementation of the ironstone pebble layers,
which give the unit a distinctive deep red colour. The upper Jurassic Awingak Formation
overlies the Heiberg Formation and consists of fine grained marine sandstone unit with
poor exposure. It has a poorly defined upper contact, and is approximately 148 m thick.

Unconformably overlying the Awingak Formation is the Cretaceous Isachsen
Formation, a sandstone unit with minor silt, shale and pebbly conglomeratic layers. The
outcrop exposure of the Isachsen Formation is very poor, especially in comparison with
the Vesley Fiord section (see above), and the unit is over 100 m thick. The Isachsen
Formation is overlain by the Christopher Formation but the quality of the outcrop
deteriorates to the point where it is not possible to define the actual formation contacts and
Dr. Embry's stratigraphic log ends at this point. Traces of the bedding plane insure that
the measurement of the stratigraphic offset remains accurate and a total stratigraphic offset
of 695 m was recorded as undefined Cretaceous-Tertiary before accurately identifying the
Eureka Sound Group. This stratigraphically undefined measured section is surmised to
include the top of the Christopher Formation, the Hassel and Kanguk Formations and the
basal Eureka Sound Group where accurate stratigraphic identification is once again
possible. With an additional section of 564 m of Eureka Sound Group, the section ends in
Eureka Sound Group strata, (possibly in the Strand Bay Formation based on the shale
content) in the centre of a syncline.

2.4.2.2 Section 2

The hangingwall measured section begins at an altitude of 500 m on the south-west
side of Mt. Bridgeman and moves down dip to the west along a creek bed. Bedding is

sub-parallel to the gradient of the traverse, requiring a long distance traverse to measure relatively small amounts of stratigraphic offset.

The section commences in the Permian Sabine Bay Formation, 380 m thick, which consists of light coloured, massive, arkosic, fine grained sandstones. Sulphide zones weather to distinctive red iron oxides in some horizons. The conformable overlying Assistance Formation is 400 m thick and is characterised by grey-black siltstone to very fine sandstone. Thin layers of brachiopods, bryozoans, and calcareous cementation are characteristic of this formation. The Trold Fiord Formation above is 320 m thick and is dominated by a fine grained green sandstone, with interbedded burgundy-coloured bioclastic limestone, and chert. The overlying Bjorne Formation is easily identified by the red weathering of the tan, subaerial sandstone, and 1450 m of strata were measured up to the edge of a strike-parallel valley, assumed to mark the bottom of the more friable Heiberg Formation.

2.5   Summary

The lithological packages in the hangingwall and the footwall of the Vesley Fiord Thrust are both bedding-parallel to the fault plane and exhibit remarkably little deformation. These relationships suggest that the thrust is located on a ramp flat with a horizontal pre-folding direction of movement and that the fault offset must be as large as the stratigraphic offset, if not larger. Conversely, the Mount Bridgeman cross-section has a hangingwall that is sub-parallel to the fault plane and a footwall where the truncated strata are close to perpendicular to the fault plane. This suggests that the fault contact at Mt. Bridgeman is a hangingwall flat on a footwall ramp and that thrusting occurred during or after the formation of the syncline.

CHAPTER 3: FISSION TRACK ANALYSIS

3.1   Introduction

The apatite fission track method is based on the measured density and etchable length distribution of linear tracks of crystal damage produced during the spontaneous fission decay of trace amounts of ^{238}U in apatite (Fig. 3.1). Fission track (FT) dating is similar to other isotopic dating methods in that fission tracks are the physical expression or "daughter product" of the decaying ^{238}U parent isotope, and accumulate through time. Fission track density is defined by counting spontaneous tracks within a given area of a polished apatite grain. Measurement is done at under high magnification under a microscope (Hubert and Green, 1982, 1983). A number of different methods exist for determining fission track ages. In the external detector method used in this thesis, the track density over a specific grain area is compared with the density of a new set of tracks, formed by the decay of ^{235}U induced by thermal neutron flux in a reactor, recorded on a low-uranium mica wafer in close contact with the apatite grain in question. ^{238}U and ^{235}U have a constant relative abundance and the induced track density is proportional only to the uranium content, hence the ratio of induced tracks to spontaneous tracks thus obtained permits the calculation of a fission track age.

Fission tracks fade or anneal by progressive length shortening. Fission track densities provide a measure of cooling age with respect to the low-temperature thermal history of a rock sample, as the effective retention of fission tracks in apatite occurs at temperatures in the range 90 to 135°C for cooling rates between 0.1°C/Ma and 100°C/Ma, respectively. The precise temperature at which fission tracks in apatite are effectively retained also depends on the composition of the apatite and in particular the chlorine content (Green et al, 1986). Corresponding etchable track length distributions contain valuable

Figure 3.1   Detrital apatite grains with etched fission track pits. Different magnification reveals the variation in grain shape, condition, density of etch pits in different grains.
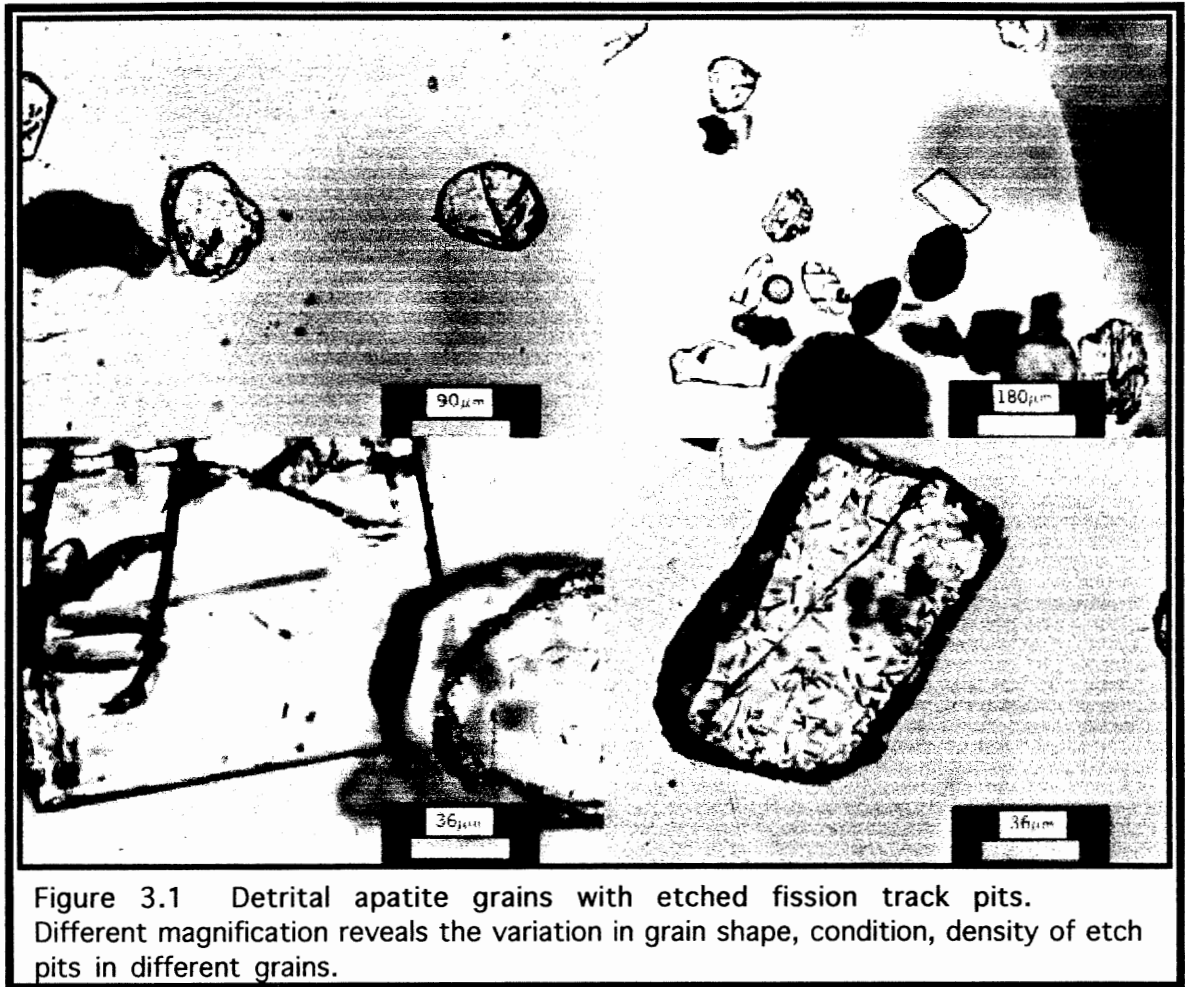
information on the thermal history of the mineral because fission tracks form continuously through time, and thus each track records a unique time-temperature history (Andriessen, 1995). The interpretation of fission track data has recently been assisted by the development of a number of forward and inverse modelling procedures that incorporate fission track age and length data to test possible thermal history scenarios in sedimentary basins (Laslett et al, 1987; Carlson, 1990; Willett, 1992; Ravenhurst and Donelick, 1992).

For this study apatite samples from the Vesley Fiord measured section and the East Cape/Mount Bridgeman measured section were analysed. As previously indicated samples

were collected by Dr. D. Arne and the author. Mineral separation was performed by the

author. Sample preparation was done by Gudong Li (MSc) and the author. Alexander

Grist (MSc), technical manager of the Dalhousie Fission Track Research Laboratory

performed the age and length measurements with the participation of the author increasing

towards the end of this study.

3.2   Technique

3.2.1 Apatite separation

Apatite occurs naturally in small amounts as an accessory mineral in a wide range of

igneous and metamorphic rocks and is also found in most detrital sedimentary rocks.

Apatite is separated using a variety of physical procedures. Samples are first crushed and

milled until >70% of the sample passes through 60 mesh (Tyler equivalent) sieve. Next the

sample is washed and separated on a Wilfley shaker table, which sorts the grains based on

a combination of size, shape, and density. The high density (apatite bearing) fraction is

subsequently washed and dried for further processing while the medium density and light

fractions are washed and stored. The heavy minerals (minerals with densities greater than

2.8) are then separated from the lighter (mainly quartz and feldspars constituting the

majority of the sample) either by using the toxic heavy liquid, tetrabromoethane (density =

2.96), or by centrifugation of the sample in the non-toxic sodium polytungstate, (density =

2.8). Magnetic separation is then utilised to separate more-magnetic minerals from less-

magnetic minerals including apatite. The non-magnetic fraction is further subdivided using

the toxic heavy liquid diiodomethane (density of 3.3). If the sample contains sufficient

apatite and the separation process is successful, the resulting apatite separate is mounted in

epoxy and polished to expose internal grain surfaces.

Spontaneous tracks were revealed by etching the polished grainmounts in 5M

HNO_3 for 20 seconds at 24°C. The etched grainmounts are irradiated and analysed using

the external detector method (see Sect. 3.2.2: Track density determination). If spontaneous

track densities are relatively low and sufficient sample material exists, a second grainmount

can be made solely to improve track length analysis. These duplicate samples are exposed

to radiation from ^{252}Cf fission (under vacuum for 5 days at a distance of 9 cm) to increase

the number of confined tracks that are revealed by etching. This ^{252}C irradiation is done

under contract at the Irradiation Laboratory at Rensselaer Polytechnic Institute, Troy, New

York.

3.2.2 Track density determination

In this study track density was measured using the external detector method

(Hurford and Green, 1982, 19983). A thin sheet of low-uranium muscovite was placed in

contact with each grainmount to serve as a detector for neutron-induced radiation.

Samples where irradiated at the Dalhousie Slowpoke-2 reactor. A glass neutron dosimeter

(CN5; U=12.44+/- 0.32 ppm; Bellemans et al., 1993) was placed in the package to

calibrate neutron dosage. The total thermal-neutron was approximately 9×10^{15}

neutrons/cm^2. Tracks in the mica detectors were exposed by etching in 48% HF for 30

minutes at 24°C.

Tracks were counted at 1000X magnification with dry objectives using a Zeiss

Axioplan binocular microscope fitted with an Autoscan™ computer controlled stage and a

486DX computer with Autoscan software. The computerised system registers the location

of the grainmount and the external detector in relation to a fixed point. This allows for the

rapid and accurate translation between grains and their respective induced track image.

Logging the grain locations ensures the grains are counted once. Where possible 25 grains

and images were counted to produce a fission track age (see Appendix F).

3.2.3 Track length measuring

Track lengths were also measured at 100X magnification with dry objectives using a Zeiss Axioplan binocular microscope fitted with a drawing tube, a 486DX computer and a digitising tablet. Where possible, grainmounts used in track density determination were also used for length measurement. In cases where the insufficient track lengths were present to produce meaningful length data a second grainmount was irradiated with ^{252}Cf to produce a density of approximately $3x10^6$ fission fragment pits.. These pits serve as channels for the HF etchant, allowing for increased efficiency in the etching of contained fission tracks and a greater number of confined track lengths to be measured.

The lengths and angles of tracks, relative to the c-axis of the grain were determined using a calibrated digitising puck, on a digitising pad with a tiny red diode which appears in the microscope field of view. The diode was aligned at either end of the track and the position of the two points recorded on the digitising pad. Age and length statistics were done using fission track dating software developed by Donelick (1988).

3.2.4 Single grain age analysis

When fission track analysis demonstrates that a detrital apatite sample is unannealed (the sample has an inherited fission track age that is older than its stratigraphic age) it may be possible to look at the distribution of the single-grain fission track ages and define one or more cooling ages of the sediment source area(s).

Single grain ages can be plotted using scatter diagrams but a 2-dimensional scatter diagram does not show the level of certainty or precision associated the individual grain ages. As well, the mean pooled age derived from a scatter plot does not place any weight on the relative certainty of the individual grain ages. A better way to graphically plot single grain ages is to use radial plots (Fig. 3.2)(Galbraith, 1990).

(a)

estimate z   →   standardised estimate $y = (z - z_0)/\sigma$

standard error σ precision $x = 1/\sigma$

(z_0 is a convenient central value)

draw a scatter plot of (x,y):

(b)   **(c)**
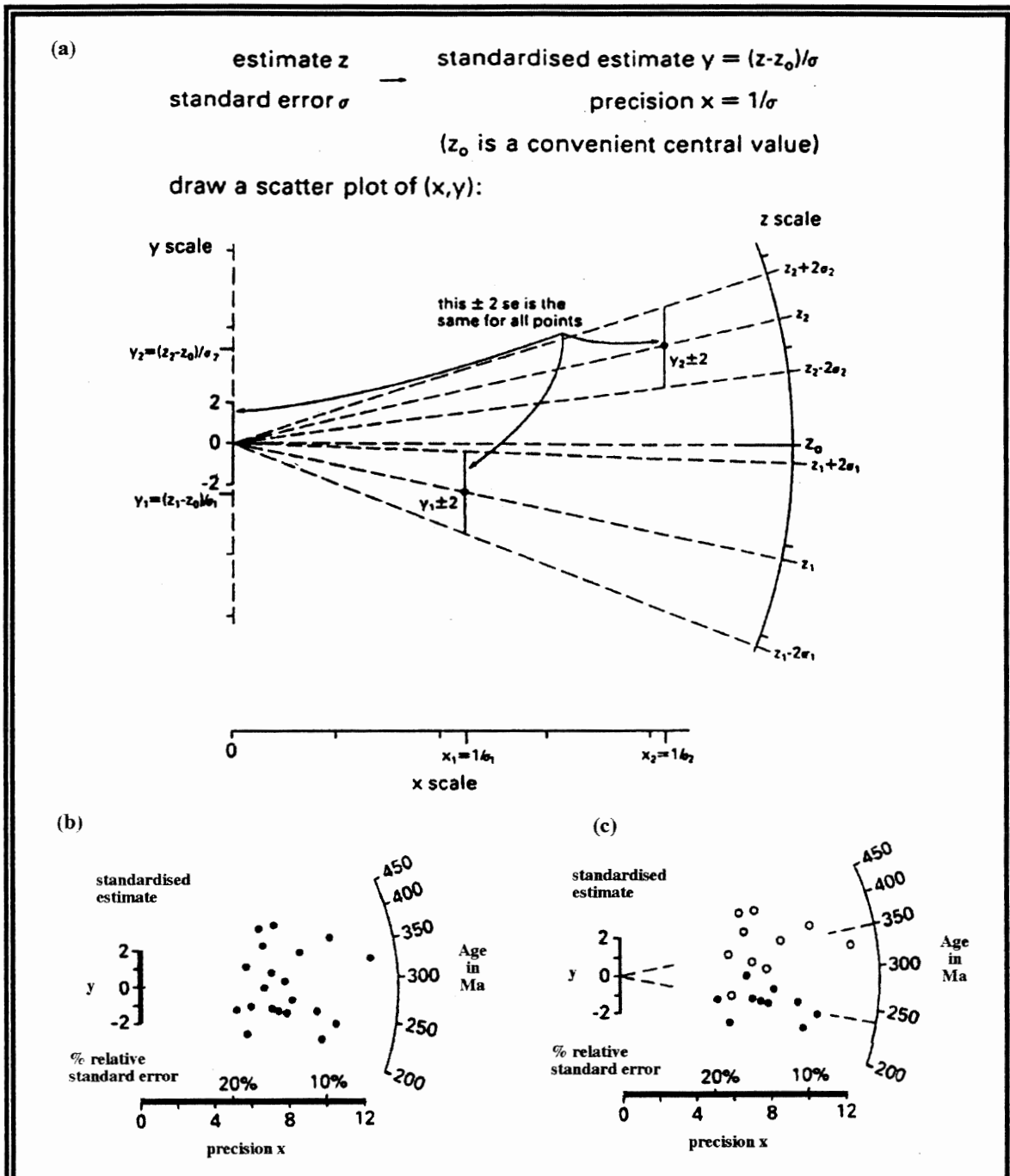
Figure. 3.2 Principle of the radial plot.   (a) An estimate z with standard error σ is plotted as the point (x,y) where $x=1/\sigma$ and $y=(z-zo)/\sigma$ for some z chosen so the average y is near 0. Each estimate has unit standard error on the y scale. Points with larger x have higher precision. To read off the values of z and $z+/- 2\sigma$, extrapolate lines from (0,0) through (x,y) and from (0,0) through (x, y+/-2) to the z scale.
(b) a radial plot of single grain ages from a mixture of two samples/age groups.
(c) reveals which group each grain actually belongs to. There are 10 grains with ages of ~350 Ma and10 grains with ages of ~240 Ma.   (modified after Galbraith, 1990)

The radial plot provides a more accurate measurement of the age of an annealed sample. The "central" age of a sample is similar to a mean age of all grains but the individual grain ages are weighted according to their standard deviation. This procedure reduces the effect of outliers on the data. Where there are visually discrete groups of grains in a radial plot, the derived groups of grains can be analysed separately to define inherited fission track ages for the different populations (Fig. 3.2) (see Sect. 3.3.2: Analysis of data).

3.3   Samples

3.3.1 Sampled sections

Samples from both sections (Table 3.1) have been analysed for fission track data. The Vesley Fiord cross section (Fig. 3.3) is particularly good for presenting fission track data. 6 successful samples were obtained over good intervals and with a close spatial relationship with the Vesley Fiord Fault. The two sections at Mt. Bridgeman (Fig. 3.4) are not as closely spatially related, with major offset between the footwall and hangingwall sections. The 6 samples from the Vesley Fiord section are divided evenly between the hangingwall and the footwall and define the relationship of the fission track ages with the fault movement in the Vesley Fiord Thrust Fault. The samples from the Mt. Bridgeman section are located in the footwall of the East Cape Thrust and add information about the relationship of inherited apatite fission track ages to the derived mean pooled age.

3.3.2 Analysis of data

Six samples were analysed in the Vesley Fiord section (Fig. 3.3 and Tables 3.1, and 3.2) and 6 samples were analysed on the Mt. Bridgeman sections (Fig. 3.4 and Tables 3.1, and 3.2). The Vesley Fiord Thrust juxtaposes older Permian and Triassic age
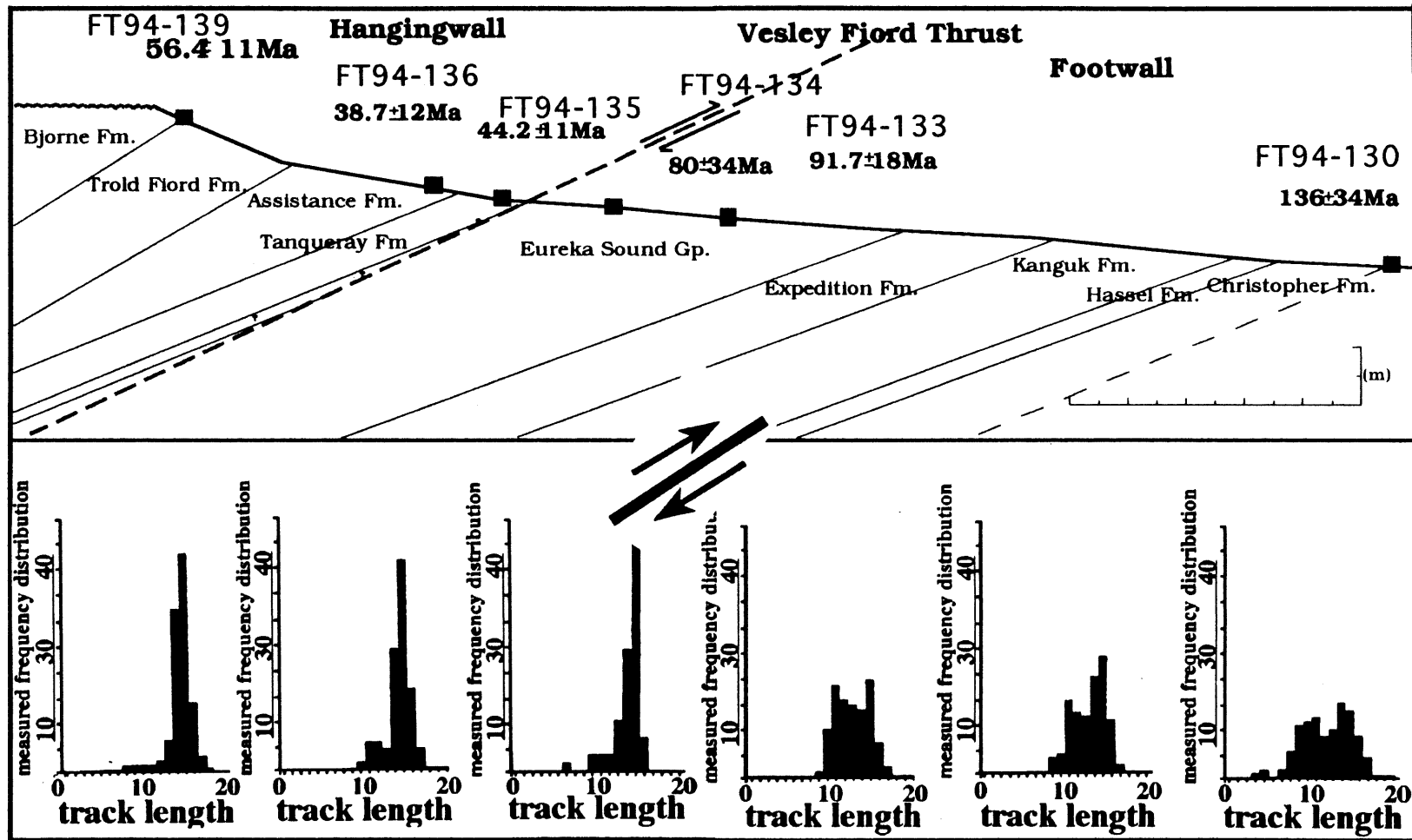
Figure 3.3 The Measured section at Vesley Fiord. With derived fission track age and length data. The Vesley Fiord Thrust juxtaposes older Permian- and Triassic-aged Formations on Tertiary and Cretaceous strata. The fission track ages of the hangingwall samples are much younger than their stratigraphic ages. Corresponding track length distributions are narrow and peaked, indicating that these samples were totally annealed until the Eocene. In contrast, fission track ages of the footwall samples exceed stratigraphic ages and corresponding track length distributions are relatively broad, indicating that these samples were only partially annea led after deposition.
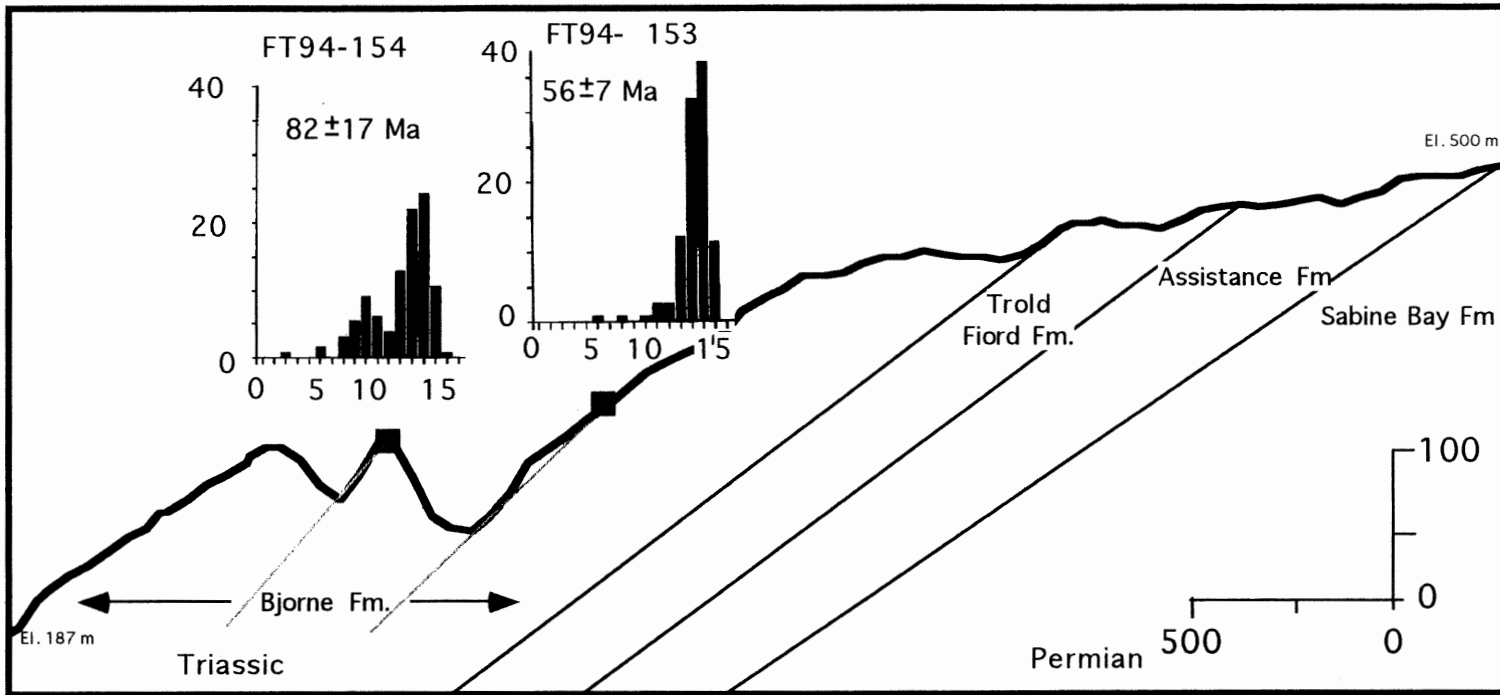
Figure 3.4a   Hangingwall of the East Cape Thrust at Mt. Bridgeman: with track length histograms and fission track ages. Note the histogram for sample FT94-153 has a narrow base and a tall peak, characteristic of a rapid cooling history. The histogram for FT94-154 is bimodal and has a wide distribution, characteristics of a partially annealed sample.
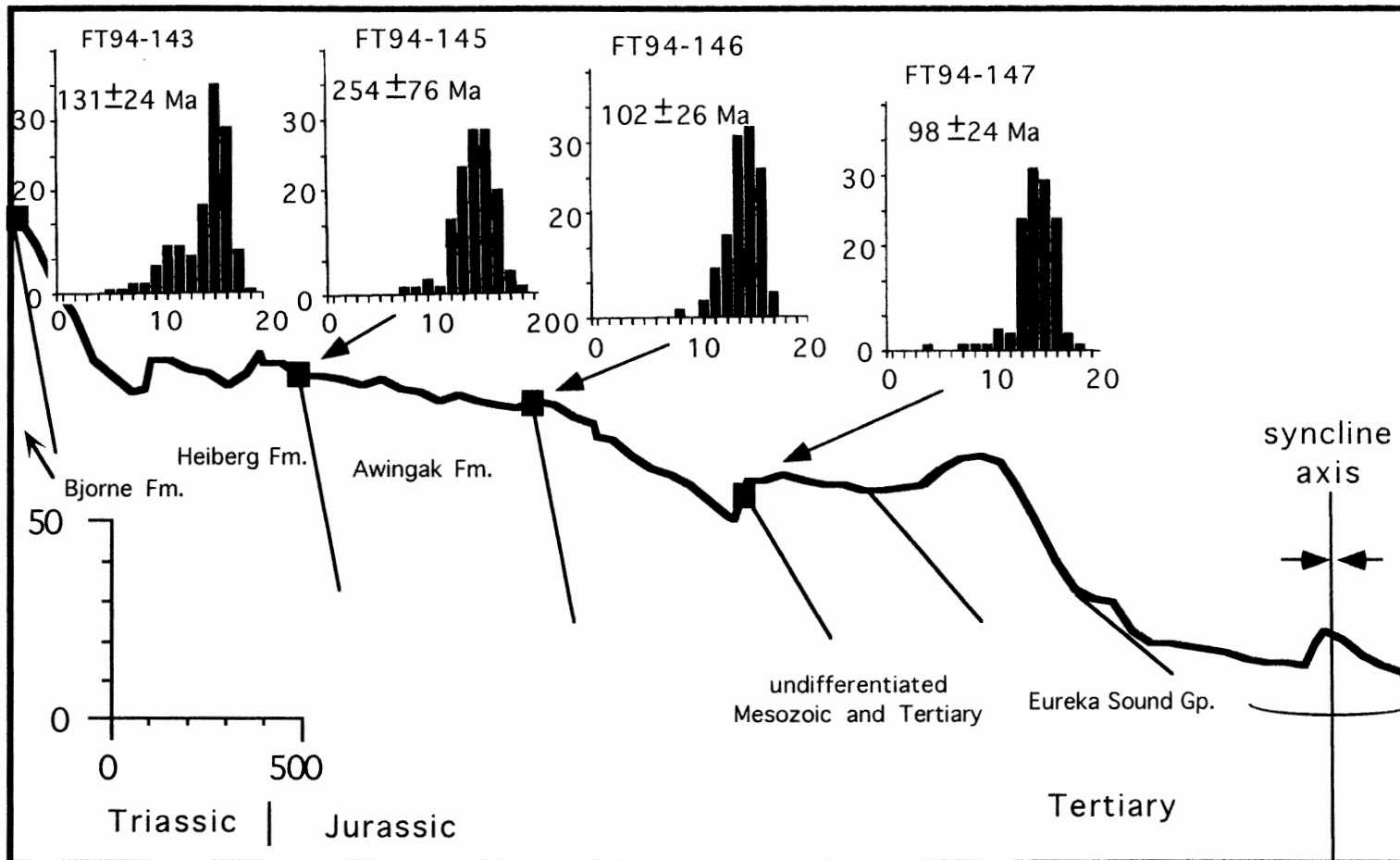
Figure 3.4b Footwall of the East Cape Thrust at Mt. Bridgeman. Histograms and fission track ages of the four successful samples in the footwall section. The relatively wide distribution and large 2 sigma errors are indicative of unannealed fission track samples.

FTLab Number	Sample Number	Grains Counted	N_s	N_i	Rho_s	Rho_i	Chi-square	N_d	FT Age (Ma)	Formation	Stratigraphic Age (Ma)
FT94-130*	DA94-074	28	513	702	8.40	11.5	.0000	9000	136+/-34	Christopher Fm.	Early C., Albian 112-98.9
FT94-133*	DA94-080	18	132	205	3.87	6.02	.0000	9000	80+/-34	Mount Lawson Fm.	Late Paleocene 60.5-56.5
FT94-134	DA94-082	25	389	653	7.01	11.8	.0173	6000	92+/-18	Mount Lawson Fm.	Late Paleocene: 60.5-56.5
FT94-135	DA94-084	13	82	325	4.74	18.8	.7919	6000	44+/-11	Assistance Fm.	Middle Permian 264-260
FT94-136	DA94-085	29	55	249	0.75	3.38	.9738	6000	39+/-12	Cretaceous Dyke	Assumed Cretaceous Age
FT94-139	DA94-088	24	758	2463	7.86	25.5	.0000	6000	56+/-11	basal Bjorne Fm.	Lower Triassic 250-244
FT94-143	DA94-093	24	3848	4145	26.2	28.2	.0000	6000	131+/-24	upper Bjorne Fm.	Lower Triassic 250-244
FT94-145	DA94-097	9	428	314	28.6	20.9	.0000	6000	254+/-76	Awingak Fm.	Late Jurassic 159-150
FT94-146	DA94-099	16	109	186	6.50	11.1	.9096	6000	102+/-26	Christopher Fm. (?)	Early C., Albian 112-98.9
FT94-147	DA94-100	25	117	209	2.00	3.57	.9655	6000	98+/-24	Mount Lawson Fm.	Late Paleocene 60.5-56.5
FT94-153	DA94-109	25	597	1957	7.02	23.0	.5733	8600	56+/- 7	mid Bjorne Fm.	Lower Triassic 250-244
FT94-154	DA94-110	27	646	1463	10.7	24.0	.0000	8600	82+/-17	mid Bjorne Fm.	Lower Triassic 250-244

TABLE 3.2 A SUMMARY OF TRACK COUNT DATA. Samples with chi^2 probability of >0.05 pass the chi^2 test at a 95% confidence level. Ages for samples that pass the chi^2 test are calculated using pooled statistics. Samples that failed the chic^2 test have ages that are calculated using the radial plot statistical method. Age summary sheets are given in Appendix F. Formation and Stratigraphic age columns refer to the formation that was sampled. Abbreviations are as follows: N_s and N_i are the number of spontaneous(fossil) tracks and induced tracks respectively; Rh_o and Rh_i are the density of spontaneous and induced tracks respectively($10^5/cm^2$); N_d is the number of flux dosimeter (CN5 or CN1 glass) tracks counted. Ages of samples marked with an asterisks(*) were calculated using a zeta factor of 105.4+/-1.8(CN1 glass). All other ages use a value of 345.3 +/-12 (CN5 glass) for a zeta factor. Age error estimates are at the 95% (2-s) confidence level. Analysis by A.M. Grist. (modified after Grist and Collins, 1996)

Age	Formation	Vesley Fiord Footwall	Vesley Fiord Hangingwall	Mt. Bridgeman Footwall	Mt. Bridgeman Hangingwall
		Fault contact		Top of section	
Tertiary	Eureka Sd. Gp.	134,FT,C 133,FT,C			
Undivided Cretaceous-Tertiary					
Cretaceous	Kanguk Fm. Hassel Fm. Christopher Fm. Isachsen	130,FT (Base of		— — — — 147,FT —	
Jurrasic	Awingak Fm.	section)			
Triassic- Jurassic	Heiberg Fm.			145,FT,C	
Triassic	Barrow Fm Pat Bay Fm. Hoyle Bay Fm. Roche Point Fm. C. Caledonia Fm. Bjorne Fm.		top of section 139,FT,C —	143, FT,C start of section	end of section 154,FT,C 153, FT,C
Permian	Trold Fiord Fm. Assistance Fm Tanqueray Fm. Sabine Bay Fm.		136,FT,C 135,FT (fault contact)		start of section

Table 3.2   The stratigraphic relationships between units, and measured sections.   Thickness of strata measured in sections at Vesley Fiord and Mt. Bridgeman. Dotted lines (--)indicate an unconformity. Successful samples (FT94-XXX)are marked on the table. (FT) indicates FT analysis, C indicates compositional analysis.

Formations on Tertiary and Cretaceous strata. The 3 samples from the footwall have fission track ages that are older than their stratigraphic age. Histograms of the track lengths of the footwall samples are have a broad distribution and more than one peak. This indicates that all the footwall samples are unannealed and the fission track ages derived from them are inherited from the exhumation history of their provenance areas.

The 3 Vesley Fiord hangingwall samples are fully annealed. The derived fission track ages are significantly younger than the stratigraphic age of the sample locations (Fig. 3.4 and Table 3.2). Track length distribution is very narrow and the mean track lengths of

the samples are high (Appendix G) indicating that the samples cooled through the $100\,^\circ C$ isotherm rapidly. The hangingwall fission track age closest to the thrust has a fission track closure age of 44 ± 11 Ma, which can be seen as a finite constraint on movement of the Vesley Fiord Thrust. The juxtaposition of unannealed samples in the footwall with annealed hangingwall samples indicated maximum basinal heating predated the thrust movement. The rising hangingwall block underwent rapid thermal relaxation and passed cooled through the $100\,^\circ C$ geotherm as it was thrust up over the cooler footwall block. The close spatial relationship of the hangingwall sample to the thrust plane would suggest that the closure date of 44 ± 11 Ma is related to the normalisation of a inverted geotherm. A more conservative analysis would suggest the date is reflects the uplift, erosion and cooling of the hangingwall block. The later analysis conflicts with the AFTA age of sample FT94-136 (Fig. 3.3) which is stratigraphically up section from the sample (FT94-134) closest to the fault plane If AFTA dates are related to uplift and erosion, then the AFTA date of sample FT94-136 should be older than FT94-134 as it would have passed through the $100\,^\circ C$ isotherm before sample FT94-134.

The samples from the Mt. Bridgeman section (Figure 3.4 and Table 3.2) do not have as close a linkage the East Cape Thrust as the Vesley Fiord sample set does with the Vesley Fiord Thrust. There is a significant offset between the hangingwall and footwall sections. In addition, the first successful sample in the hangingwall is 1000 m up-section from the start of the section (see Sect. 2.4.2.2.) However, analysis of the fission track data supports the same model of uplift and cooling as the Vesley Fiord section. Samples from the footwall section of the Vesley Fiord Thrust are unannealed with wide track length distribution, and exhibiting FT ages significantly older than their respective source formations. Samples located in the hangingwall of the thrust are fully annealed and have fission track ages that are significantly younger than their source formations(Fig. 3.4).

The analysis of fission track ages with radial plots show that hangingwall samples from the Vesley Fiord section (Fig. 3.5b) are totally annealed and the derived ages represent the time of cooling in relation to the uplift and exhumation of the formations as they moved up the fault plane of their respective faults. Of the two samples from the Mt. Bridgeman hangingwall section the one closest to the fault contact (FT94-153) (Fig. 3.5a) is completely annealed and exhibits the characteristic steep peaked track length histogram that is diagnostic of a sample that has been rapidly cooled. The sample located up-section (FT94-154) is partially annealed and has a bimodal track length distribution. This relationship suggests that FT94-154 lies in the zone of partial annealing, when the basinal geotherm was at a maximum.

Samples from the footwall of both sections have fission track ages that are older than the stratigraphic age of their respective formations (Fig. 3.3 and 3.4). The use of radial plotting statistical techniques shows that the footwall samples have a have significant spreads in their single grain fission track age and the certainty of these ages. The spread is so significant in several of the footwall samples that it suggests that it is possible to discern two or more different inherited fission track ages from the single track ages plotted radially (Figures 3.5a, 3.5c, and 3.6).

Figure 3.5 Radial plots of samples from the Vesley Fiord and Mt. Bridgeman sections. 3.5a) These three samples are from the footwall of the Vesley Fiord Thrust. There is significant spread in the single grain ages in samples FT94-130 and -133, indicating that there may be several discrete populations of detrital apatite in this sample. Located just below the fault contact, sample FT94-134 has a slightly tighter grouping and younger age which indicates either a younger-unimodal source area or some partial annealing related to an inverted geotherm from the fault movement. 3.5b) these samples are taken from the hangingwall at Vesley Fiord. Samples FT94-135 and 136 are both totally reset samples and represent the cooling age of the hangingwall. Sample FT94-139 has an older age and more spread than the previous samples in the hangingwall. 3.5c) Samples FT94-143, -147 and -153 are from the foot wall at Mt. Bridgeman. Sample FT94-143 is from the Bjorne Formation up section from the fault plane. There is a wide scatter in this plot indicating an unannealed sample with several source areas. Samples FT94-147 and -153 are the youngest samples obtained from the Sawtooth Range. The tight distribution and single grain ages of these samples would seem to refute the logic behind relating depth with annealing. But if they are considered in terms of the rapid collapse and closure of the Sverdrup basin, the young, unimodal distribution of the single grain ages suggest a rapidly uplifted, local source area or a discrete igneous source.
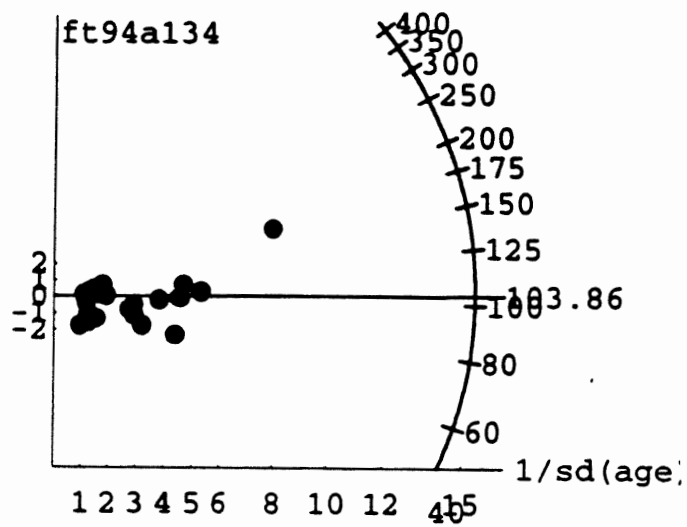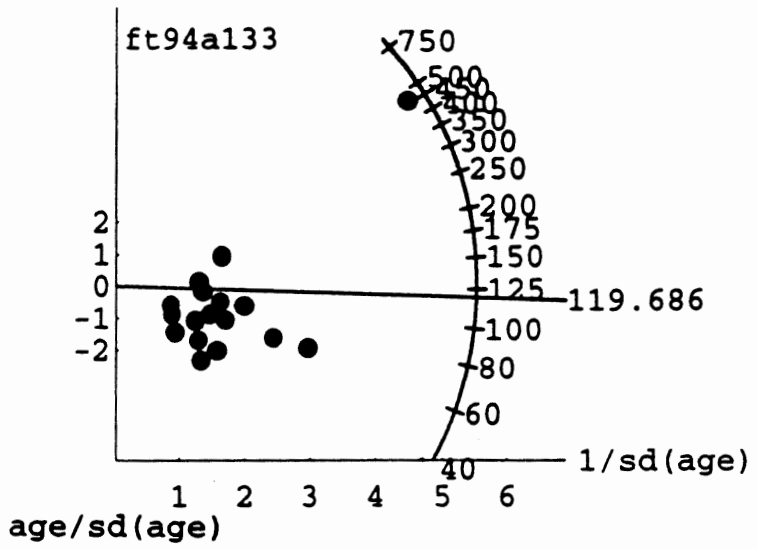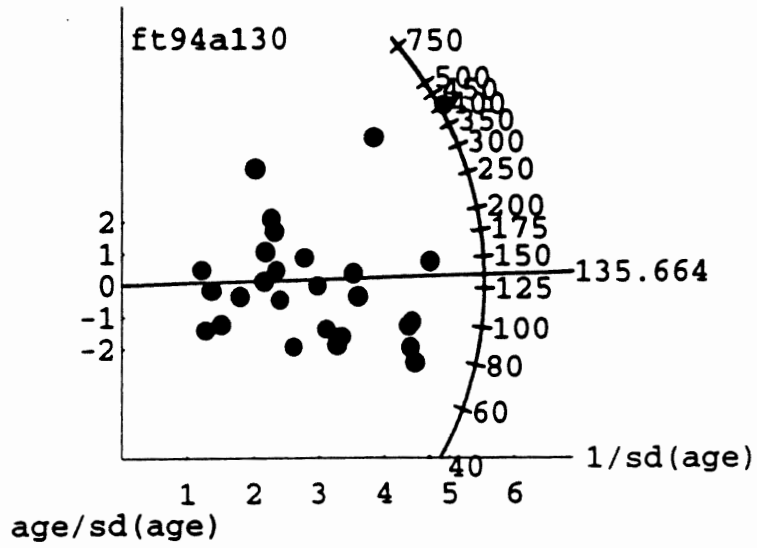
Figure 3.5a

age/sd(age)

ft94a135

1/sd(age)

44.1932

age/sd(age)

ft94a136

1/sd(age)

age/sd(age)

ft94a139

Figure 3.5b

1/sd(age)

age/sd(age)

ft94a135

age/sd(age)

ft94a136

age/sd(age)

ft94a139
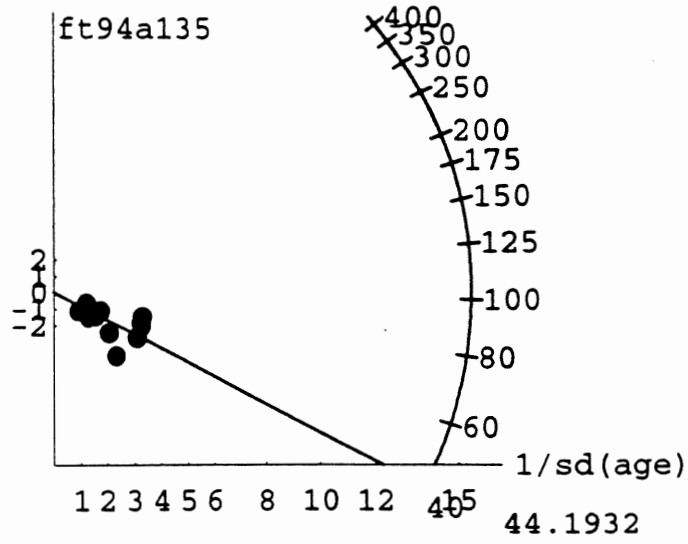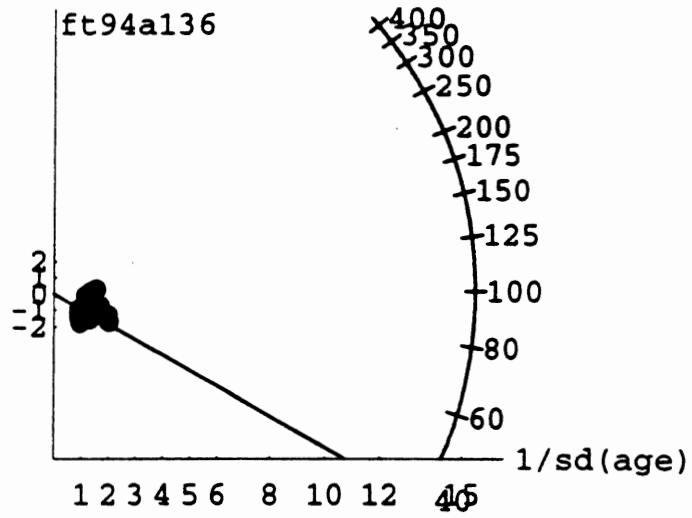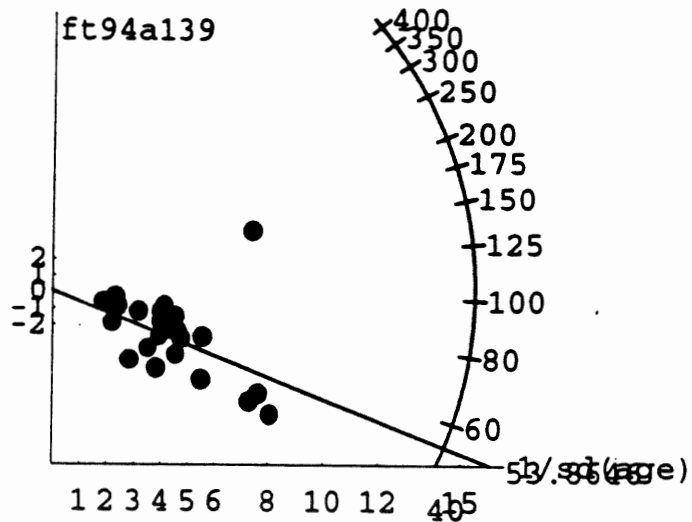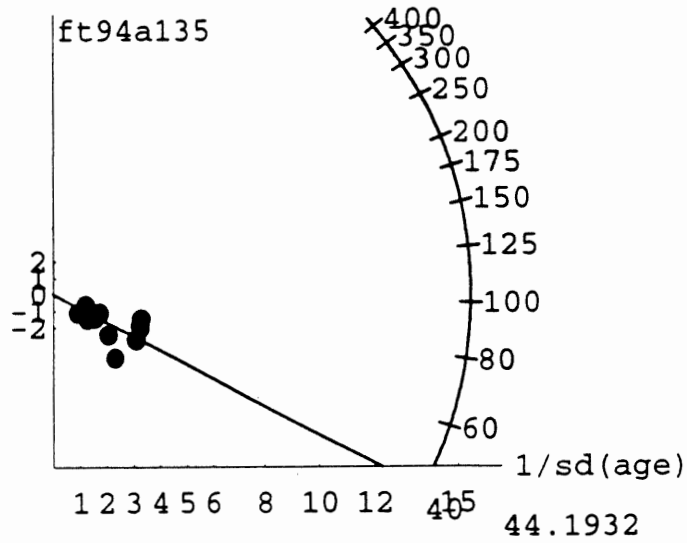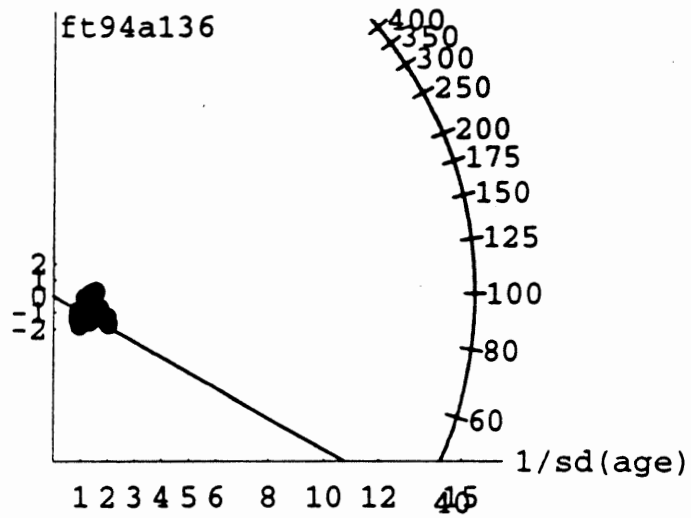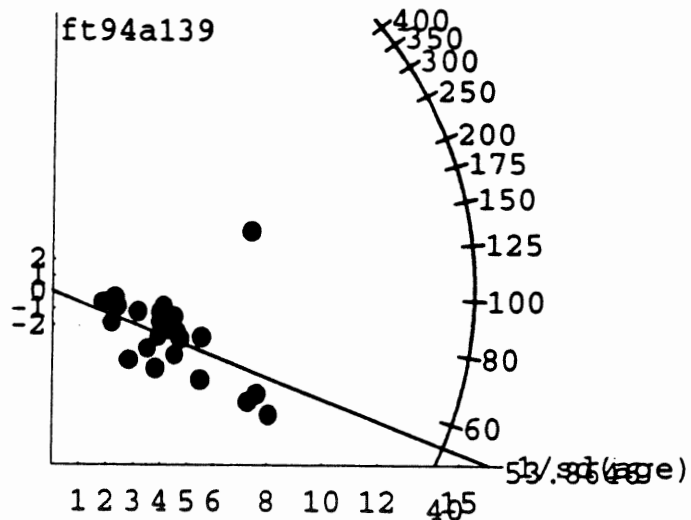
Figure 3.5c

The majority of grains in the unannealed Cretaceous and Tertiary samples have ages around 120 Ma. One small group of outliers has ages that cluster around 420 Ma. The former group, representing the majority of grains, is clearly related to the on set of the Eurekan Orogeny in the Cretaceous. The 420 Ma group was probably derived from distal outcrop that was cooled and uplifted during the Ellesmerian orogeny
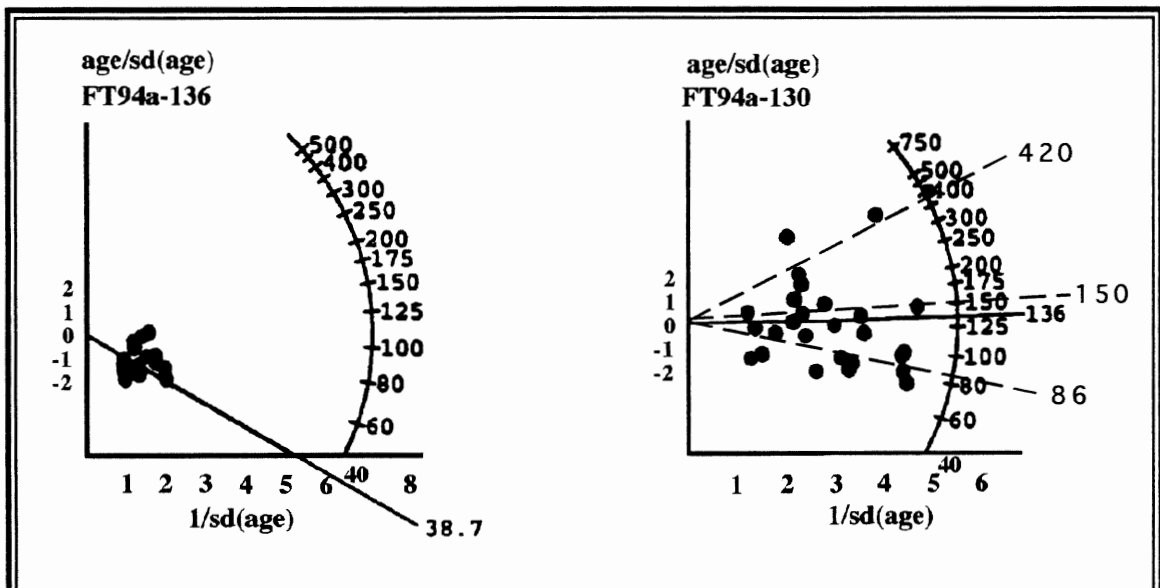
Figure 3.6 Radial plots of single grain ages. Sample FT94-136 is a totally annealed hangingwall sample and the single grain ages plot very tightly and close to the Y axis. Sample FT94-130 is a unannealed footwall sample and the single grain ages show significant spread. Dotted lines (— —)define possible populations of inherited ages that may represent different sediment sources. By definition exhumation and cooling in these sediment source areas would have occurred at 420, 150 and 86 Ma respectively.

3.4   Summary

Two measured sections in the Sawtooth Range were sampled for analysis of their thermochronology based on the apatite fission track analysis technique.   Apatite fission track dating of the two measured sections in the Sawtooth Range suggests that fault thrusting, and associated uplift and erosion, occurred in the Eocene. The thrusting dating is based on the fission track age of the first sample up-section from the fault contact. Thrusting is dated at 44±11 Ma at the Vesley Fiord section and 56±7 Ma on the East Cape Thrust at Mt. Bridgeman. Samples in the footwall sections of the Vesley Fiord Thrust have FT ages that are significantly younger than their stratigraphic age and partially or completely unannealed. Samples from the footwall of the East Cape Thrust are cover a greater stratigraphic range and range from possible partial annealing to unannealed. Radial plotting techniques allow for the disaggregation of discrete populations of inherited fission track ages in the unannealed samples and shed some light on their provenance from the perspective of the cooling history of the grain source area.

Chapter 4   Apatite Geochemistry And Provenance

4.1   Introduction

The apatite group, $(Ca_5(PO_4)_3(F, Cl, OH))$ is a solid solution group of phosphate minerals with the end member minerals fluoroapatite, chlorapatite and hydroxy-apatite. The group as a whole is generally referred to simply as apatite. Occurring as a common accessory mineral in a wide variety of igneous and metamorphic rocks, apatite has a hardness of 5 on the Mohs scale, a density of 3.15 to 3.20 and a relatively high resistance to chemical alteration or dissolution.

In addition to variation of major element composition, apatite also exhibits a wide range of rare earth element (REE) trace composition. This generally varies in relation to the REE trace composition of the magma from which the apatite crystallised. From this it follows that detrital apatite will reflect the composition of the parent magma from which it was derived. The matching of detrital samples and possible igneous or metamorphic source areas defines a possible provenance history for the sedimentary deposits involved.

4.2   Single Mineral Compositional Studies vs. Conventional Provenance Studies

As previously indicated traditionally provenance studies have been based on grain characterisation and analysis, or heavy mineral assemblages such as the Rutile-Zircon index (RZi) or Apatite-Rutile index (ATi)(Hubert, 1962). Grain shape and mineral distribution can be heavily influenced by environmentally controlled factors such as: distance of transport, pH, temperature, time in, and the energy level of transitional environments, diagenetic processes and differential sorting. The presence of specific minerals or mineral assemblages can be highly dependent on the natural occurrence of the minerals or member minerals, respectively, in suitable source areas (Force, 1980). Thus, the provenance

analysis based on indices of minerals are influenced by factors that can not always be detected or adjusted for.

Conversely by using a single mineral type for a provenance study the problems associated with natural occurrence, differential sorting and mineral dissolution or diagenesis are minimised. It is important to note that while the absence of the chosen indicator mineral indicated neither a positive nor a negative correlation of provenance it does not affect the overall results by skewing ratios or ternary plots. Conversely the absence of a component mineral in a "ratio" study may result in misleading conclusions.

Apatite ($Ca_5(PO_4)_3(F,Cl,OH)$ is well suited for single mineral compositional studies: it is formed in a wide range of igneous and metamorphic environments, apatite resists dissolution by acidic ground water, with a hardness of ~5, it is well suited to surviving the harsh abrasion of sediment transport and of great importance apatite has a wide compositional range, thus improving the chances that a discrete population will have a discrete compositional signature.

4.3   Compositional Range Of Apatite

4.3.1 Igneous apatite

Apatite forms as an accessory mineral in a wide range of igneous rocks. Work at the Dalhousie Fission Track Research Laboratory has derived apatites from igneous rocks ranging in type from granites and volcanic rocks to kimberlites and ophiolites. Igneous rocks that were analysed as a part of this study are limited to a single gabbroic dyke but igneous-derived apatite appears to constitute the majority of the detrital apatite found in the Sverdrup Basin (see 4.3.2 Metamorphic apatite).

Studies have been done on both the major ion and REE composition of igneous apatite. Studies of major ion composition focus on the solid solution of apatite between Fluoro-, Chlor- and Hydroxy-, (F,Cl,OH) apatite end-members. Literature review

(Boudreau, 1993), suggests that the composition of apatite derived from single igneous complex should plot within a discrete field (Fig. 4.1) in terms of the F, Cl, OH composition of individual grains.

Trivalent REE can easily substitute for Ca in apatite, so apatite tends to act as a concentrator of REE in melts (Muecke and Möller, 1988) and has concentration levels significantly higher than background. The affinity between apatite and REE means that the apatite REE composition will mirror the REE composition of the melt that it is derived from. Apatite can be defined as having REE compositions that are unique with respect to the melt from which it is derived. REE plots (Fig. 4.2) of igneous apatite also define discrete signatures(Punchelt and Emmermann, 1976; Dill, 1994) in relationship with the respective source magma. It should be noted that in large igneous bodies, partitioning of magma may result in unique REE compositions in relationship with the fractionation of the melt (e.g. cumulate in intrusive complexes (Boudreau, 1993)).

4.3.2 Metamorphic apatite

Metamorphic apatite is very interesting in terms of provenance studies as the processes of partial melts in high grade metamorphic terrains and supersaturated fluids tend to be highly enriched in REE and heavy metals (Muecke and Möller, 1988). REE-enriched metamorphic apatites can have unique compositional signatures (Deer et al , 1992) in terms of replacement of Ca by heavy metals such as strontium or partitioning of REE. Some metamorphic apatite has higher overall percentages REE (Muecke and Möller, 1988) as a result of melt partitioning or concentration through fluid flow. If there is no magmatic partitioning or concentration through rock/fluid interaction, the resulting metamorphic apatite will have a compositional signature that is indistinguishable from the signature of the source rock.
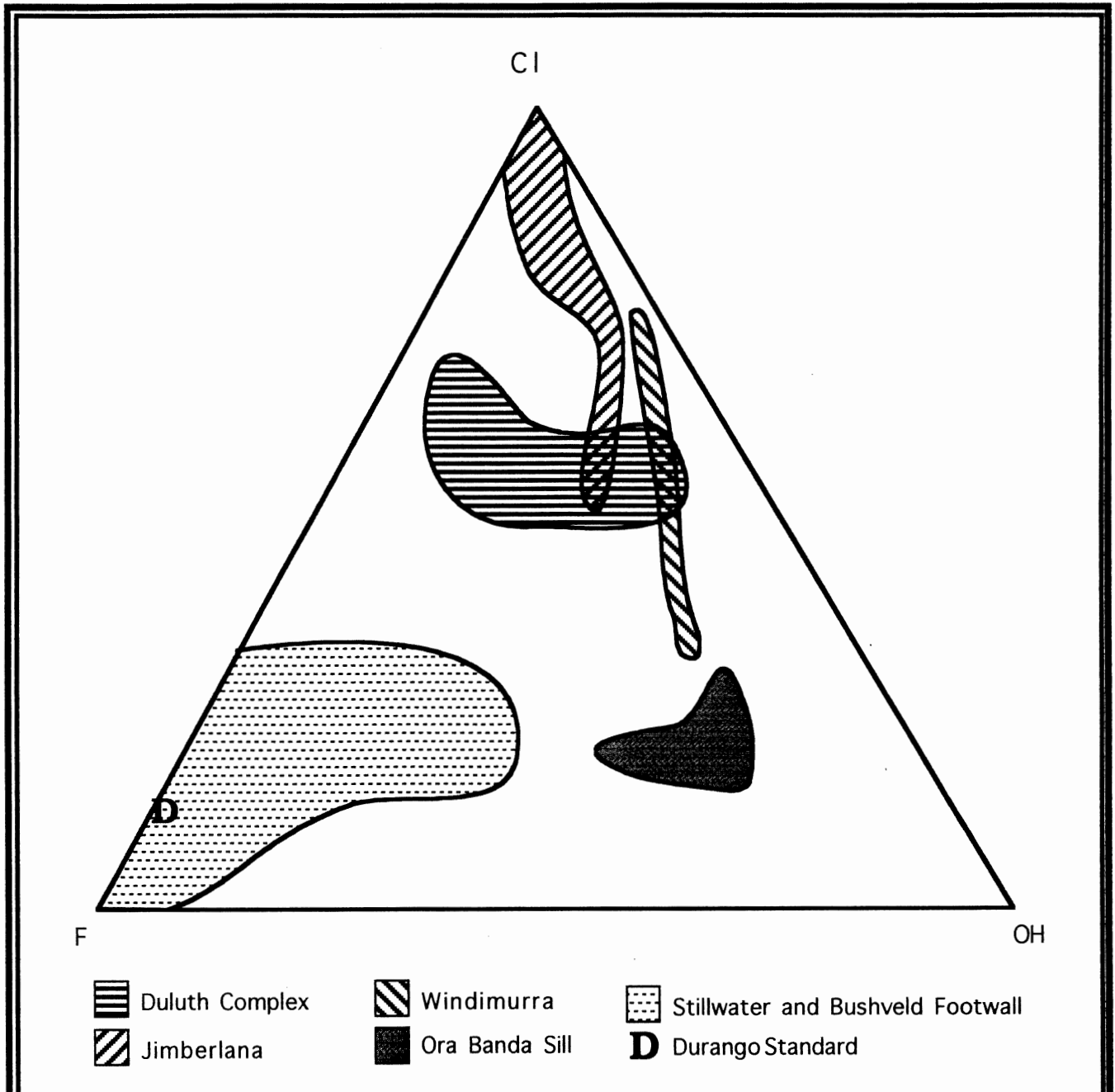
Figure 4.1 Ternary plots of the compositional range of selected apatites of igneous derivation. Apatite from different source areas plots in discrete fields. Equilateral fields, (i.e. Ore Banda Sill) may suggest hemogeneous composition in the original melt. Elongate fields, (i.e. Windimurra) suggest that compositional partitioning may have played a role in the crystallization of the intrusive complex.   (modified after Boudreau, 1993)

Figure 4.2   REE composition plot of 5 different Igneous apatites.   Each sample has a charateristic set of slopes (ratios) between element points. Although residual melts may become progressively enriched as the melt crystallizes, the ratios of REE remains the same unless melt fractionation occurs.

(modified after Punchelt and Emmermann,1976)
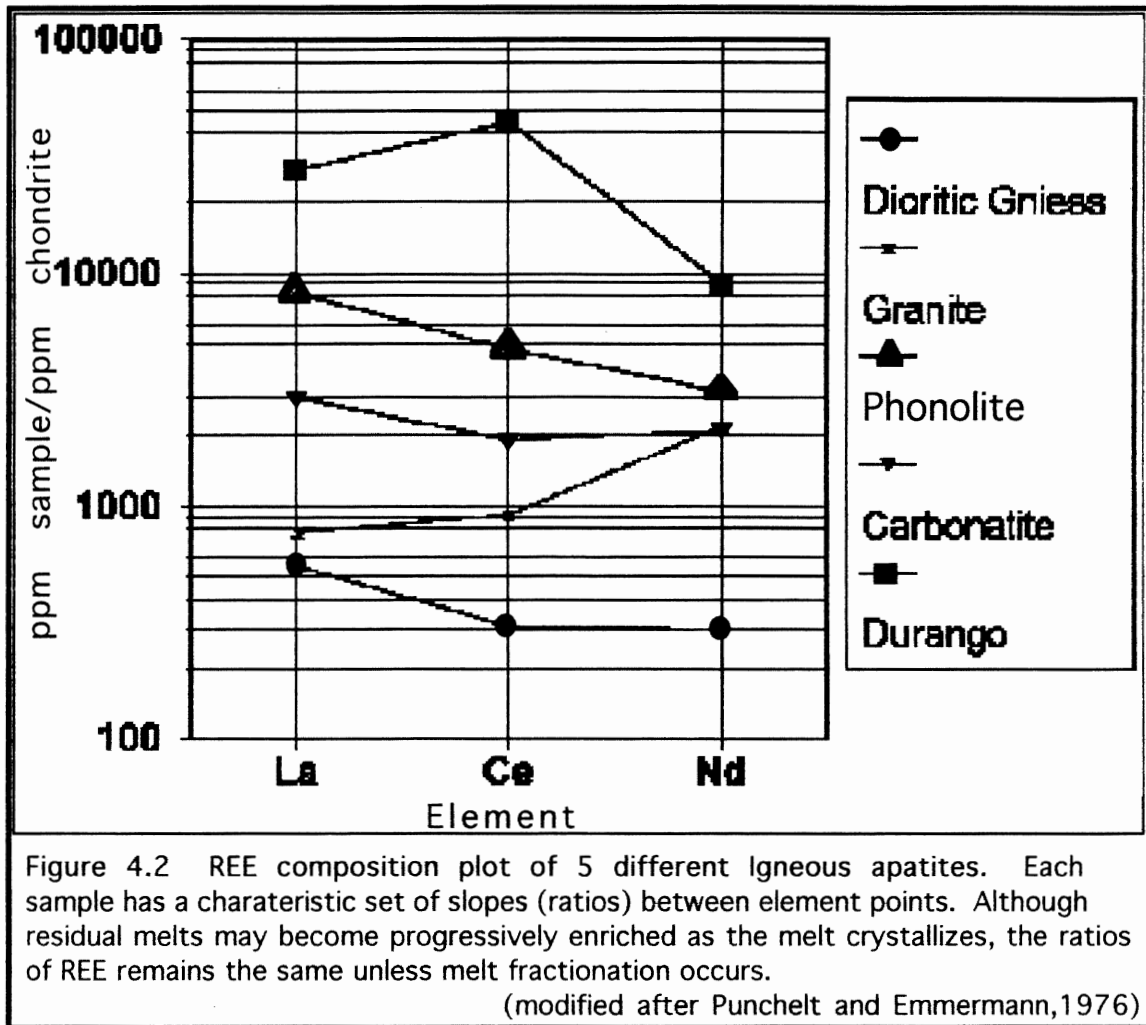
Microprobe work at Dalhousie has defined populations of Sr rich, (~2wt%) apatite in detrital samples (pers. comm. Casey Ravenhurst, Nov., 1995). This suggests that metamorphic apatite can be an important component in detrital apatite separates. Metamorphic apatite is not of significant importance in this study as the compositional range of samples is well within the range expected from apatite of igneous derivation (see appendix C).   It is probable that the gneiss in the crystalline basement of the Sverdrup Basin had igneous protoliths.

4.4   Detrital Apatite

Previous work has shown that detrital apatite can be used as an identifier of sedimentary provenance. Dill, (1994), defines depositional source areas for late Paleozoic and Triassic red bed clastic rocks in S.E. Germany by analysing detrital apatite with several techniques including REE composition. The derived data was compared with apatite REE patterns from granites, gneisses, volcanics and phosporites of NE Bavarian basement rocks (Fig. 4.1). With a conspicuous contrast in the REE patterns of the different source areas, Dill (1994) was able to define two relationships between discrete source areas and two adjacent basinal areas. This is the relationship addressed by this thesis.

4.5   Geochemistry Of Apatite From The Fosheim Peninsula and Axel Heiberg Island

4.5.1 Methods

Compositional analysis was performed at the Dalhousie Microprobe Laboratory under the supervision of Robert McKay using a JEOL 733 Superprobe with a Link-Analytical data processing package. Live probe count times were 9 and 40 seconds for the energy dispersive spectrometry (EDS) and wave detection spectrometry (WDS) respectively. The microprobe was calibrated and checked for drift with the Durango apatite standard. The precision for the EDS is $\pm 2\%$ at 1wt% of the measured element. The WDS

has significantly higher accuracy, with a precision of $\pm 3\%$ at 0.5wt% of the measured

element. Statistical analysis of ten spot analysis of the Durango standard had a standard deviation ranging from 0.02 to 0.04wt% for elements measured using the WDS. The chondrite rare earth element normalising factors are from Evensen (1978), in Taylor (1985).

The geochemical aspect of defining populations based on microprobe analysis used the WDS for trace elements, and the EDS for major element constituents. OH and CO_2 values are derived iteratively from excess oxygen assuming a 21 unit atom molecule. The primary geochemical constraint is the F-Cl-OH ternary relationship. Solid solution exists between end-member apatite crystals but populations derived from a unique melt occupy discrete areas in the ternary field (see below in Chapter 4). The secondary identifier is the relationship of chondrite normalised LREE, (La, Ce, Nd) and Y. In apatite of igneous origin, these elements exhibit unique patterns based on the melt type from which they were derived (Taylor, 1985).

Samples from the Sawtooth Range were chosen for analysis because of the stratigraphic range they covered. Four samples are grainmounts that were specially prepared and etched for fission track analysis. Ten additional grainmounts were prepared from excess apatite separates for use in the microprobe. Grainmounts for either purpose are prepared by embedding grains in catalysed epoxy and polishing the resulting puck with 600 μm grit sand paper and then with 3 μm diamond polish. The polished grainmounts are coated with carbon to close the circuit of the electron beam. The conductivity of the carbon coating is measured using a bridge to insure consistency between microprobe samples.

Each sample was surveyed prior to compositional analysis to define physical groups within the sample based on grain shape, habit and etching or corrosion characteristics. Individual grains were chosen to represent the cross section of different grain types found in any-one sample. Grains were probed between two and five times to ascertain the homogeneity of the sample and ensure the validity of the analysis of physically poor grains.

4.5.2 Samples

The analysed samples were apatite concentrates left over from the fission track analysis work. This was a major constraint on the compositional analysis study as there

was not sufficient apatite left to allow for the analysis of a full suite of samples throughout

the cross sections (Table 3.1). Of the nine samples analysed, two samples were obtained

from Dr. G. K. Muecke of Dalhousie University. These samples (Appendix E) were from

bentonite deposits in the Cretaceous Kanguk Formation on the Kanguk Peninsulas on Axel

Heiberg Island on the western edge of the Sverdrup Basin (see Fig. 2.1). While the

bentonite samples were clearly distal to the Sawtooth Range they where chosen for

analysis because they are know to be good examples of unaltered Cretaceous bentonites

(Parsons, 1994) and by inference it was hoped that the bentonites would define a

characteristic signature for Cretaceous volcanic activity that extended into the Sawtooth

region. Primary separation of these two samples was carried out by Michael Parsons

(1994) and diiodomethane (heavy liquid) separation , mounting and polishing was carried

out by the author.

4.5.3 Analytical results

Major element analysis demonstrates that apatite in the Sverdrup Basin is primarily

fluorine rich. Out of over two hundred spot analyses only three grains (Fig. 4.3, FT94-

153) were found that exceeded the chlorine content of Durango (standard) apatite, (at

0.5wt%). Six of the nine apatite separates have a compositional range that extended

between a fluorapatite end member and a intermediate fluoro-hydroxyapatite. The other 3

separates are dominantly fluoroapatite. The fluorapatite samples are all located in the

hangwall block of the Vesley Fiord Thrust, but the lack of congruencies of these samples

with others of a similar stratigraphic age as well as the long geological time span, late

Permian to early Triassic, suggests that the result was coincidence or processing error. The

composition of the samples plot over such a narrow area that it is not possible to define

distinct fields for the samples.
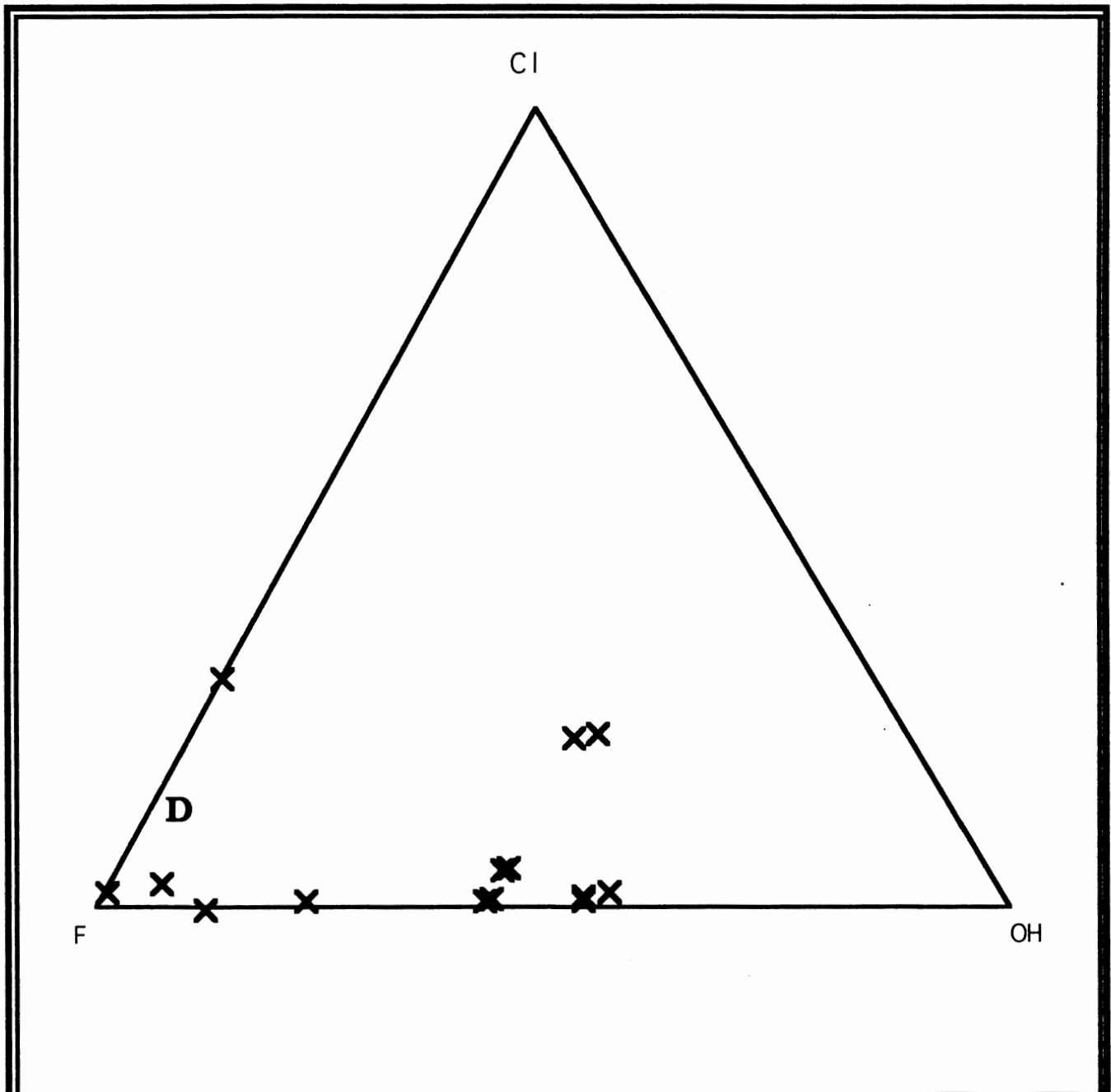
Figure 4.3   A representative sample demonstrating compositional variation in detrital apatite from the Sawtooth Range. The comosition of probed grains generally ranges between fluoro and hydroxyapatite endmembers with rare clorapatites.

Figure 4.4 ppm/chondrite normalised REE PLOT
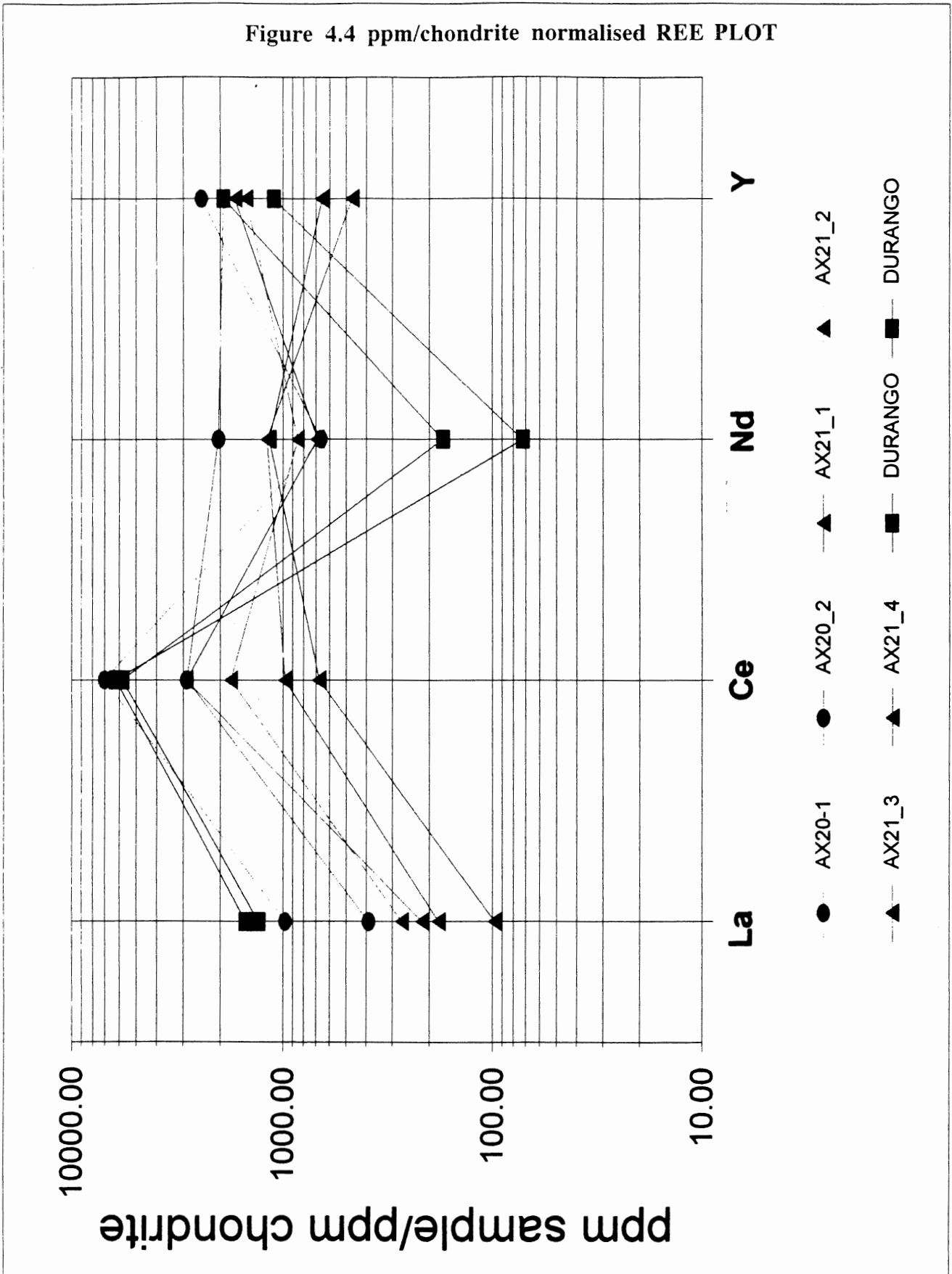
The results of REE analyses have much more scatter than expected. While the REE chondrite normalised plots for the Cretaceous bentonites have a general signature (Fig. 4.4), a gabbroic dyke (FT94-136) and the purely detrital samples do not have much uniformity or definable populations. The lack of consistency extends to the grain level as well. Some grains where probed up to five times and returned five unique analyses.

Although the compositional analysis did not prove fruitful in illuminating the questions of provenance in the Sawtooth Range. the data derived from the study was very useful in constraining the fission track model in terms of the relationship between annealing rates and compositional variation (see Chapt. 3).

4.6   Summary

Major ion composition is relatively uniform in all the samples analysed. Compositional ranges plot in a relatively narrow field between a pure fluoroapatite end-member and solid solution between fluoro- and hydroxyapatite. The limited variation in the samples made it impossible to discern different populations of apatite from whole apatite separates. The similarity of the plotted ranges of the samples does not allow for the definition of shifts in source areas, through time , based on the shifting compositional ranges.

The variation in REE suggests that there are discrete compositional populations within some of the samples. However, these unique populations within specific samples do not show any correlation with other unique populations in stratigraphically related samples. Conversely the one Cretaceous gabbroic dyke that was analysed exhibits a wide range of REE values which would suggest several phases of crystallisation. Because of the variation in the Cretaceous dyke it is not possible to use it as a signature for the para-autochthonous erosion and deposition of Cretaceous and older sediments in Tertiary formations.

Chapter 5   Discussion and Conclusions

5.1   Introduction

This study is a modest contribution to the better understanding of the timing, and style of tectonic transport and deformation of the Eurekan Orogeny. Single grain fission track analysis and compositional data provides some restrictions on the possible source of sediment in the Sverdrup Basin during the late Tertiary. Fission Track dates provide clear constraints on the timing of thrusting during the compression and collapse of the Sverdrup Basin, and this age relationship in turn, has serious implications for the hydrocarbon potential of the Sawtooth Range region.

5.2   Structural Development of the Sawtooth Range

From the sections examined the Sawtooth Range Thrusts may be considered "pure" reverse faults (Davis, 1984). Lineations, where observable, are perpendicular to the strike of the fault plane. The fault contact is a rampflat at Vesley Fiord and a footwall ramp at Mount Bridgeman. Hangingwall and footwall contacts are remarkably undeformed when considered in terms of the minimum (stratigraphic) offset. This model conflicts with the work of De Paor et al, (1989) who observed dextral transpression with significant hangingwall and footwall deformation in localities near the centre of the Sawtooth Range. This thesis work suggests that this specific style of deformation, described by De Paor et al., is only a local phenomenon and could possibly be related to changes in the nature of the basal décollement. It could be speculated that the décollement was pinned at depth in the centre section of the Sawtooth Range where it was studied by De Paor et al. (1989), whereas it moved freely in the northern and southern ends of the Sawtooth Range where work for this study was carried out.

5.3 Time of Thrusting

Compositional data indicate that fluoroapatite is predominant in samples from the Permian to the Miocene. The unimodal distribution of apatite composition indicates that the Durango (standard) based fission track model is valid in the analysis of the data. Even if the calculated error in the FT dates overlaps with the analytical uncertainty (2 sigma confidence interval), it is suggested the age difference is geologically significant. Analysis of the fission track data from the Vesley Fiord measured section constrains the maximum age of thrusting, uplift and exhumation to 44 ± 11 Ma during Eocene times (Table 3.1). This date is defined by the fission track age of the sample closest to the fault contact (FT94-134), which is the first sample to pass through the 100°C isotherm as the inverted geotherm relaxes and normalises. In the southern end of the Sawtooth Range, structural data indicate that movement was pure reverse thrust. The hangingwall and footwall appear to be undeformed except for centimetre-scale thrusts, and bedding-parallel slickenlines in the hangingwall. There is some rotation of the bedding plane (going from 30° to 45°) in the hangingwall that may be related to interbed slip.

This interpretation is supported by fission track data from the Mount Bridgeman measured section. The relationship of samples to the East Cape thrust is more distal than at Vesley Fiord, but the relationship of reset fission track ages in the hangingwall and inherited fission track ages still holds. The stratigraphic offset of the first sample (FT94-153) is 1100 m of section, plus an undetermined distance to the actual fault contact. Because of the great distance, the sample would not have cooled through the 100°C geotherm in a direct relationship to the fault movement. Even with this in mind, the hangingwall is constrained to an exhumation time of 56 ± 7 Ma, as defined by the Paleocene-Eocene fission track age of the sample (Table 3.1). This age matches

remarkably well with its stratigraphic correlative sample (both samples are located at the
bottom of the Bjorne Formation) at Vesley Fiord (FT94-139), which has a fission track age
of 56 ± 11 Ma.

The Structure of the East Cape Thrust is obscured by scree but it is recognisable as
a linear feature on air photos and from helicopter. The hangingwall and footwall blocks are
relatively undeformed in relation to the fault contact even though they are juxtaposed at high
angles. No strike-slip faults were observed on the measured sections or proximal to them
although a few deeply incised linear valleys, oriented perpendicular to the strike of the
fault, could be observed in the hangingwall block. Because no stratigraphic offset was
observed in the valleys, they may represent the physical expression of the strike-slip faults.

These two analyses of the structure of the Sawtooth Range contrast with the
analysis of De Paor et al. (1989), who delineated east-vergent thrusts and dextral wrench
faults as the main expressions of the indentation of the Greenland craton on the Sverdrup
Basin. This thesis suggests that the east-vergent thrusts and dextral wrench faults observed
by De Paor are the exception and not the rule for the closure of the Sverdrup Basin.
Another model, advocated by Oakey (1994) proposes dominance by pure reverse thrusts
and sub-perpendicular sinistral strike-slip faults. It is speculated that structural features
observed by De Paor may just be local structure related to the anomalous sub-surface
conditions or a sticky décollement.

5.4   Hydrocarbon Prospectivity

Previous hydrocarbon exploration in the north central Sverdrup Basin targeted
Tertiary structural traps. These structures formed during the Eurekan orogeny and parallel
the formation of the Sawtooth Range. Analysis of apatite fission track data from the
Sawtooth Range demonstrates that maximum basinal temperatures were reached before the
structural traps formed. This relationship is defined by the offset of fission track ages

across fault structures. If the maximum basinal temperatures post-dated thrusting the apatite fission track ages would vary in relationship with elevation as opposed to varying in terms of stratigraphic and fault plane offset.

If maximum basinal temperatures predate the formation of structural traps it is probable that hydrocarbon maturation and migration also occurred much earlier than the formation of Eocene structural traps. This would suggest that Eurekan Orogeny thrusts and faults may have served as conduits for the dispersal of hydrocarbons that had already formed rather than traps for maturing hydrocarbons. This relationship explains, in part the rather disappointing results of expensive oil exploration in the northeast part of the Sverdrup Basin.

5.5   Sediment source areas

The homogeneity of the compositional data makes it impossible to identify any specific shifts in source areas based on either the major ion data or the REE. Decomposition of inherited fission track age data, from detrital samples, into single age radial plots does suggests that Cretaceous strata were being eroded from advancing thrust-related uplands and subsequently redeposited within the Sverdrup Basin in the Eocene. The analysis of radially plotted fission track age dates promises to become a valuable tool in provenance analysis.

5.6   Conclusions

The main conclusions of this thesis are:

1)   The large scale uplift and exhumation on the Vesley Fiord Fault has a maximum age of 44±11 Ma. Thrusting on the East Cape Thrust, at Mt. Bridgeman is constrained to a maximum age of 56±7 Ma.

2)   At the Vesley Fiord field location the movement on the Vesley Fiord Fault was

        observed to be pure reverse thrusting.

3)   Oil maturation in Cretaceous source rocks predates the formation of structural traps

        in the Sawtooth Range.

4)   Radial plots of single grain fission track ages have excellent potential for

        differentiating populations of apatite grains with discrete age groupings and this

        information can be useful for provenance studies.

5.7   Unanswered Questions: Future Work

        The Eureka Orogeny is a unusual orogeny in that it does not have a foreland basin,

and thrusting verges towards the orogenic highlands on the eastern edge of the Sverdrup

Basin. The strike of these verging thrust faults in the basin generally have a northeast-

southwest orientation and are controlled by the a single compressive event oriented at 67°

west of north (Oakey, 1994). This study constrains the timing of thrusting on the Vesley

Fiord and East Cape Thrusts in the Sawtooth Range. By extending the study to major

thrusts belts to the east and west of the Sawtooth Range; the Parrish and Stolze Thrust

Belts, respectively, would define the order of propagation of thrusting and deformation in

the central Sverdrup Basin. This information would allow for the development of a more

comprehensive model of the closure of the Sverdrup Basin.

        This thesis shows that there is not a clear linkage between apatite composition and

provenance in the central Sverdrup Basin. However, given the ability to discern discrete

populations of unannealed apatite grains in detrital samples it would be interesting to test if

populations of single grain ages could be related to fission track models of potential source

areas. The development of apatite fission track models could also shed light on the

kinematics in the collisional belt to the east where compressional action of the Eurekan orogeny started.

Future work in combined fission track and provenance studies should cross-reference grains analysed for fission track data with grains that are microprobed for compositional data. Cross-referencing would match the coordinant system in the FT microscope stage with the coordinate system in the microprobe. The cross-referencing of grains would remove any bias in the selection of grains for microprobe work, thus ensuring that a representative cross section of grains are analysed and allow for single grain fission track ages to be cross-referenced with compositional data. The cross referencing on a grain level provides a higher level of certainty in the meaning of any compositional variation. Cross referencing allows for more exact modelling in cases where a fraction of a sample exceeds the compositional limitations of the apatite model being used.

REFERENCES

Andriessen, P. A. M. (1995). Fission-track analysis: principles, methodology and implications for tectono-thermal histories of sedimentary basins, orogenic belts and continental margins. Geologie en Mijnbouw, v74, pp. 1-12.

Arne, D. C. & Zentilli, M., (1994) Apatite fission track thermochronology integrated with vitrinite reflectance- a review; Reevaluation of Vitrinite Reflectance as a Maturity Parameter: Applications and limitations. American Chemical Society, pp. 249-268

Arne, D. C. (1995). Dalhousie University Fission Track Research Laboratory Report 94-5:Apatite Fission Track Analysis of 33 well samples from the Canadian Arctic Archipelago (open file report No. Geological Survey of Canada).

Bellemans, F., De Corte, F., Van den haute, P. (1993) Suitablity of SRM and CN glasses as netron fluence monitors in FT dating: in Benton, E.V., McKeever, S.W.S., Omar, G.I. & Giegengack, R. (eds.) Nuclear Tracks and Radiation Measurements. v21, pp.624

Boudreau, A. E. (1993). Chlorine as an exploration guide for the platinum-group elements in layered intrusions. Journal of Geochemical Exploration, v48, pp.21-37.

Carlson, W.D. (1990) Mechanisms and kinetics of apatite fission track annealing. American Mineralogist. v75, nos 9 & 10, pp.1120-1139

Christie, R. L., & Dawes, P. R. (1991). Geography and Geological Exploration, Chapter 2 in. In H. P. Trettin (Ed.), Geology of the Innuitian Orogen and Arctic Platform of Canada and Greenland Geological Survey of Canada.

Davies, G. R., & Nassichuk, W. W. (1991). Carboniferous and Permian History of the Sverdrup Basin, Arctic Islands, Chapter 13 in. In H. P. Trettin (Ed.), Geology of the Innuitian Orogen and Arctic Platform of Canada and Greenland Geological Survey of Canada.

Davis, H.G. (1984) Chapter 9: in Structural Geology of Rocks and Regions. (John Whiley & Sons: New York), pp.261-324

Deer, W.A., Howie, R.A., & Zussman, J. (1992) Rock Forming Minerals 2nd edition (John Whiley &Sons: New York), pp. 507-509

De Paor, D. C., Bradley, D. C., Eisenstadt, G., & Phillips, S. M. (1989). The Arctic Eurekan orogen: A most unusual fold-and-thrust belt. Geological Society of America Bulletin, v101, pp. 952-967.

Dill, H. G. (1994). Can REE patterns and U-TH variations be used as a tool to determine the origin of Apatite in clastic rocks? Sedimentary Geology, v92, pp. 175-196.

Donelick, R.A. (1988) Model time-temperature paths from apatite fission track age and confined track length measurements: Chapter 4 in Donelick, R.A. <u>Etchable fission track length reduction in apatite: experimental observations, theory and geological applications</u>. Unpublished Ph.D. thesis, Rensselaer Polytechnic Institute, Truy, New York. pp.186 -288

Embry, A. F. (1991). Mesozoic History of the Arctic Islands: Chapter 14 in. In T. H.P. (Ed.), <u>Geology of the Innuitian Orogen and Arctic Platform of Canada and Greenland</u> Geological Survey of Canada.

Embry, A. F. (1992). Crockerland -the northwest source area for the Sverdrup Basin, Canadian Arctic Islands. In T. O. Vorren, E. Bergsager, O. A. Dahl-Stamnes, E. Holter, E. Johnansen, E. Lie, & T. B. Lund (Eds.), <u>Arctic Geology and Petroleum Potential</u> (Elsevier: Amsterdam). pp. 205-216

Embry, A. F. (1993). Transgressive-regressive (T-R) sequence analysis of the Jurassic succession of the Sverdrup Basin, Canadian Arctic Archipelago. <u>Canadian Journal of Earth Sciences</u>, v30, pp.301-320.

Evensen, M.N. et al. (1978) For type 1 chondrites. <u>Geological Association of America Bulletin</u>. v42, p.1203

Fortier, Y.O., McNair, A.H. & Thorsteinsson, R., (1950) Geology and petroleum possiblities in the Canadian Arctic Islands. <u>Bulletin of the Americam Association of Petroleum Geologists</u>, v38, pp.2075-2109

Force, E.R., (1980) The Provenance of Rutile. <u>Journal of Sedimentary Petrology</u>. v50, pp.485-488

Galbraith, R.F. (1990) The radial plot: graphical assessment of spread in ages. <u>Nuclear Tracks and radiation Measurement</u>, v17, pp.207-214

Green, P.F., Duddy, I.R., Gleadow, A.J., Tingate, P.R., & Laslett, G.M. (1986). Thermal annealing of fission tracks in apatite: 1. A qualitative description. <u>Chemical Geology.(Isotope Geoscience Section)</u>. v59, pp.237-253

Grist, A.M., & Collins, M. (1996) Dalhousie University Fission Track Laboratory Report 96-2: Phase 3 of the Sverdrup Basin fission track study: Analysis of 35 outcrop samples from the central Ellesmere Island. Report prepared for the Institute of Sedimentary and Petroleum Geology, Geological Survey of Canada, Calgary.

Hubert, J. F. (1962). A Zircon-Tourmaline-Rutile Maturity index and interdependence of the composition of heavy mineral assemblages with the gross composition and texture of sandstones. <u>Journal of Sedimentary Petrology</u>, v32, pp. 440-450.

Hurford, A.J., & Green, P.F. (1982). A users guide to fission track dating calibration. <u>Earth and Planetary Science Letters</u>, v59, pp.343-3554

Huford, A.J., & Green, P.F. (1983). The zeta age calibration of fission track dating. <u>Isotope Geoscience</u>. v1, pp.285-317

Laslett, G.M., Green, I.R., and Gledow, A.J.W., (1987). Thermal annealing of fission tracks in apatite 2. A quantitative analysis: Chemical Geology (Isotope Geoscience Section). v65, pp.1-13

Morton, A. C. (1985). A new approach to provenance studies: electron probe analysis of detrital garnets from Middle Jurassic sandstones of the northern North Sea. Sedimentology, v32, pp. 553-566.

Morton, A. C. (1991). Geochemical studies of detrital heavy minerals and their application to provenance research. In A. C. Morton, S. P. Todd, & P. D. W. Hauton (Eds.), Developements in Sedimentary Provenance Studies (pp. 31-45). Geological Society Special Pubication.

Morton, A. C., & Hallsworth, C., (1994). Identifying provenance-specific features of detrital heavy mineral assemblages in sandstones. Sedimentary Geology, v90, pp. 241 -256.

Muecke, G.K., & Moller, P. (1988) The not-so-rare earths. Scientific American, v256, pp. 72-77

Oakey, G. (1994) A structural fabric defined by topographic lineaments: Correlation with Tertiary deformation of Ellesmere and Axel Heiberg Islands, Canadian Arctic. Journal of Geophysical Research. v99, pp.20,311-2,021

Okulitch, A. V. (1995). Geological time scale. (open File 3040, Geological Survey of Canada).

Parsons, M. (1994) Geochemistry and Petrogenesis Of Late Cretaceous Bentonites From The Kanguk Formation,Axel Heiberg and Ellesmere Islands, Canadian High Arctic. Thesis, B.Sc. Honours,Dahousie University.

Punchelt, H., & Emmermann, R., (1976). Bearing of Rare Earth patterns of Apatite from Igneous and Metamorphic rocks. Earth and Planetary Science Letters, v31, pp.279-286.

Ravenhurst, C. E., & Donelick, R. A. (1992). Fission track Thermolchronology. In M. Zentilli & P. H. Reynolds (eds.), Short Course Handboook on Low Temperature Thermochronology. Mineralogical Association of Canada. (pp. 21-43)

Ricketts, B. D. (1994). Basin Analysis, Eureka Sound Group, Axel Heiberg and Ellesmere Islands, Canadian Arctic Archipelago. Geological Survey of Canada.

Ricketts, B. D., & Stephenson, R. A. (1994). The demise of the Sverdrup Basin: Late Cretateous-Paleogene Sequence Stratigraphy and Forward Modeling. Journal of Sedimentary Research, B64(4), 516-530.

Taylor, S. R., & McLennan, S. M. (1985). The Continental Crust: its Composition and Evolution. (Blackwell Scientific Publications: Oxford)

Trettin, H. P. (1991a). Geology of the Innuitian Orogeny, and Arctic Platform of Canada and Greenland. Geological Survey of Geology.

Trettin, H. P. (1991b). Tectonic Framework; Chapter 4 in. In Trettin (Ed.), in Current Research, Part A. Geological Survey of Canada. (pp. 59-67)

Willett, S.D. (1992). Modeling thermal annealing of fissiontracks in apatite: in M. Zentilli & P. H. Reynolds (eds.), <u>Short Course Handboook on Low Temperature Thermochronology</u>. Mineralogical Association of Canada. v20, pp.43-72

Appendix A

Sample Log

FT Lab#	Sample#	STN#	REGION	Formation Sampled	Lithology	Structural Position	UTM coordinates
FT94-130	DA94-74	34	S. Sawtooth R.	Christopher Fm.	Siltstone	Footwall to Vesle Fiord Thrust Fault	4-40-230E 17 89-99-615N
	DA94-75	35	S. Sawtooth R.	Upper Christopher Fm.	Shale	Footwall to Vesle Fiord Thrust Fault	4-39-875E 17 87-99-807N
FT94-131	DA94-76	36	S. Sawtooth R.	Upper Hassel Fm.	Sandstone	Footwall to Vesle Fiord Thrust Fault	4-39-719E 17 87-99-889N
	DA94-77	36	S. Sawtooth R.	Lr Kanguk Fm. (77A mineraliz Shale	Footwall to Vesle Fiord Thrust Fault	4-39-719E 17 87-99-889N
FT94-132	DA94-78	37	S. Sawtooth R.	Mount Bell Fm.	Sandstone	Footwall to Vesle Fiord Thrust Fault	4-39-194E 17 80-00-298N
	DA94-79	38	S. Sawtooth R.	Mount Lawson Fm.	Shale	Footwall to Vesle Fiord Thrust Fault	4-38-861E 17 88-00-556N
FT94-133	DA94-80	39	S. Sawtooth R.	Mount Lawson Fm.	Sandstone	Footwall to Vesle Fiord Thrust Fault	4-38-505E 17 88-00-874N
	DA94-81	39	S. Sawtooth R.	Mount Lawson Fm.	Coal	Footwall to Vesle Fiord Thrust Fault	4-38-505E 17 88-00-874N
FT94-134	DA94-82	40	S. Sawtooth R.	Mount Lawson Fm.	Sandstone	Footwall to Vesle Fiord Thrust Fault	4-38-126E 17 88-01-251N
	DA94-83	40	S. Sawtooth R.	Mount Lawson Fm.	Coal	Footwall to Vesle Fiord Thrust Fault	4-38-126E 17 88-01-251N
FT94-135	DA94-84	41	S. Sawtooth R.	Assistance Fm.	Sandstone	Hangingwall to Vesle Fiord Thrust Fault	4-37-884E 17 88-01-529N
FT94-136	DA94-85	42	S. Sawtooth R.	Mafic dyke in Assistance Fm.	Gabbro	Hangingwall to Vesle Fiord Thrust Fault	4-37-769E 17 88-01-936N
FT94-137	DA94-86	42	S. Sawtooth R.	Assistance Fm. mafic dyke	Sandstone	Hangingwall to Vesle Fiord Thrust Fault	4-37-769E 17 88-01-936N
FT94-138	DA94-87	43	S. Sawtooth R.	Trold Fiord Fm.	Siltstone	Hangingwall to Vesle Fiord Thrust Fault	5-61-795E 16 88-02-196N
FT94-139	DA94-88	44	S. Sawtooth R.	Lower Bjorne Fm.	Sandstone	Hangingwall to Vesle Fiord Thrust Fault	5-61-458E 16 88-02-277N
	DA94-89	45	NE Sawtooth R.	Chilled margin of mafic sill	Gabbro	Hangingwall to East Cape Thrust Fault	4-66-879E 17 88-71-710N
FT94-140	DA94-90	45	NE Sawtooth R.	Bjorne Fm.	Sandstone	Hangingwall to East Cape Thrust Fault	4-66-879E 17 88-71-710N
FT94-141	DA94-91	46	NE Sawtooth R.	Assistance Fm.	Siltstone	Hangingwall to East Cape Thrust Fault	4-67-405E 17 88-70-504N
FT94-142	DA94-92	47	NE Sawtooth R.	Sabine Fm.	Sandstone	Hangingwall to East Cape Thrust Fault	4-68-285E 17 88-70-059N
FT94-143	DA94-93	48	NE Sawtooth R.	Bjorne Fm.	Sandstone	Footwall to East Cape Thrust Fault	4-69-831E 17 88-70-921N
	DA94-94	49	NE Sawtooth R.	Cape Caledonia Fm.	Shale	Footwall to East Cape Thrust Fault	4-69-917E 17 88-70-942N
FT94-144	DA94-95	50	NE Sawtooth R.	Pat Bay Fm.	Sandstone	Footwall to East Cape Thrust Fault	4-70-161E 17 88-70-841N
	DA94-96	51	NE Sawtooth R.	Barrow Fm.	Shale	Footwall to East Cape Thrust Fault	4-70-222E 17 88-70-850N
FT94-145	DA94-97	52	NE Sawtooth R.	Awingak Fm.	Conglomerate	Footwall to East Cape Thrust Fault	4-70-606E 17 88-70-891N
	DA94-98	52	NE Sawtooth R.	Upper Heiberg Fm.	Coal	Footwall to East Cape Thrust Fault	4-70-606E 17 88-70-891N
FT94-146	DA94-99	53	NE Sawtooth R.	Christopher or Kanguk Fm.	Sandstone	Footwall to East Cape Thrust Fault	4-71-235E 17 88-71-017N
FT94-147	DA94-100	54	NE Sawtooth R.	Mount Lawson Fm.	Sandstone	Footwall syncline	4-71-770E 17 88-70-822N
	DA94-101	54	NE Sawtooth R.	Mount Lawson Fm.	Coal	Footwall syncline	4-71-770E 17 88-70-822N
FT94-148	DA94-102	55	NE Sawtooth R.	Mount Lawson Fm.	Sandstone	Footwall syncline	4-73-604E 17 88-70-581N
	DA94-103	55	NE Sawtooth R.	Mount Lawson Fm.	Coal	Footwall syncline	4-73-604E 17 88-70-581N

Appendix B

Vesley Fiord Measurements

FT LAB NUMBER	SAMPLE NUMBER	STATION NUMBER	Horizontal Distance	THICKNESS SECT.	Total	ELEVATION CHANGE	Total.	GPS	ALTIM	Location (UTM)	DISTANCE section	total	Chain Angle	Trend Cor.	COS of DIST.	Ttl. HOZ Dist.
										Section on west side of Mount Bridgeman in the hanging wall of the East Cape Thrust						
										All measurements in Metres and degrees						
							80									
FT94-130	DA94-074	34	48.5	22	22	4.36	84	146	75	4-40-230 89-99-615N	50	50	5	0.97437	0.99619	49
	LEG#1		97.3	22	44	0.00	84				50	100	0	0.97437	1.00000	97
			146.0	22	66	0.00	84				50	150	0	0.97437	1.00000	146
			194.5	22	88	-4.36	80				50	200	-5	0.97437	0.99619	195
			243.2	22	110	-1.74	78				50	250	-2	0.97437	0.99939	243
			291.2	22	132	8.68	87				50	300	10	0.97437	0.98481	291
			338.6	22	154	11.25	98				50	350	13	0.97437	0.97437	339
	DA94-75	35	387.2	24	178	3.49	102	196	100	4-39-875E 17 87-99-207N	50	400	4	0.97437	0.99756	387
			435.4	24	202	7.82	109				50	450	9	0.97437	0.98769	435
			484.0	24	226	3.49	113				50	500	4	0.97437	0.99756	484
FT94-131	DA94-76	36	532.4	34	260	5.23	118	397	160	4-39-719E 17 87-99-889N	50	550	6	0.97437	0.99452	532
	leg 2		582.0	34	295	-6.09	112				50	600	-7	1	0.99255	582
			631.6	34	329	6.96	119				50	650	8	1	0.99027	632
			675.6	31	360	9.36	128				45	695	12	1	0.97815	676
			725.4	35	394	4.36	133				50	745	5	1	0.99619	725
			775.2	35	429	4.36	137				50	795	5	1	0.99619	775
			830.0	38	467	-4.79	132				55	850	-5	1	0.99619	830
			879.6	34	501	6.09	138				50	900	7	1	0.99255	880
			929.5	35	536	-3.49	135				50	950	-4	1	0.99756	929
			948.5	13	549	6.18	141				20	970	18	1	0.95106	949
			998.4	35	584	3.49	145				50	1020	4	1	0.99756	998
			1056.6	40	624	14.52	159				60	1080	14	1	0.97030	1057
			1111.1	38	662	7.65	167				55	1135	8	1	0.99027	1111
			1160.3	34	696	8.68	175				50	1185	10	1	0.98481	1160
FT94-132		37	1209.5	28	724	8.68	184	315	250		50	1235	10	1	0.98481	1210
	leg 3		1258.5	28	753	5.23	189				50	1285	6	0.984808	0.99452	1259
			1307.6	28	781	4.36	194				50	1335	5	0.984808	0.99619	1308
			1356.7	28	809	3.49	197				50	1385	4	0.984808	0.99756	1357
			1405.8	28	837	3.49	201				50	1435	4	0.984808	0.99756	1406
			1455.0	28	865	2.62	203				50	1485	3	0.984808	0.99863	1455
			1504.2	28	893	2.62	206				50	1535	3	0.984808	0.99863	1504
			1528.5	14	907	3.48	209				25	1560	8	0.984808	0.99027	1529
			1553.2	14	922	0.00	209				25	1585		0.984808	1.00000	1553
			1602.4	28	950	0.00	209				50	1635		0.984808	1.00000	1602
			1651.6	28	978	0.00	209				50	1685		0.984808	1.00000	1652
	day2 leg4		1701.6	29	1007	2.62	212				50	1735	3	1	0.99863	1702
			1751.4	29	1035	4.36	216				50	1785	5	1	0.99619	1751
		38	1779.4	14	1049	0.98	217	216	270		28	1813	2	1	0.99939	1779
			1801.3	11	1060	0.77	218				22	1835	2	1	0.99939	1801

FT LAB NUMBER	SAMPLE NUMBER	STATION NUMBER	Horizontal Distance	THICKNESS SECT.	THICKNESS Total	ELEVATION CHANGE	ELEVATION Total	GPS	ALTIM	Location (UTM)	DISTANCE section	DISTANCE total	Chain Angle	Trend Cor.	COS of DIST.	Ttl. HOZ Dist.
			1850.9	25	1085	6.96	225				50	1885	8	1	0.99027	1851
			1900.7	25	1110	3.49	229				50	1935	4	1	0.99756	1901
			1950.7	25	1135	2.62	231				50	1985	3	1	0.99863	1951
			2000.6	25	1160	2.62	234				50	2035	3	1	0.99863	2001
			2050.5	25	1185	3.49	237				50	2085	4	1	0.99756	2050
			2100.5	25	1210	1.74	239				50	2135	2	1	0.99939	2100
			2150.3	25	1235	3.49	243				50	2185	4	1	0.99756	2150
			2200.3	25	1260	2.62	245				50	2235	3	1	0.99863	2200
			2250.0	25	1285	5.23	250				50	2285	6	1	0.99452	2250
FT94-133		39	2299.5	21	1305	5.23	256				50	2335	6	0.996195	0.99452	2300
			2348.7	21	1326	7.82	263	321	350		50	2385	9	0.996195	0.98769	2349
			2398.2	21	1347	6.09	270				50	2435	7	0.996195	0.99255	2398
			2443.0	19	1366	0.79	270				45	2480	1	0.996195	0.99985	2443
			2496.9	23	1389	9.55	280				55	2535	10	0.996195	0.98481	2497
			2546.6	21	1410	3.49	283				50	2585	4	0.996195	0.99756	2547
			2596.0	21	1431	6.96	290				50	2635	8	0.996195	0.99027	2596
			2645.6	21	1452	3.49	294				50	2685	4	0.996195	0.99756	2646
FT94-134	DA94-82	40	2695.5	29	1480	0.00	294	392	375		50	2735	0	0.996195	1.00000	2695
			2742.0	27	1507	-4.91	289				47	2782	-6	0.996195	0.99452	2742
			2794.5	30	1537	5.54	294				53	2835	6	0.996195	0.99452	2795
			2844.1	28	1566	5.23	300				50	2885	6	0.996195	0.99452	2844
			2893.7	29	1594	3.49	303				50	2935	4	0.996195	0.99756	2894
			2943.4	28	1623	4.36	308				50	2985	5	0.996195	0.99619	2943
			2992.4	28	1651	8.68	316				50	3035	10	0.996195	0.98481	2992
		leg5	3038.4	26	1677	0.00	316				50	3085	0	0.920505	1.00000	3038
FT94-135	DA94-84	41	3084.2	24	1701	5.23	321	289	400		50	3135	6	0.920505	0.99452	3084
			3129.4	24	1725	9.54	331				50	3185	11	0.920505	0.98163	3129
			3175.0	24	1749	6.96	338				50	3235	8	0.920505	0.99027	3175
			3220.6	24	1774	6.96	345				50	3285	8	0.920505	0.99027	3221
			3265.9	24	1798	8.68	354				50	3335	10	0.920505	0.98481	3266
FT94-136	DA94-85		3275.0	5	1802	1.56	355				10	3345	9	0.920505	0.98769	3275
FT94-137	DA94-86	42	3311.3	19	1822	6.26	361	438	430		40	3385	9	0.920505	0.98769	3311
			3357.3	24	1846	2.62	364				50	3435	3	0.920505	0.99863	3357
		leg6	3407.0	21	1867	3.49	367				50	3485	4	0.996195	0.99756	3407
			3456.0	21	1888	8.68	376				50	3535	10	0.996195	0.98481	3456
			3504.2	20	1908	12.94	389				50	3585	15	0.996195	0.96593	3504
			3552.3	20	1928	12.94	402				50	3635	15	0.996195	0.96593	3552
			3600.4	20	1949	12.94	415				50	3685	15	0.996195	0.96593	3600
			3649.4	21	1970	8.68	424				50	3735	10	0.996195	0.98481	3649
			3699.1	21	1990	4.36	428				50	3785	5	0.996195	0.99619	3699
			3748.5	21	2011	6.09	434				50	3835	7	0.996195	0.99255	3748
			3797.8	21	2032	6.96	441				50	3885	8	0.996195	0.99027	3798

FT LAB NUMBER	SAMPLE NUMBER	STATION NUMBER	Horizontal Distance	THICKNESS SECT.	Total	ELEVATION CHANGE	Total.	GPS	ALTIM	Location (UTM)	DISTANCE section	total	Chain Angle	Trend Cor.	COS of DIST.	Ttl. HOZ Dist.
		leg7	3844.5	20	2052	12.94	454				50	3935	15	0.965926	0.96593	3844
FT94-138	DA94-86	leg8, stn.	3890.7	20	2071	14.62	469	433	440		50	3985	17	0.965926	0.95630	3891
			3935.4	19	2090	18.73	487				50	4035	22	0.965926	0.92718	3935
			3979.6	19	2109	20.34	508				50	4085	24	0.965926	0.91355	3980
			4023.7	19	2128	20.34	528				50	4135	24	0.965926	0.91355	4024
			4068.8	19	2147	17.92	546				50	4185	21	0.965926	0.93358	4069
			4112.5	18	2165	21.13	567				50	4235	25	0.965926	0.90631	4113
			4156.3	18	2184	21.13	588				50	4285	25	0.965926	0.90631	4156
FT94-139	DA94-88	44	4190.7	15	2198	18.16	606	596	675	5-61-458E 16-88-02-277N	40	4325	27	0.965926	0.89101	4191

FT LAB	Bedding		Stratigraphy		Trend
NUMBER	Plunge	Dip	N of B Ang	Sin of Ch.	Angle
FT94-130	27	25	0.45399	0.087156	30
	27	25	0.45399	0	30
	27	25	0.45399	0	30
	27	25	0.45399	-0.08716	30
	27	25	0.45399	-0.0349	30
	27	25	0.45399	0.173648	30
	27	25	0.45399	0.224951	30
	30	20	0.5	0.069756	30
	30	20	0.5	0.156434	30
	30	20	0.5	0.069756	30
FT94-131	44	17	0.69466	0.104528	30
	44	17	0.69466	-0.12187	35
	44	17	0.69466	0.139173	35
	44	17	0.69466	0.207912	35
	44	17	0.69466	0.087156	35
	44	17	0.69466	0.087156	35
	44	17	0.69466	-0.08716	35
	44	17	0.69466	0.121869	35
	44	17	0.69466	-0.06976	35
	44	17	0.69466	0.309017	35
	44	17	0.69466	0.069756	35
	44	17	0.69466	0.241922	35
	44	17	0.69466	0.139173	35
	44	17	0.69466	0.173648	35
FT94-132	35	20	0.57358	0.173648	35
	35	20	0.57358	0.104528	25
	35	20	0.57358	0.087156	25
	35	20	0.57358	0.069756	25
	35	20	0.57358	0.069756	25
	35	20	0.57358	0.052336	25
	35	20	0.57358	0.052336	25
	35	20	0.57358	0.139173	25
	35	20	0.57358	0	25
	35	20	0.57358	0	25
	35	20	0.57358	0	25
	35	20	0.57358	0.052336	30
	35	20	0.57358	0.087156	30
	30	20	0.5	0.034899	30
	30	20	0.5	0.034899	30

FT LAB	Bedding		Stratigraphy		Trend
NUMBER	Plunge	Dip	N of B Ang	Sin of Ch.	Angle
	30	20	0.5	0.139173	30
	30	20	0.5	0.069756	30
	30	20	0.5	0.052336	30
	30	20	0.5	0.052336	30
	30	20	0.5	0.069756	30
	30	20	0.5	0.034899	30
	30	20	0.5	0.069756	30
	30	20	0.5	0.052336	30
	30	20	0.5	0.104528	30
FT94-133	25	25	0.42262	0.104528	30
	25	25	0.42262	0.156434	30
	25	25	0.42262	0.121869	30
	25	25	0.42262	0.017452	30
	25	25	0.42262	0.173648	30
	25	25	0.42262	0.069756	30
	25	25	0.42262	0.139173	30
	25	25	0.42262	0.069756	30
FT94-134	35	25	0.57358	0	30
	35	25	0.57358	-0.10453	30
	35	25	0.57358	0.104528	30
	35	25	0.57358	0.104528	30
	35	25	0.57358	0.069756	30
	35	25	0.57358	0.087156	30
	35	25	0.57358	0.173648	30
	35	25	0.57358	0	55
FT94-135	32	22	0.52992	0.104528	55
	32	22	0.52992	0.190809	55
	32	22	0.52992	0.139173	55
	32	22	0.52992	0.139173	55
	32	22	0.52992	0.173648	55
FT94-136	32	22	0.52992	0.156434	55
FT94-137	32	22	0.52992	0.156434	55
	32	22	0.52992	0.052336	55
	25	30	0.42262	0.069756	20
	25	30	0.42262	0.173648	20
	25	30	0.42262	0.258819	20
	25	30	0.42262	0.258819	20
	25	30	0.42262	0.258819	20
	25	30	0.42262	0.173648	20
	25	30	0.42262	0.087156	20
	25	30	0.42262	0.121869	20
	25	30	0.42262	0.139173	20

FT LAB	Bedding		Stratigraphy		Trend
NUMBER	Plunge	Dip	N of B Ang	Sin of Ch.	Angle
	25	30	0.42262	0.258819	40
FT94-138	25	32	0.42262	0.292372	10
	25	32	0.42262	0.374607	20
	25	32	0.42262	0.406737	20
	25	32	0.42262	0.406737	20
	25	32	0.42262	0.358368	20
	25	32	0.42262	0.422618	20
	25	32	0.42262	0.422618	20
FT94-139	25	32	0.42262	0.45399	20

Appendix C

Mt. Bridgeman:
Footwall Measurements

FT Lab. Number	Sample# Number	Station Number	Horizontal Distance	Thickness section	Thickness total	Elevation change	Elevation Total	Elevation GPS	Chain Angle angle	Chain Angle SIN	Chain Angle COS	Distance section	Distance total	Bedding Angle Angle	Bedding Angle SIN
						Starts At	230	230				0	0		
FT94-143	DA94-93	48	49.5134	48.8	48.8	6.959	223	210	8	0.1392	0.99	50	50	80	0.9848
	DA94-94	49	98.4208	48.2	96.9	10.4	212.6		12	0.2079	0.98	50	100	80	0.9848
			147.934	48.8	146	6.959	205.7		8	0.1392	0.99	50	150	80	0.9848
			196.653	48	194	11.25	194.4		13	0.225	0.97	50	200	80	0.9848
			246.462	49.1	243	4.358	190.1		5	0.0872	1	50	250	80	0.9848
			296.341	49.1	292	3.488	186.6		4	0.0698	1	50	300	80	0.9848
			346.333	49.2	341	-0.87	187.5	170	-1	-0.017	1	50	350	80	0.9848
FT94-144	DA94-95	50	382.771	35.9	377	-6.42	193.9		-10	-0.174	0.98	37	387	80	0.9848
			395.771	12.8	390	0	193.9	160	0	0	1	13	400	80	0.9848
	DA94-96	51	445.74	49.2	439	1.745	192.1		2	0.0349	1	50	450	80	0.9848
			495.733	49.2	488	0.873	191.3		1	0.0175	1	50	500	80	0.9848
			545.611	49.1	537	3.488	187.8		4	0.0698	1	50	550	80	0.9848
			595.489	49.1	586	-3.49	191.3		-4	-0.07	1	50	600	80	0.9848
			644.571	48.3	635	-9.54	200.8		-11	-0.191	0.98	50	650	80	0.9848
			694.084	48.8	684	6.959	193.9	150	8	0.1392	0.99	50	700	80	0.9848
				0	684	0	193.9			0		0			1
			743.962	49.1	733	3.488	190.4	160	4	0.0698	1	50	750	80	0.9848
FT94-145	DA94-97	52	793.962	49.2	782	0	190.4	180	0	0	1	50	800	80	0.9848
	DA94-98	52		0	782	0	190.4			0		0			1
			843.955	49.2	831	0.873	189.5		1	0.0175	1	50	850	80	0.9848
			893.924	49.2	880	1.745	187.8		2	0.0349	1	50	900	80	0.9848
			943.894	49.2	930	-1.74	189.5		-2	-0.035	1	50	950	80	0.9848
			993.825	49.2	979	2.617	186.9		3	0.0523	1	50	1000	80	0.9848
			1043.82	49.2	1028	0.873	186		1	0.0175	1	50	1050	80	0.9848
			1093.79	49.2	1077	1.745	184.3		2	0.0349	1	50	1100	80	0.9848
			1143.78	49.2	1126	-0.87	185.1		-1	-0.017	1	50	1150	80	0.9848
			1193.77	49.2	1176	0.873	184.3		1	0.0175	1	50	1200	80	0.9848
			1243.76	49.2	1225	0.873	183.4		1	0.0175	1	50	1250	80	0.9848
			1293.76	49.2	1274	0.873	182.5		1	0.0175	1	50	1300	80	0.9848
			1343.73	49.2	1323	-1.74	184.3	150	-2	-0.035	1	50	1350	80	0.9848
FT94-146	DA94-99	53	1393.72	49.2	1373	0.873	183.4		1	0.0175	1	50	1400	80	0.9848
			1443.6	49.1	1422	3.488	179.9		4	0.0698	1	50	1450	80	0.9848
			1493.57	49.2	1471	1.745	178.2		2	0.0349	1	50	1500	80	0.9848
			1543.5	49.2	1520	2.617	175.5		3	0.0523	1	50	1550	80	0.9848
			1553.44	9.79	1530	1.045	174.5		6	0.1045	0.99	10	1560	80	0.9848
			1593.22	38.9	1569	4.181	170.3		6	0.1045	0.99	40	1600	78	0.9781
			1643.1	48.2	1617	3.488	166.8		4	0.0698	1	50	1650	75	0.9659
			1693.09	47.8	1665	0.873	166		1	0.0175	1	50	1700	73	0.9563
			1743.03	46.9	1712	2.617	163.3		3	0.0523	1	50	1750	70	0.9397
			1792.84	48.7	1760	4.358	159		5	0.0872	1	50	1800	78	0.9781
			1842.71	45.2	1806	3.488	155.5		4	0.0698	1	50	1850	65	0.9063
			1892.71	44.5	1850	0.873	154.6		1	0.0175	1	50	1900	63	0.891
			1915.66	20.3	1870	-7.02	161.6	150	-17	-0.292	0.96	24	1924	62	0.8829
FT94-147	DA94-100	54	1941.52	22.4	1893	-2.72	164.4	150	-6	-0.105	0.99	26	1950	60	0.866
	DA94-101	54		0	1893	0	164.4			0					1
			1991.51	41	1934	-0.87	165.2		-1	-0.017	1	50	2000	55	0.8192

FT Lab. Number	Sample# Number	Station Number	Horizontal Distance	Thickness		Elevation			Chain Angle			Distance		Bedding Angle	
				section	total	change	Total	GPS	angle	SIN	COS	section	total	Angle	SIN
			2041.5	39.9	1974	0.873	164.4		1	0.0175	1	50	2050	53	0.7986
			2091.49	38.3	2012	0.873	163.5		1	0.0175	1	50	2100	50	0.766
			2141.49	37.7	2050	0	163.5		0	0	1	50	2150	49	0.7547
			2191.46	35.9	2086	1.745	161.7		2	0.0349	1	50	2200	46	0.7193
			2241.46	34.1	2120	0	161.7		0	0	1	50	2250	43	0.682
			2291.45	32.1	2152	-0.87	162.6		-1	-0.017	1	50	2300	40	0.6428
			2341.33	29.3	2181	-3.49	166.1		-4	-0.07	1	50	2350	36	0.5878
			2391.14	23.4	2205	-4.36	170.5		-5	-0.087	1	50	2400	28	0.4695
			2440.95	17	2222	-4.36	174.8		-5	-0.087	1	50	2450	20	0.342
			2490.94	14.6	2236	0.873	173.9		1	0.0175	1	50	2500	17	0.2924
			2540.88	12.1	2248	2.617	171.3		3	0.0523	1	50	2550	14	0.2419
			2590.5	8.62	2257	6.093	165.2		7	0.1219	0.99	50	2600	10	0.1736
			2639.74	6.85	2264	8.682	156.5		10	0.1736	0.98	50	2650	8	0.1392
			2688.82	4.28	2268	9.54	147		11	0.1908	0.98	50	2700	5	0.0872
			2738.34	2.59	2271	6.959	140		8	0.1392	0.99	50	2750	3	0.0523
			2788.27	1.74	2272	2.617	137.4		3	0.0523	1	50	2800	2	0.0349
			2838.26	0.87	2273	0.873	136.6		1	0.0175	1	50	2850	1	0.0175
			2887.78	0.86	2274	6.959	129.6		8	0.1392	0.99	50	2900	1	0.0175
			2937.71	0	2274	2.617	127		3	0.0523	1	50	2950	0	0
			2987.71	0	2274	0	127		0	0	1	50	3000	0	0
			3037.7	0	2274	0.873	126.1		1	0.0175	1	50	3050	0	0
			3087.69	0	2274	0.873	125.2		1	0.0175	1	50	3100	0	0
			3137.68	0	2274	0.873	124.4		1	0.0175	1	50	3150	0	0
			3187.65	0.87	2275	1.745	122.6		2	0.0349	1	50	3200	1	0.0175
			3237.65	0.87	2276	0.873	121.7		1	0.0175	1	50	3250	1	0.0175
			3287.65	1.74	2278	0	121.7		0	0	1	50	3300	2	0.0349
			3312.65	0.87	2278	0	121.7		0	0	1	25	3325	2	0.0349
			3337.64	1.31	2280	0.436	121.3		1	0.0175	1	25	3350	3	0.0523
			3387.37	2.6	2282	-5.23	126.5		-6	-0.105	0.99	50	3400	3	0.0523
			3412.12	1.3	2284	-3.48	130		-8	-0.139	0.99	25	3425	3	0.0523
			3436.99	1.3	2285	2.613	127.4		6	0.1045	0.99	25	3450	3	0.0523
			3486.8	2.61	2288	4.358	123		5	0.0872	1	50	3500	3	0.0523
			3536.77	3.49	2291	1.745	121.3		2	0.0349	1	50	3550	4	0.0698
			3586.74	3.49	2295	1.745	119.6		2	0.0349	1	50	3600	4	0.0698
			3636.62	3.48	2298	3.488	116.1	50	4	0.0698	1	50	3650	4	0.0698
FT94-148	DA94-102	55	3670.62	2.96	2301	0	116.1		0	0	1	34	3684	5	0.0872

To the rivers edge

Appendix D

Mt. Bridgeman:
Hangingwall Measurements

FT Lab. Number	Sample Number	Station Number	Horizontal Distance	Thickness sect.	Thickness total	Elevation change	Elevation total	GPS	Alti-meter	Location (UTM)	Distance section	Distance total
							500			Leg #1		
FT94-150	DA94-105	56	50	29	29	2.62	497	230	550	4-63-123E 17 88-65-141N	50	50
			100	29	57	2.62	495				50	100
			150	29	86	0.87	494				50	150
			200	29	115	0.87	493				50	200
			250	29	143	1.74	491				50	250
			299	28	172	7.82	483				50	300
			349	29	200	3.49	480				50	350
			399	29	230	4.36	476				50	400
			449	29	259	-3.49	479				50	450
			499	29	288	2.62	476				50	500
			549	29	318	0.87	476				50	550
			599	30	348	2.62	473				50	600
			649	30	378	-1.74	475				50	650
			699	30	408	1.74	473				50	700
			749	30	438	1.74	471				50	750
			798	31	468	6.09	465				50	800
			848	30	499	7.82	457				50	850
FT94-151	DA94-106	57	897	31	529	-3.49	461	347	525	4-62-172E 17 88-65-180N	50	900
			947	31	560	0.00	461				50	950
			997	31	592	-3.49	464				50	1000
			1019	14	605	0.77	464				22	1022
			1069	31	637	1.74	462				50	1072
			1097	17	654	3.90	458				28	1100
			1146	32	686	9.54	448				50	1150
			1196	32	718	6.96	441				50	1200
			1245	32	750	3.49	438				50	1250
FT94-152	DA94-107	58	1295	32	782	-2.62	441	340		4-61-627E 17 88-65-482N	50	1300
			1345	33	815	0.87	440				50	1350
			1395	33	848	-1.74	441				50	1400
FT94-152	DA94-108	59	1445	33	880	-2.62	444	275	475	4-61-342E 17 88-66-164N	50	1450
			1495	33	913	3.49	441				50	1500
			1545	33	946	0.87	440				50	1550
			1595	33	980	4.36	435				50	1600
			1645	33	1013	6.09	429				50	1650
Traverse continued, Bearing			1695	33	1046	1.74	427				50	1700
035 following the sill up to			1745	34	1081	0.87	427				50	1750
the north, starting on a bench			1745	0	1081	0.00	427					
Leg #2, Measured distances			1794	34	1114	6.96	420				50	1800
are added to Leg #1			1844	34	1148	6.96	413				50	1850

FT Lab. Number	Sample Number	Station Number	Horizontal Distance	Thickness sect.	Thickness total	Elevation change	Elevation total	GPS	Alti-meter	Location (UTM)	Distance section	Distance total
			1893	34	1182	9.54	403				50	1900
			1941	34	1216	12.94	390				50	1950
			1990	34	1250	9.54	381				50	2000
			2040	34	1284	6.09	375				50	2050
			2089	35	1319	6.09	368				50	2100
			2139	35	1354	6.96	362				50	2150
			2188	34	1389	11.25	350				50	2200
FT94-153	DA94-109	60	2236	35	1423	10.40	340	485	500	4-60-887E 17 88-66-498N	50	2250
			2286	35	1459	8.68	331				50	2300
			2334	35	1494	11.25	320				50	2350
			2383	36	1530	9.54	310				50	2400
			2433	36	1566	7.82	303				50	2450
			2478	34	1600	21.13	281		500		50	2500
			2526	36	1635	14.62	267				50	2550
			2575	36	1672	9.54	257				50	2600
			2625	38	1709	-1.74	259				50	2650
			2674	37	1747	-7.82	267				50	2700
			2718	33	1780	-24.24	291				50	2750
			2764	35	1815	-20.34	311				50	2800
FT94-154	DA94-110	61	2788	18	1833	-10.16	322	450	520	4-60-206E 17 88-67-100N	26	2826
			2811	17	1850	7.42	314				24	2850
			2856	35	1885	21.13	293				50	2900
			2903	36	1921	16.28	277				50	2950
			2952	37	1959	-11.25	288				50	3000
			2999	36	1995	-17.10	305				50	3050
			3048	38	2032	-7.82	313				50	3100
			3089	31	2064	0.72	312				41	3141
			3130	31	2095	5.71	307				41	3182
			3138	6	2101	3.95	303				9	3191
			3187	38	2139	7.82	295				50	3241
			3237	38	2177	7.82	287				50	3291
			3286	38	2214	9.54	277				50	3341
			3335	38	2252	7.82	270				50	3391
			3355	15	2268	0.70	269				20	3411
			3383	21	2289	10.75	258				30	3441
			3433	38	2327	6.96	251				50	3491
			3482	38	2365	9.54	242				50	3541
			3531	38	2402	7.82	234				50	3591
			3581	38	2440	6.09	228				50	3641
			3630	37	2478	10.40	217				50	3691
			3660	23	2501	5.92	211				31	3722
			3706	36	2537	18.73	193				50	3772
FT94-155	DA94-111	62	3725	14	2551	5.24	187	530	450	4-61-522E 17 88-69-172	19	3791

FT Lab.	Chain Angle			Bedding Angle	
Number	angle	SIN	COS	Angle	SIN
FT94-150	3	0.0523	0.9986	35	0.5736
	3	0.0523	0.9986	35	0.5736
	1	0.0175	0.9998	35	0.5736
	1	0.0175	0.9998	35	0.5736
	2	0.0349	0.9994	35	0.5736
	9	0.1564	0.9877	35	0.5736
	4	0.0698	0.9976	35	0.5736
	5	0.0872	0.9962	36	0.5878
	-4	-0.0698	0.9976	36	0.5878
	3	0.0523	0.9986	36	0.5878
	1	0.0175	0.9998	36	0.5878
	3	0.0523	0.9986	37	0.6018
	-2	-0.0349	0.9994	37	0.6018
	2	0.0349	0.9994	37	0.6018
	2	0.0349	0.9994	37	0.6018
	7	0.1219	0.9925	38	0.6157
	9	0.1564	0.9877	38	0.6157
FT94-151	-4	-0.0698	0.9976	38	0.6157
	0	0.0000	1.0000	38	0.6157
	-4	-0.0698	0.9976	39	0.6293
	2	0.0349	0.9994	39	0.6293
	2	0.0349	0.9994	39	0.6293
	8	0.1392	0.9903	39	0.6293
	11	0.1908	0.9816	40	0.6428
	8	0.1392	0.9903	40	0.6428
	4	0.0698	0.9976	40	0.6428
FT94-152	-3	-0.0523	0.9986	40	0.6428
	1	0.0175	0.9998	41	0.6561
	-2	-0.0349	0.9994	41	0.6561
FT94-152	-3	-0.0523	0.9986	41	0.6561
	4	0.0698	0.9976	41	0.6561
	1	0.0175	0.9998	42	0.6691
	5	0.0872	0.9962	42	0.6691
	7	0.1219	0.9925	42	0.6691
	2	0.0349	0.9994	42	0.6691
	1	0.0175	0.9998	43	0.6820
		0.0000	1.0000		0.0000
	8	0.1392	0.9903	43	0.6820
	8	0.1392	0.9903	43	0.6820

FT Lab. Number	Chain Angle			Bedding Angle	
	angle	SIN	COS	Angle	SIN
	11	0.1908	0.9816	44	0.6947
	15	0.2588	0.9659	44	0.6947
	11	0.1908	0.9816	44	0.6947
	7	0.1219	0.9925	44	0.6947
	7	0.1219	0.9925	45	0.7071
	8	0.1392	0.9903	45	0.7071
	13	0.2250	0.9744	45	0.7071
FT94-153	12	0.2079	0.9781	45	0.7071
	10	0.1736	0.9848	46	0.7193
	13	0.2250	0.9744	46	0.7193
	11	0.1908	0.9816	47	0.7314
	9	0.1564	0.9877	47	0.7314
	25	0.4226	0.9063	48	0.7431
	17	0.2924	0.9563	48	0.7431
	11	0.1908	0.9816	48	0.7431
	-2	-0.0349	0.9994	49	0.7547
	-9	-0.1564	0.9877	49	0.7547
	-29	-0.4848	0.8746	49	0.7547
	-24	-0.4067	0.9135	50	0.7660
FT94-154	-23	-0.3907	0.9205	50	0.7660
	18	0.3090	0.9511	50	0.7660
	25	0.4226	0.9063	50	0.7660
	19	0.3256	0.9455	50	0.7660
	-13	-0.2250	0.9744	50	0.7660
	-20	-0.3420	0.9397	50	0.7660
	-9	-0.1564	0.9877	50	0.7660
	1	0.0175	0.9998	50	0.7660
	8	0.1392	0.9903	50	0.7660
	26	0.4384	0.8988	50	0.7660
	9	0.1564	0.9877	50	0.7660
	9	0.1564	0.9877	50	0.7660
	11	0.1908	0.9816	50	0.7660
	9	0.1564	0.9877	50	0.7660
	2	0.0349	0.9994	50	0.7660
	21	0.3584	0.9336	50	0.7660
	8	0.1392	0.9903	50	0.7660
	11	0.1908	0.9816	50	0.7660
	9	0.1564	0.9877	50	0.7660
	7	0.1219	0.9925	50	0.7660
	12	0.2079	0.9781	50	0.7660
	11	0.1908	0.9816	50	0.7660
	22	0.3746	0.9272	50	0.7660
FT94-155	16	0.2756	0.9613	50	0.7660

Appendix E

Axel Heiberg
Descriptions and Sample Locations

Collected by Prof.G.K. Muecke and M.Parsons on Axel Heiberg Island in the summer of 1990 (Parsons, 1991)

Kanguk Peninsula, Axel Heiberg Island (79°15'N, 91°31'W)

AX90-020
Section: 90-05   Stratigraphic position: 48.2 m   Rock type: Bentonite
Physical description: 2-3 cm thick, over ~10 m interval below the sample at least 6 thin bentonite
        horizons occur, usually <1 cm thick, which could not be sampled because of poor outcrop
        and thickness of units, yellowish green colour, no mixing with surrounding black shale
        observed.

AX90-021
Section: 90-01   Stratigraphic position: 99.7 m   Rock type: Bentonite
Physicl description: 2-4 cm thick, but up to 20 cm due to slumping, at least onemore bentonite
        horizon <2 cm thick observed between this unit and AX90-020, overlies ~10 cm thick
        ironstone bed, yellowish green, small crystals visible, overlain by black shale, highly
        contorted by slumping.

Appendix F

Age and Track Length Data

```
SAMPLE LOCATION (OR STD)...DA94-74 CHRISTOPHER FM,
DATE OF ANALYSIS...........21/08/95 SAWTOOTH RANGE SVERDRUP
LAB IDENTIFICATION CODE....FT94-130
IRRADIATION CODE...........
DISKETTE...................A
DATAFILE...................FT94A130.AlL
MINERAL ANALYZED...........A
ANALYSIS BY...............AMG
```

FT LENGTH DATA POINTS IN µm

12.56	12.73	13.03	15.60	9.26	7.78	12.11	15.61	12.43	8.82
10.22	9.81	6.68	13.97	12.65	14.41	14.31	14.86	14.97	15.59
8.21	9.89	16.59	16.47	6.10	9.77	9.70	9.29	10.99	10.98
10.15	10.44	8.63	14.61	7.14	10.27	12.31	10.09	7.61	14.83
9.86	9.76	7.94	7.47	16.19	15.44	10.67	13.86	15.11	13.35
10.72	14.54	11.73	11.34	11.05	11.10	13.61	11.81	13.49	13.29
3.13	15.78	9.10	9.36	11.83	9.06	8.15	8.18	9.07	9.98
8.87	4.36	12.52	15.38	13.21	13.73	10.44	7.85	13.85	13.04
15.27	11.18	8.07	12.63	15.75	8.62	8.12	14.77	14.42	13.60
8.72	14.75	8.86	7.14	15.07	14.04	12.97	9.35	13.90	13.67
11.91	13.26	12.83	14.33	14.02	12.89	10.80	11.79	9.14	12.56
8.15	14.21	10.04	11.23	10.54	8.47	14.02	10.46	14.53	13.85
16.43	16.37	11.47	13.98	15.28	14.71	11.56	14.35	13.15	4.85
10.39	8.62	10.42	12.42	13.73					

SUMMARY OF MEASURED STATISTICS

```
                              135 FT LENGTHs MEASURED
THE MEAN IS              11.707
THE STD DEV IS           2.848
THE STD ERROR IS         0.246
THE SKEWNESS IS         -0.389
THE KURTOSIS IS         -0.476
```

MEASURED FREQUENCY TABLE

INTERVAL RANGE FROM	TO	INT. MID. POINT	FREQUENCY VALUE	CUMULATIVE FREQUENCY	%
0.000-	1.000	0.500	0.00	0	0
1.000-	2.000	1.500	0.00	0	0
2.000-	3.000	2.500	0.00	0	0
3.000-	4.000	3.135	0.01	1	1
4.000-	5.000	4.609	0.01	2	1
5.000-	6.000	5.500	0.00	2	0
6.000-	7.000	6.389	0.01	4	1
7.000-	8.000	7.557	0.05	9	5
8.000-	9.000	8.464	0.10	19	10
9.000-	10.000	9.492	0.11	30	11
10.000-	11.000	10.475	0.12	42	12
11.000-	12.000	11.540	0.08	50	8
12.000-	13.000	12.593	0.10	60	10
13.000-	14.000	13.532	0.15	75	15
14.000-	15.000	14.482	0.13	88	13
15.000-	16.000	15.442	0.08	96	8
16.000-	17.000	16.411	0.04	100	4
17.000-	18.000	17.500	0.00	100	0
18.000-	19.000	18.500	0.00	100	0
19.000-	20.000	19.500	0.00	100	0

MEASURED FREQUENCY DISTRIBUTION (%)

DA94-74 CHRISTOPHER FM, SAWTOOTH RANGE SVERDRUP
AMG

FT94-130
21/08/95

INT
MID PT

TRACK LENGTH μ

MID PT	5	10	15	20	25	30	35	40	45	50
0.5										
1.5										
2.5										
3.1										
4.6										
5.5										
6.4										
7.6										
8.5										
9.5										
10.5										
11.5										
12.6										
13.5										
14.5										
15.4										
16.4										
17.5										
18.5										
19.5										
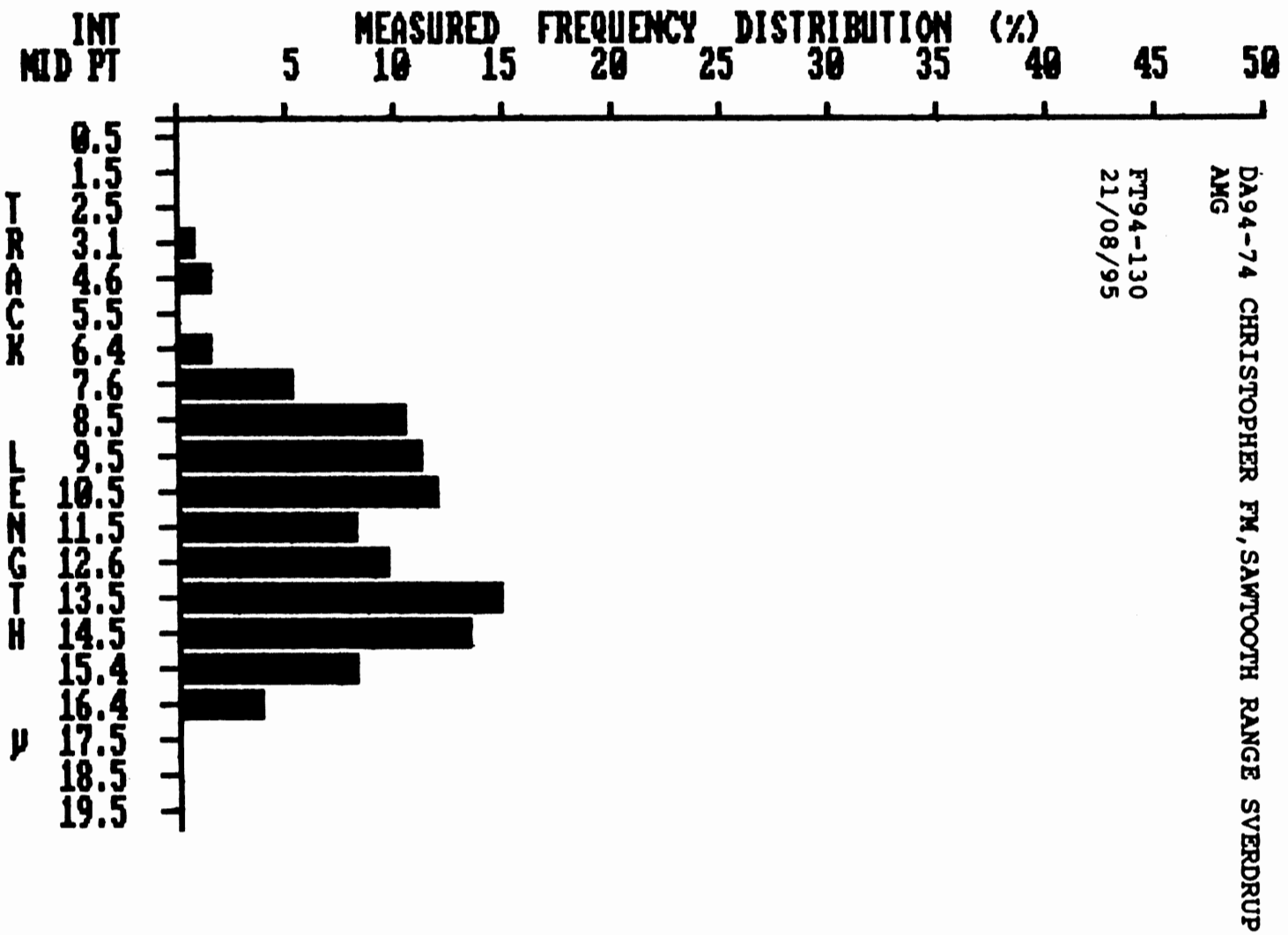
```
SAMPLE LOCATION (OR STD)...DA94-80,SAWTOOTH RANGE SVERDRUP
DATE OF ANALYSIS...........21/01/96
LAB IDENTIFICATION CODE....FT94-133
IRRADIATION CODE...........
DISKETTE...................A
DATAFILE...................FT94A133.A1L
MINERAL ANALYZED...........A
ANALYSIS BY................AMG
```

FT LENGTH DATA POINTS IN µm

13.60	11.10	14.12	9.28	12.00	12.21	10.61	14.68	8.33	15.13
13.03	15.06	8.45	11.10	13.74	13.24	10.02	13.16	10.78	15.23
15.93	10.67	14.75	6.39	13.93	10.55	14.23	11.45	12.20	13.96
13.95	12.54	14.85	14.10	4.64	12.11	15.38	13.39	12.57	12.84
13.69	13.24	12.49	12.25	14.02	13.35	15.32	12.25	10.61	13.62
10.30	14.36	11.22	10.49	13.54	16.11	9.21	14.89	15.08
13.66	11.59	14.13	11.07	10.98	13.64	10.02	11.20	14.06	13.92
14.60	14.89	14.08	11.03	11.55	15.02	9.54	11.20	14.48	13.53
13.87	13.93	15.24	14.09	14.17	15.10	11.79	12.82	10.50	10.54
11.76	11.02	14.29	14.78	15.49	15.09	9.78	15.45	12.55	12.42
11.50	12.35	10.73	10.25	13.37	13.87	11.08	15.14	10.48	8.52
10.78	9.64	14.16	13.79	11.72	14.08	14.97	12.34	14.88	10.13
10.79	14.37	14.59	14.65	11.74	13.18	13.18	12.96	14.91	14.82

SUMMARY OF MEASURED STATISTICS

```
                          130  FT LENGTHs MEASURED
THE MEAN IS               12.841
THE STD DEV IS             1.926
THE STD ERROR IS           0.170
THE SKEWNESS IS           -0.435
THE KURTOSIS IS           -0.846
```

MEASURED FREQUENCY TABLE

INTERVAL RANGE FROM	TO	INT. MID. POINT	FREQUENCY VALUE	CUMULATIVE FREQUENCY	%
0.000-	1.000	0.500	0.00	0	0
1.000-	2.000	1.500	0.00	0	0
2.000-	3.000	2.500	0.00	0	0
3.000-	4.000	3.500	0.00	0	0
4.000-	5.000	4.500	0.00	0	0
5.000-	6.000	5.500	0.00	0	0
6.000-	7.000	6.500	0.00	0	0
7.000-	8.000	7.500	0.00	0	0
8.000-	9.000	8.424	0.03	3	3
9.000-	10.000	9.492	0.04	7	4
10.000-	11.000	10.523	0.15	22	15
11.000-	12.000	11.384	0.12	34	12
12.000-	13.000	12.460	0.12	45	12
13.000-	14.000	13.560	0.19	65	19
14.000-	15.000	14.479	0.23	88	23
15.000-	16.000	15.267	0.11	98	11
16.000-	17.000	16.064	0.02	100	2
17.000-	18.000	17.500	0.00	100	0
18.000-	19.000	18.500	0.00	100	0
19.000-	20.000	19.500	0.00	100	0

MEASURED FREQUENCY DISTRIBUTION (%)

DA94-80 , SAWTOOTH RANGE SVERDRUP
AMG

FT94-133
21/01/96
CF006
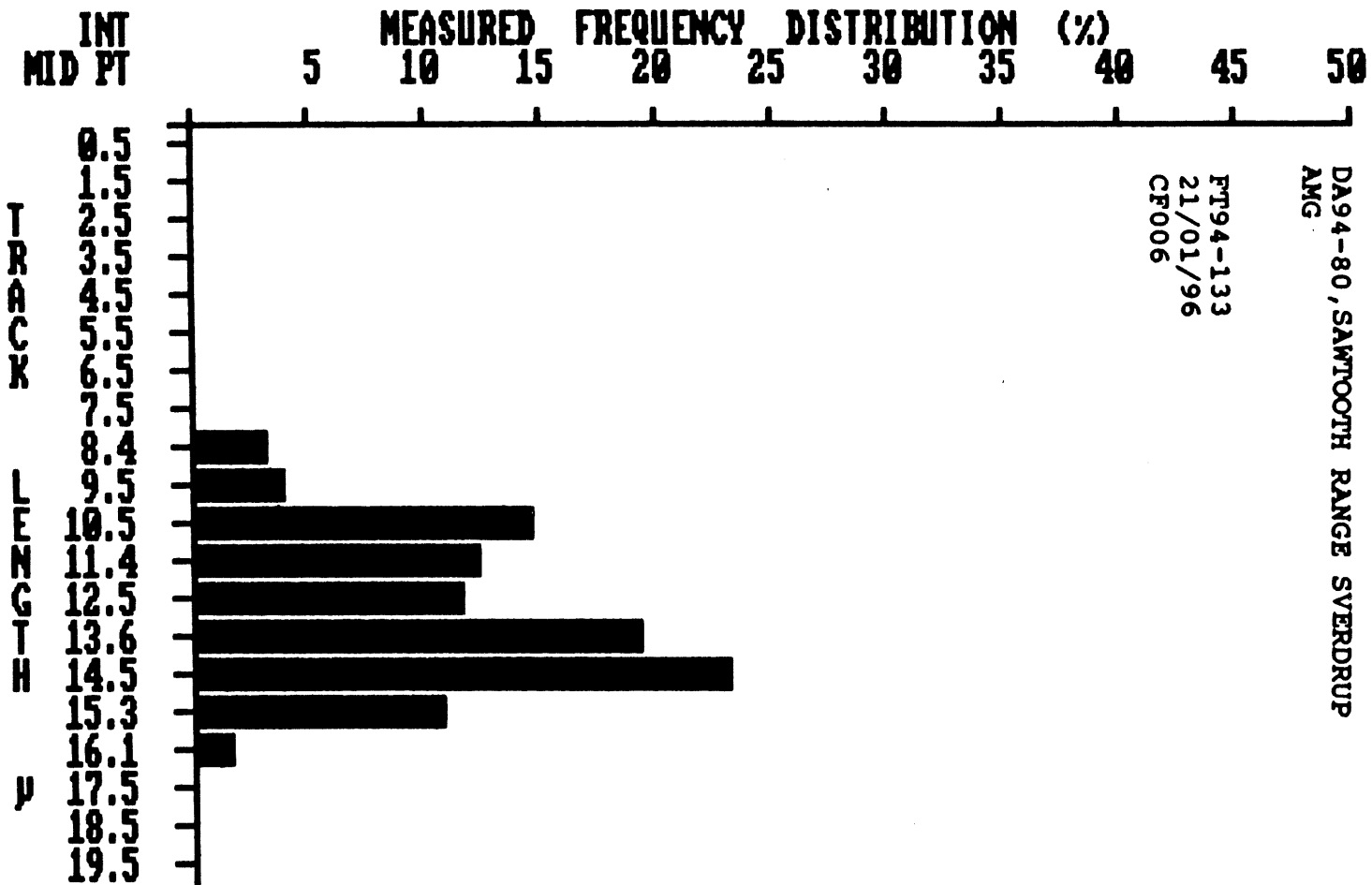
```
SAMPLE LOCATION (OR STD)...DA94-93,SSTR/EAST CAPE
DATE OF ANALYSIS...........24/10/95
LAB IDENTIFICATION CODE....FT94-143
IRRADIATION CODE...........
DISKETTE...................A
DATAFILE...................FT94A143.AlL
MINERAL ANALYZED...........A
ANALYSIS BY................AMG
```

FT LENGTH DATA POINTS IN μm

13.23	15.25	13.90	10.32	14.63	14.61	14.01	14.45	12.80	14.31
14.54	16.05	13.39	10.97	14.15	14.82	12.34	4.57	9.28	10.26
9.43	13.56	8.48	13.71	12.48	9.64	13.46	12.09	13.64	9.71
12.49	14.09	13.48	10.37	11.68	13.41	12.39	5.43	13.76	13.73
8.34	12.21	13.53	13.70	15.42	13.88	14.03	14.93	14.21	13.82
9.62	11.73	11.22	14.40	15.13	7.06	14.06	4.58	6.25	15.61
15.33	12.42	14.99	11.43	13.40	11.49	14.25	9.89	9.92	9.70
13.39	12.89	13.13	15.36	14.00	14.73	14.00	14.62	10.85	13.88
14.06	15.32	13.77	12.60	12.84	11.16	10.35	9.55	13.46	13.16
13.26	10.63	14.91	13.30	13.82	12.49	14.65	15.00	13.07	13.75
13.19	14.19	14.90	10.67	11.34	12.99	14.19	15.07	12.75	8.02
14.39	13.59	12.45	7.25	12.94	13.57	6.17	9.50	12.68	13.73
14.62	10.77	13.93	14.54	15.44	13.74	14.95	10.00	11.03	14.24
10.65	13.46	12.65	13.71	11.00	12.84	13.41	8.60	14.40	14.68
13.11	14.54	15.54	13.36	14.00	13.21	14.97	13.22	14.20	13.11

SUMMARY OF MEASURED STATISTICS

```
                              150  FT LENGTHs MEASURED
THE MEAN IS                 12.684
THE STD DEV IS               2.242
THE STD ERROR IS             0.184
THE SKEWNESS IS             -1.301
THE KURTOSIS IS              1.360
```

MEASURED FREQUENCY TABLE

INTERVAL RANGE FROM	TO	INT. MID. POINT	FREQUENCY VALUE	CUMULATIVE FREQUENCY	%
0.000-	1.000	0.500	0.00	0	0
1.000-	2.000	1.500	0.00	0	0
2.000-	3.000	2.500	0.00	0	0
3.000-	4.000	3.500	0.00	0	0
4.000-	5.000	4.581	0.01	1	1
5.000-	6.000	5.425	0.01	1	1
6.000-	7.000	6.213	0.01	3	1
7.000-	8.000	7.157	0.01	4	1
8.000-	9.000	8.460	0.04	8	4
9.000-	10.000	9.653	0.07	15	7
10.000-	11.000	10.584	0.07	21	7
11.000-	12.000	11.300	0.05	27	5
12.000-	13.000	12.597	0.13	39	13
13.000-	14.000	13.526	0.30	69	30
14.000-	15.000	14.466	0.24	93	24
15.000-	16.000	15.270	0.06	99	6
16.000-	17.000	16.048	0.01	100	1
17.000-	18.000	17.500	0.00	100	0
18.000-	19.000	18.500	0.00	100	0

INT
MID PT

MEASURED FREQUENCY DISTRIBUTION (%)

5 10 15 20 25 30 35 40 45 50

DA94-93,SSTR/EAST CAPE
AMG

FT94-143
24/10/95
NON IRRAD

TRACK LENGTH μ

0.5
1.5
2.5
3.5
4.6
5.4
6.2
7.2
8.5
9.7
10.6
11.3
12.6
13.5
14.5
15.3
16.0
17.5
18.5
19.5
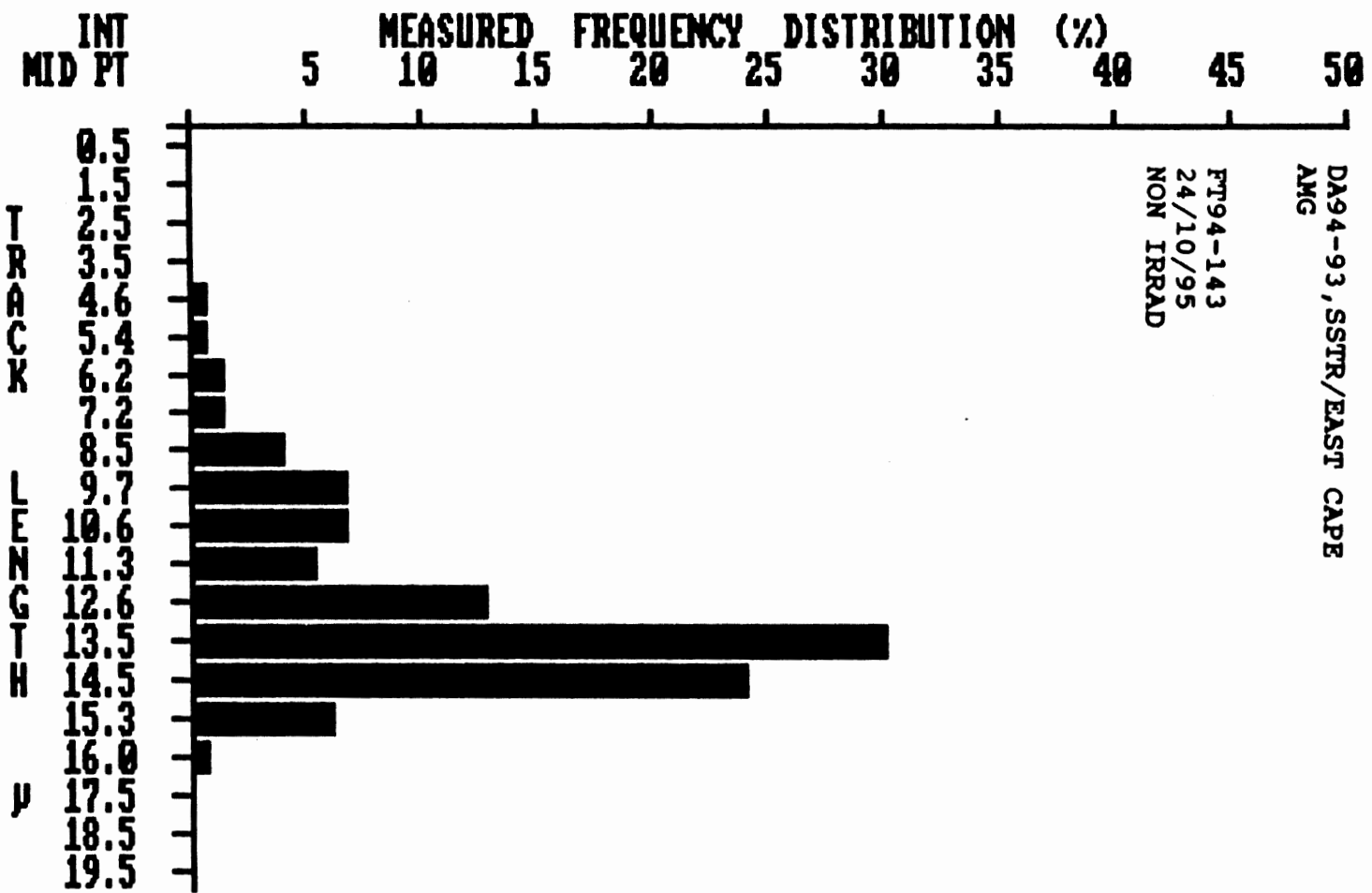
```
SAMPLE LOCATION (OR STD)...DA94-88 BJORNE FM,
DATE OF ANALYSIS...........24/08/95  SAWTOOTH RANGE SVERDRUP
LAB IDENTIFICATION CODE....FT94-139
IRRADIATION CODE...........
DISKETTE...................A
DATAFILE...................FT94A139.A1L
MINERAL ANALYZED...........A
ANALYSIS BY................AMG
```

FT LENGTH DATA POINTS IN μm

13.22	15.14	14.35	15.63	13.04	13.26	14.38	14.42	13.75	14.77
14.07	10.89	14.07	14.30	14.64	14.65	13.07	14.22	14.14	14.02
14.59	14.99	13.46	13.47	14.75	13.83	13.08	13.69	14.50	14.33
13.32	12.76	12.59	14.51	16.26	14.92	14.06	14.35	14.39	14.05
14.69	15.45	14.19	14.22	14.48	14.45	15.78	14.97	12.59	13.52
13.09	13.54	13.91	14.01	14.01	13.17	14.72	16.07	13.41	14.75
11.12	14.98	13.87	12.78	12.29	13.21	14.72	15.46	15.46	9.54
14.30	14.74	13.89	15.01	14.62	13.68	13.87	15.17	13.26	13.96
13.23	13.73	13.84	13.92	13.02	14.35	14.42	15.90	14.69	15.18
15.30	15.04	14.85	11.81	12.97	13.28	15.19	13.98	14.12	14.89
14.41	14.99	14.95	15.22	15.09	14.65	14.31	14.91	15.53	13.86
13.64	14.22	13.23	14.13	14.61	16.07	8.47	13.86	15.75	7.03
15.33									

SUMMARY OF MEASURED STATISTICS

```
                                121  FT LENGTHs MEASURED
THE MEAN IS                     14.012
THE STD DEV IS                   1.307
THE STD ERROR IS                 0.119
THE SKEWNESS IS                 -2.273
THE KURTOSIS IS                  8.505
```

MEASURED FREQUENCY TABLE

INTERVAL RANGE FROM	TO	INT. MID. POINT	FREQUENCY VALUE	CUMULATIVE FREQUENCY	%
0.000-	1.000	0.500	0.00	0	0
1.000-	2.000	1.500	0.00	0	0
2.000-	3.000	2.500	0.00	0	0
3.000-	4.000	3.500	0.00	0	0
4.000-	5.000	4.500	0.00	0	0
5.000-	6.000	5.500	0.00	0	0
6.000-	7.000	6.500	0.00	0	0
7.000-	8.000	7.033	0.01	1	1
8.000-	9.000	8.472	0.01	2	1
9.000-	10.000	9.541	0.01	2	1
10.000-	11.000	10.895	0.01	3	1
11.000-	12.000	11.467	0.02	5	2
12.000-	13.000	12.655	0.06	11	6
13.000-	14.000	13.550	0.31	42	31
14.000-	15.000	14.507	0.42	84	42
15.000-	16.000	15.299	0.13	98	13
16.000-	17.000	16.132	0.02	100	2
17.000-	18.000	17.500	0.00	100	0
18.000-	19.000	18.500	0.00	100	0
19.000-	20.000	19.500	0.00	100	0

DA94-88 BJORNE FM, SAWTOOTH RANGE SVERDRUP
AMG

FT94-139
24/08/95

MEASURED FREQUENCY DISTRIBUTION (%)

INT
MID PT

TRACK LENGTH
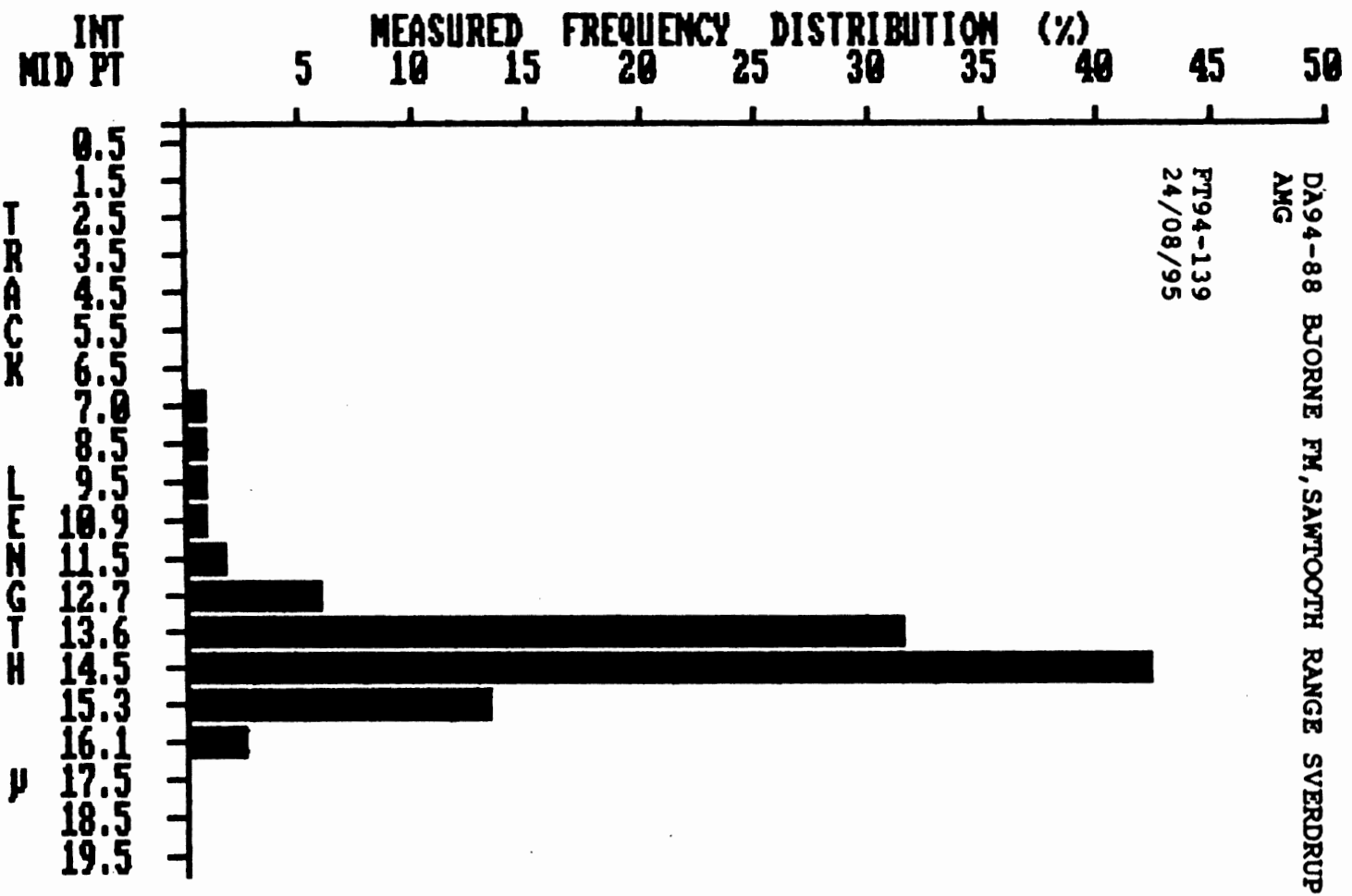
SAMPLE LOCATION (OR STD)...DA94-85 GABBRO ASST. FM,
UP   SAWTOOTH RANGE SVERDR
DATE OF ANALYSIS............19/01/96
LAB IDENTIFICATION CODE....FT94-136
IRRADIATION CODE...........
DISKETTE...................A
DATAFILE...................FT94A136.A1L
MINERAL ANALYZED...........APATITE
ANALYSIS BY...............AMG

FT LENGTH DATA POINTS IN μm

11.31	14.53	15.83	14.72	15.25	13.61	14.44	14.33	14.26	14.41
13.90	14.22	13.79	13.81	12.86	12.76	14.16	14.98	15.02	14.33
13.65	14.85	9.56	14.39	14.62	13.07	13.11	12.37	14.17	16.02
14.52	14.17	14.91	14.80	13.98	15.19	14.41	15.46	14.32	10.99
10.16	13.93	15.33	15.21	10.16	14.01	14.49	13.93	15.55	15.90
13.59	15.06	13.87	13.07	15.47	14.33	13.52	15.89	14.03	13.71
14.68	14.37	13.78	14.62	11.65	11.23	14.89	16.10	14.81	13.72
10.31	11.73	16.33	14.63	14.55	13.22				

SUMMARY OF MEASURED STATISTICS

76 FT LENGTHs MEASURED

THE MEAN IS   13.985
THE STD DEV IS   1.442
THE STD ERROR IS   0.167
THE SKEWNESS IS   -1.192
THE KURTOSIS IS   1.240

MEASURED FREQUENCY TABLE

INTERVAL RANGE FROM	TO	INT. MID. POINT	FREQUENCY VALUE	CUMULATIVE FREQUENCY	%
0.000-	1.000	0.500	0.00	0	0
1.000-	2.000	1.500	0.00	0	0
2.000-	3.000	2.500	0.00	0	0
3.000-	4.000	3.500	0.00	0	0
4.000-	5.000	4.500	0.00	0	0
5.000-	6.000	5.500	0.00	0	0
6.000-	7.000	6.500	0.00	0	0
7.000-	8.000	7.500	0.00	0	0
8.000-	9.000	8.500	0.00	0	0
9.000-	10.000	9.557	0.01	1	1
10.000-	11.000	10.402	0.05	7	5
11.000-	12.000	11.478	0.05	12	5
12.000-	13.000	12.661	0.04	16	4
13.000-	14.000	13.626	0.24	39	24
14.000-	15.000	14.482	0.41	80	41
15.000-	16.000	15.430	0.16	96	16
16.000-	17.000	16.149	0.04	· 100	4
17.000-	18.000	17.500	0.00	100	0
18.000-	19.000	18.500	0.00	100	0
19.000-	20.000	19.500	0.00	100	0

DÀ94-85 GABBRO ASST. FM,SAWTOOTH RANGE SVERDRUP
AMG
FT94-136
19/01/96
CP006

MEASURED FREQUENCY DISTRIBUTION (%)

INT
MID PT

TRACK LENGTH
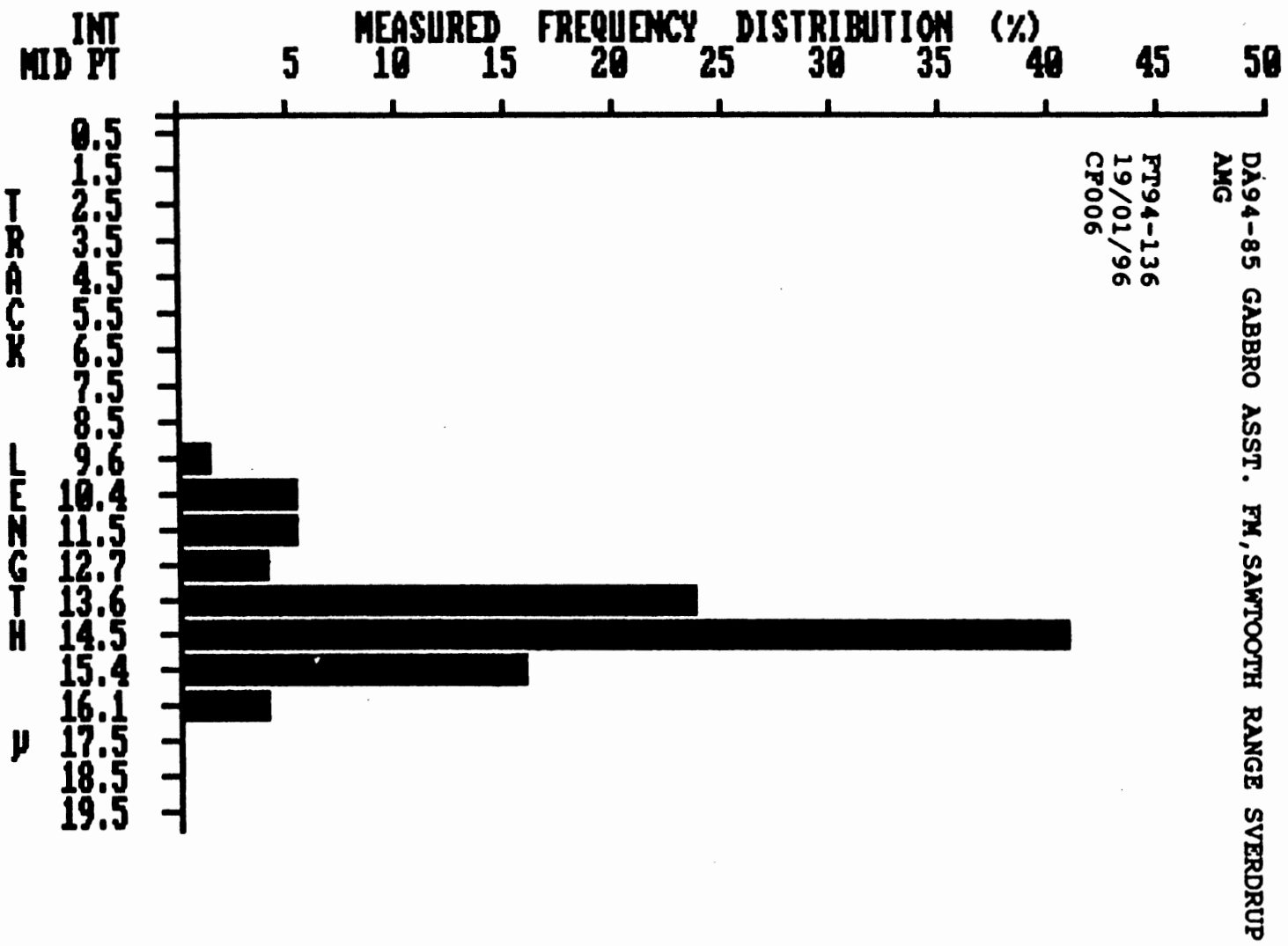
```
SAMPLE LOCATION (OR STD)...DA94-84 ASSISTANCE FM,
DATE OF ANALYSIS............20/10/95 SAWTOOTH RANGE SVERDRUP
LAB IDENTIFICATION CODE....FT94-135
IRRADIATION CODE...........
DISKETTE...................A
DATAFILE...................FT94A135.A1L
MINERAL ANALYZED...........A
ANALYSIS BY................AMG
```

FT LENGTH DATA POINTS IN μm

```
10.41    9.24   14.81   12.81   12.76   13.70   13.55   14.25   14.39   13.84
15.78   14.44   11.91   14.28   14.25   15.27   13.38   14.94   13.34   12.41
14.38   14.38   11.53   13.02   13.02   14.06   13.22   13.08   14.13   14.13
14.00   12.99   10.00   14.46   14.30   13.88   15.21   12.60   14.71   13.01
14.16   14.55   14.42   15.59    6.63   12.63   14.96   14.29   14.78   10.51
13.08   14.23   11.57   13.67   13.80   13.94   14.21   14.36
```

SUMMARY OF MEASURED STATISTICS

```
                              58  FT LENGTHs MEASURED
THE MEAN IS                   13.559
THE STD DEV IS                 1.612
THE STD ERROR IS               0.213
THE SKEWNESS IS               -1.995
THE KURTOSIS IS                4.954
```

MEASURED FREQUENCY TABLE

INTERVAL RANGE FROM	TO	INT. MID. POINT	FREQUENCY VALUE	CUMULATIVE FREQUENCY	%
0.000-	1.000	0.500	0.00	0	0
1.000-	2.000	1.500	0.00	0	0
2.000-	3.000	2.500	0.00	0	0
3.000-	4.000	3.500	0.00	0	0
4.000-	5.000	4.500	0.00	0	0
5.000-	6.000	5.500	0.00	0	0
6.000-	7.000	6.626	0.02	2	2
7.000-	8.000	7.500	0.00	2	0
8.000-	9.000	8.500	0.00	2	0
9.000-	10.000	9.619	0.03	5	3
10.000-	11.000	10.458	0.03	9	3
11.000-	12.000	11.739	0.03	12	3
12.000-	13.000	12.698	0.10	22	10
13.000-	14.000	13.484	0.24	47	24
14.000-	15.000	14.420	0.47	93	47
15.000-	16.000	15.463	0.07	100	7
16.000-	17.000	16.500	0.00	100	0
17.000-	18.000	17.500	0.00	100	0
18.000-	19.000	18.500	0.00	100	0
19.000-	20.000	19.500	0.00	100	0

MEASURED FREQUENCY DISTRIBUTION (%)

INT
MID PT

DA94-84 ASSISTANCE FM, SAWTOOTH RANGE SVERDRUP AMG
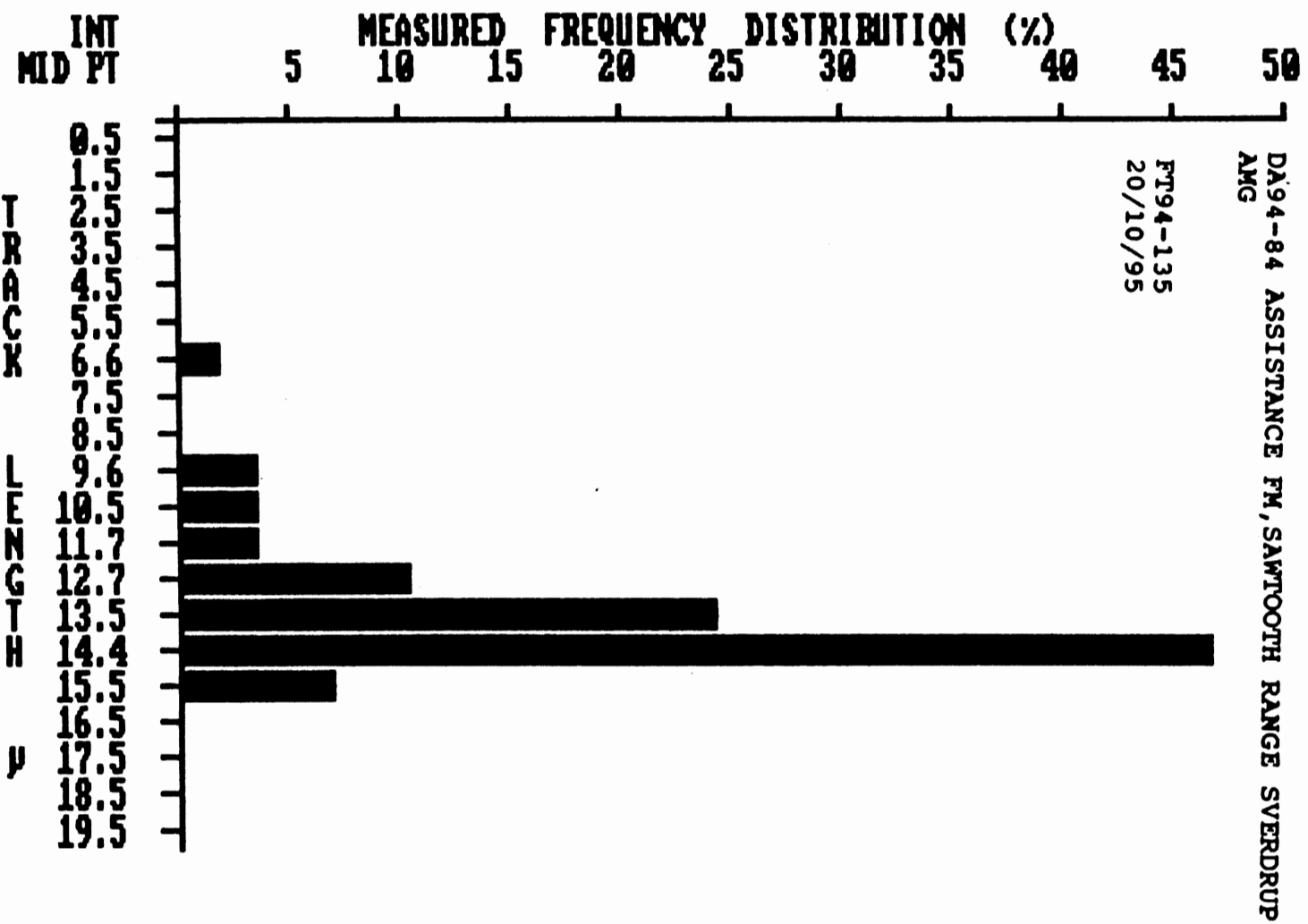
FT94-135
20/10/95

```
SAMPLE LOCATION (OR STD)...DA94-82,SAWTOOTH RANGE SVERDRUP
DATE OF ANALYSIS............22/08/95
LAB IDENTIFICATION CODE....FT94-134
IRRADIATION CODE...........
DISKETTE...................A
DATAFILE...................FT94A134.A1L
MINERAL ANALYZED...........A
ANALYSIS BY...............AMG
```

FT LENGTH DATA POINTS IN µm

13.29	13.43	13.39	14.30	13.60	10.79	10.09	10.02	10.24	14.79
14.33	9.82	12.24	14.09	15.06	14.67	11.38	12.08	9.82	13.67
14.31	9.73	12.90	11.51	10.43	3.58	11.20	10.60
14.92	15.56	11.52	10.98	12.31	12.04	12.07	11.25	10.38	10.20
10.30	10.39	9.83	12.36	12.51	11.08	14.16	15.61	13.66	15.68
11.36	16.10	13.11	13.54	9.62	10.38	11.13	14.22	8.13	14.49
11.28	14.39	12.09	10.54	10.45	11.30	9.28	14.72	13.69
12.79	14.68	14.95	10.09	11.38	9.86	12.74	9.96	9.61	12.11
13.96	11.95	15.99	12.31	16.18	10.92	15.31	10.03	14.90	14.50
15.60	13.67	10.09	11.03	11.07	10.13	11.07	13.60	12.60	13.57
15.64	10.66	12.96	14.95						

SUMMARY OF MEASURED STATISTICS

104 FT LENGTHs MEASURED

```
THE MEAN IS             12.428
THE STD DEV IS           1.985
THE STD ERROR IS         0.196
THE SKEWNESS IS          0.087
THE KURTOSIS IS         -1.195
```

MEASURED FREQUENCY TABLE

INTERVAL RANGE FROM	TO	INT. MID. POINT	FREQUENCY VALUE	CUMULATIVE FREQUENCY	%
0.000-	1.000	0.500	0.00	0	0
1.000-	2.000	1.500	0.00	0	0
2.000-	3.000	2.500	0.00	0	0
3.000-	4.000	3.500	0.00	0	0
4.000-	5.000	4.500	0.00	0	0
5.000-	6.000	5.500	0.00	0	0
6.000-	7.000	6.500	0.00	0	0
7.000-	8.000	7.500	0.00	0	0
8.000-	9.000	8.134	0.01	1	1
9.000-	10.000	9.692	0.10	11	10
10.000-	11.000	10.378	0.18	29	18
11.000-	12.000	11.323	0.15	44	15
12.000-	13.000	12.461	0.14	59	14
13.000-	14.000	13.534	0.13	72	13
14.000-	15.000	14.565	0.19	91	19
15.000-	16.000	15.591	0.07	98	7
16.000-	17.000	16.140	0.02	100	2
17.000-	18.000	17.500	0.00	100	0
18.000-	19.000	18.500	0.00	100	0
19.000-	20.000	19.500	0.00	100	0

MEASURED FREQUENCY DISTRIBUTION (%)

DA94-82, SAWTOOTH RANGE SVERDRUP

FT94-134
22/08/95
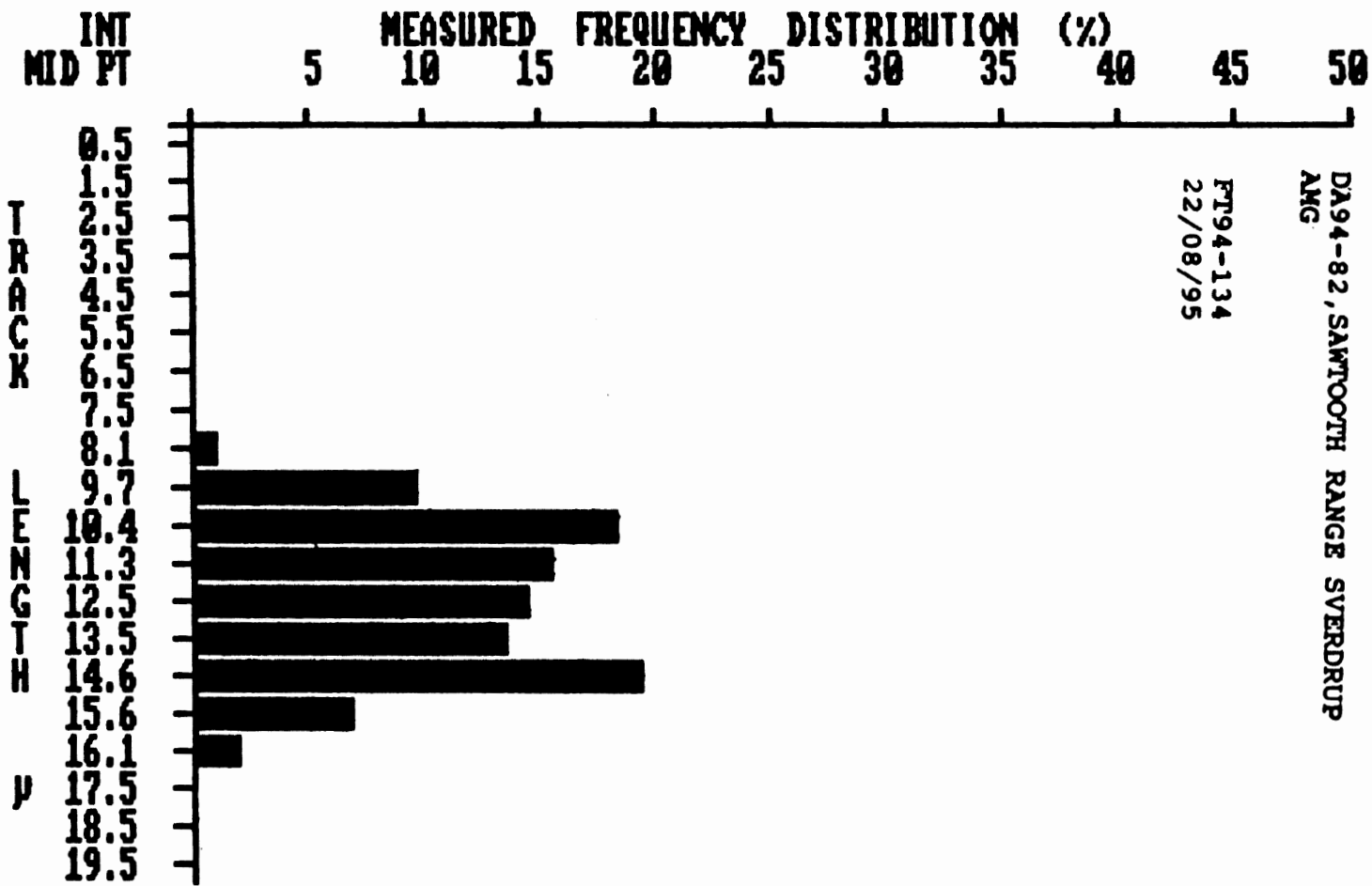
```
SAMPLE LOCATION (OR STD)...DA94-110,S.W.MT.BRIDGEMAN
DATE OF ANALYSIS...........07/10/95
LAB IDENTIFICATION CODE....FT94-154
IRRADIATION CODE...........
DISKETTE...................A
DATAFILE...................FT94A154.A1L
MINERAL ANALYZED...........A
ANALYSIS BY................AMG
```

FT LENGTH DATA POINTS IN μm

```
13.18   13.30   13.05   10.87   12.65    9.71    8.77   14.54   14.23   14.15
15.91   14.27   13.16   12.46   14.92    7.36   12.35   11.11    9.68   14.20
14.82   13.66   11.02   12.31    8.83    8.62   14.90   15.02   16.05   10.56
14.96   12.63   13.23   15.45   12.40   14.65   12.30    8.95    7.05    9.89
14.53   14.46   14.50   13.75   13.89    9.78    9.93   13.49   14.28    8.15
14.58   10.98   13.81   17.06   13.96   13.53   10.84   10.99   13.30   15.34
13.41   14.05   13.25   11.07   12.61   12.41   13.78    8.22   15.88   15.61
13.79   12.94    5.80   14.38   13.21    2.50   12.86   14.66   15.14   14.20
14.27   12.87   12.38   13.49   14.37   13.63    9.38   15.36   14.88   12.86
13.03   13.28   15.08   10.03    7.50   13.08   15.02   14.05   11.97    7.72
15.60   14.91   10.63    9.71   12.73    9.53    9.97   15.04    9.40    9.12
10.55   14.30   13.74    5.19   15.34   15.34    9.39   14.36   14.11   14.30
12.92    8.20   14.96   13.58   14.00   13.50   13.70   14.96   13.22   11.31
14.14   14.71
```

SUMMARY OF MEASURED STATISTICS

```
                          132 FT LENGTHs MEASURED
THE MEAN IS               12.580
THE STD DEV IS             2.515
THE STD ERROR IS           0.220
THE SKEWNESS IS           -1.178
THE KURTOSIS IS            1.259
```

MEASURED FREQUENCY TABLE

INTERVAL RANGE FROM	TO	INT. MID. POINT	FREQUENCY VALUE	CUMULATIVE FREQUENCY	%
0.000-	1.000	0.500	0.00	0	0
1.000-	2.000	1.500	0.00	0	0
2.000-	3.000	2.500	0.01	1	1
3.000-	4.000	3.500	0.00	1	0
4.000-	5.000	4.500	0.00	1	0
5.000-	6.000	5.492	0.02	2	2
6.000-	7.000	6.500	0.00	2	0
7.000-	8.000	7.607	0.03	5	3
8.000-	9.000	8.535	0.05	11	5
9.000-	10.000	9.624	0.09	20	9
10.000-	11.000	10.683	0.06	26	6
11.000-	12.000	11.298	0.04	30	4
12.000-	13.000	12.573	0.13	42	13
13.000-	14.000	13.483	0.22	64	22
14.000-	15.000	14.487	0.24	89	24
15.000-	16.000	15.366	0.11	99	11
16.000-	17.000	16.052	0.01	100	1
17.000-	18.000	17.500	0.00	100	0
18.000-	19.000	18.500	0.00	100	0
19.000-	20.000	19.500	0.00	100	0

INT
MID PT

MEASURED FREQUENCY DISTRIBUTION (%)

DA94-110,S.W.MT.BRIDGEMAN
AMG
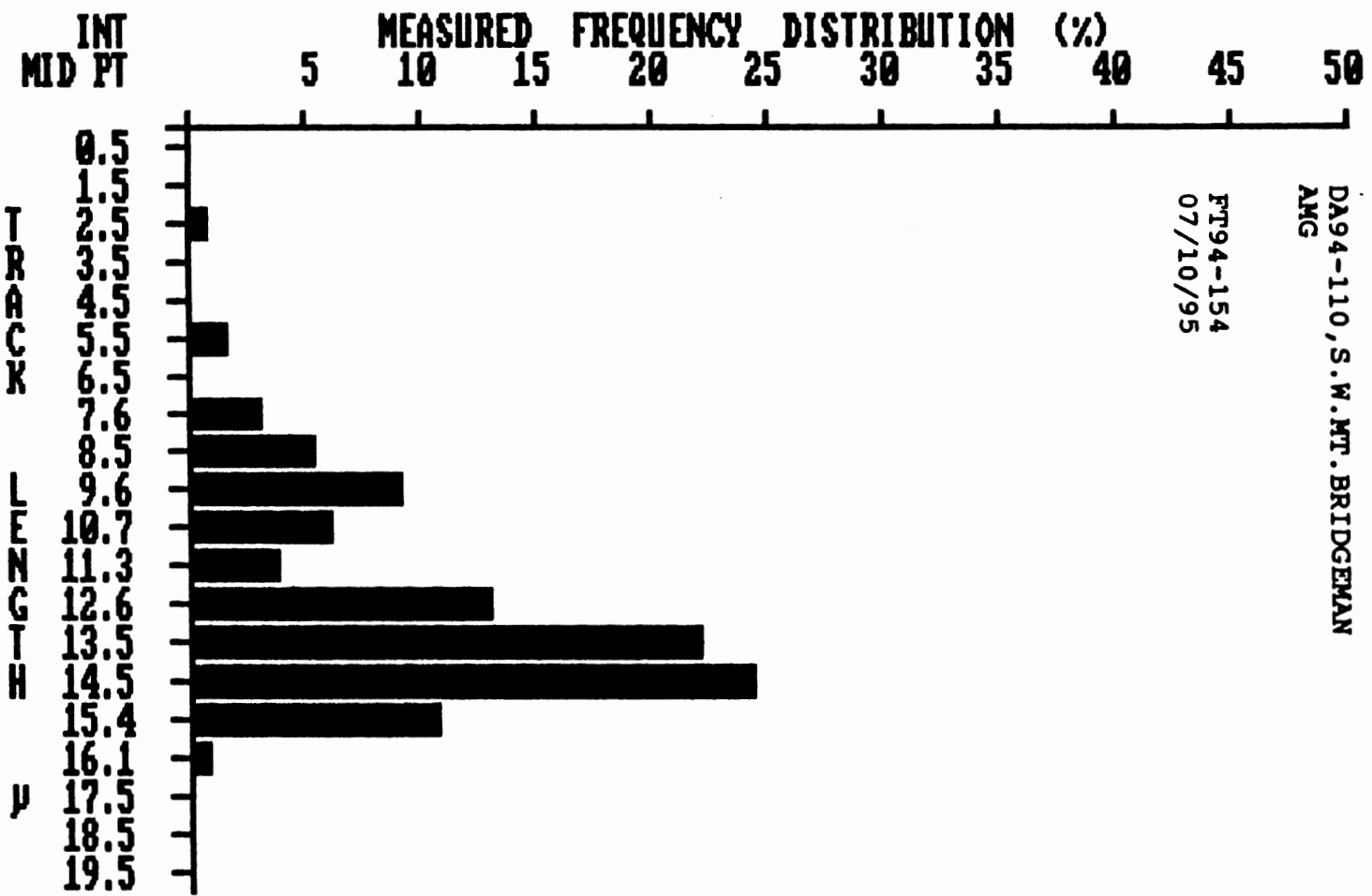
FT94-154
07/10/95

```
SAMPLE LOCATION (OR STD)...DA94-109,S.W.MT.BRIDGEMAN
DATE OF ANALYSIS...........10/10/95
LAB IDENTIFICATION CODE....FT94-153
IRRADIATION CODE...........
DISKETTE...................A
DATAFILE...................FT94A153.AlL
MINERAL ANALYZED...........A
ANALYSIS BY................AMG
```

FT LENGTH DATA POINTS IN μm

13.16	14.00	14.36	13.55	13.68	15.34	15.81	14.23	14.48	12.88
14.89	14.03	13.74	11.90	12.35	14.68	13.86	12.87	13.21	13.80
13.48	13.42	12.62	11.70	14.70	14.29	12.08	12.22	12.88	13.08
13.34	15.36	14.62	11.85	15.16	14.72	14.29	10.38	14.10	14.47
14.63	12.76	15.97	14.53	14.09	9.67	14.32	13.92	15.31	14.94
13.30	14.24	14.37	10.10	14.34	14.17	13.30	13.53	13.13	13.23
14.26	13.79	14.53	13.94	14.44	15.02	13.86	12.85	13.93	14.02
14.28	14.39	15.52	14.13	12.65	13.57	13.62	13.68	12.73	15.03
14.24	13.22	14.33	13.76	13.26	13.48	13.06	12.90	10.33	14.48
13.20	14.23	14.08	13.73	15.60	12.83	14.15	14.37	14.88	13.18
14.06	14.49	14.77	12.85	13.96	7.87	13.91	15.15	15.45	13.08
14.83	13.50	5.43	15.41	13.65	13.28				

SUMMARY OF MEASURED STATISTICS

```
                           116 FT LENGTHs MEASURED
THE MEAN IS                13.664
THE STD DEV IS              1.464
THE STD ERROR IS           0.136
THE SKEWNESS IS           -2.407
THE KURTOSIS IS            9.376
```

MEASURED FREQUENCY TABLE

INTERVAL RANGE FROM	TO	INT. MID. POINT	FREQUENCY VALUE	CUMULATIVE FREQUENCY	%
0.000-	1.000	0.500	0.00	0	0
1.000-	2.000	1.500	0.00	0	0
2.000-	3.000	2.500	0.00	0	0
3.000-	4.000	3.500	0.00	0	0
4.000-	5.000	4.500	0.00	0	0
5.000-	6.000	5.433	0.01	1	1
6.000-	7.000	6.500	0.00	1	0
7.000-	8.000	7.869	0.01	2	1
8.000-	9.000	8.500	0.00	2	0
9.000-	10.000	9.672	0.01	3	1
10.000-	11.000	10.270	0.03	5	3
11.000-	12.000	11.815	0.03	8	3
12.000-	13.000	12.675	0.12	20	12
13.000-	14.000	13.497	0.32	52	32
14.000-	15.000	14.392	0.37	89	37
15.000-	16.000	15.394	0.11	100	11
16.000-	17.000	16.500	0.00	100	0
17.000-	18.000	17.500	0.00	100	0
18.000-	19.000	18.500	0.00	100	0
19.000-	20.000	19.500	0.00	100	0

INT
MID PT

MEASURED FREQUENCY DISTRIBUTION (%)

DA94-109,S.W.MT.BRIDGEMAN
AMG
FT94-153
10/10/95

TRACK LENGTH
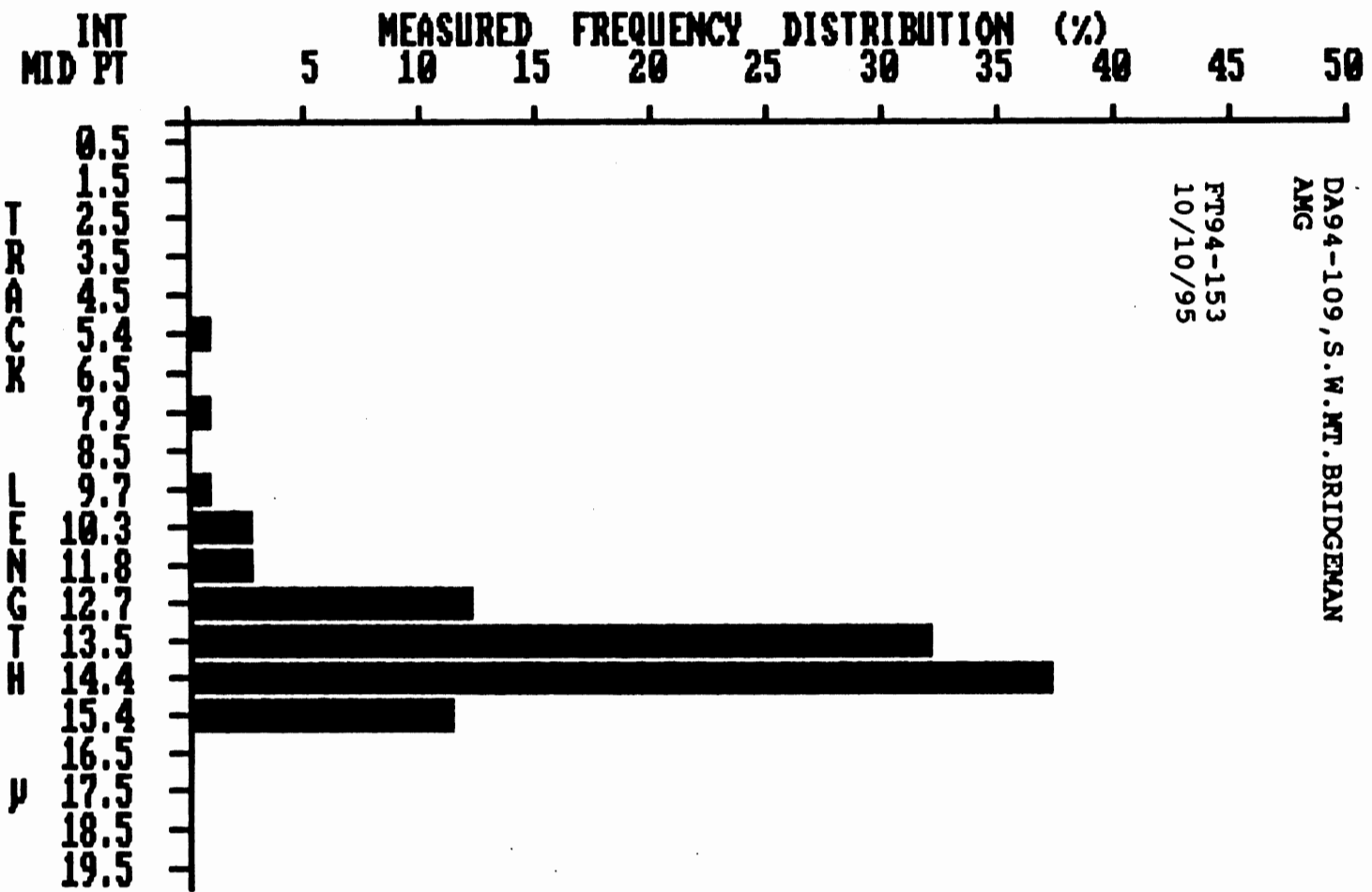
```
SAMPLE LOCATION (OR STD)...DA94-100,SSTR/EAST CAPE
DATE OF ANALYSIS...........22/10/95
LAB IDENTIFICATION CODE....FT94-147
IRRADIATION CODE...........
DISKETTE...................A
DATAFILE...................FT94A147.A1L
MINERAL ANALYZED...........A
ANALYSIS BY................AMG
```

FT LENGTH DATA POINTS IN μm

16.26	11.70	12.23	11.01	11.30	12.19	9.78	14.69	14.81	14.38
15.83	12.54	12.46	12.90	12.14	13.28	12.92	13.03	12.90	12.62
14.01	14.03	11.22	12.60	14.69	11.01	14.25	11.74	10.66	14.31
14.11	14.25	13.14	13.73	13.83	13.71	13.58	14.79	11.21	14.23
11.12	11.00	13.62	11.63	11.17	12.82	6.34	11.79	14.23	13.96
12.20	3.59	11.85	14.79	13.04	14.18	12.51	12.09	15.25	13.13
12.54	11.32	14.94	13.61	13.48	12.63	14.34	13.92	11.87	11.49
12.66	11.78	13.32	14.23	12.45	12.45	13.67	13.83	11.76	13.77
12.81	13.02	8.97	14.06	11.89	13.53	13.53	11.92	13.06	12.35
7.27	14.16	13.66	12.39	12.42	13.66	11.03	13.37	12.65	12.56
13.49	13.69	10.35	13.46	13.15	13.72	15.43	10.42	9.46	13.71
14.87	14.62	12.88	13.81	13.61	13.76	14.62	12.86	15.10	12.73
11.98	12.55	14.12	13.27	12.82	9.41	12.37			

SUMMARY OF MEASURED STATISTICS

```
                              127  FT LENGTHs MEASURED
THE MEAN IS                  12.700
THE STD DEV IS                1.757
THE STD ERROR IS              0.157
THE SKEWNESS IS              -1.722
THE KURTOSIS IS               5.814
```

MEASURED FREQUENCY TABLE

INTERVAL RANGE FROM	TO	INT. MID. POINT	FREQUENCY VALUE	CUMULATIVE FREQUENCY	%
0.000-	1.000	0.500	0.00	0	0
1.000-	2.000	1.500	0.00	0	0
2.000-	3.000	2.500	0.00	0	0
3.000-	4.000	3.592	0.01	1	1
4.000-	5.000	4.500	0.00	1	0
5.000-	6.000	5.500	0.00	1	0
6.000-	7.000	6.340	0.01	2	1
7.000-	8.000	7.273	0.01	2	1
8.000-	9.000	8.966	0.01	3	1
9.000-	10.000	9.588	0.03	6	3
10.000-	11.000	10.475	0.02	9	2
11.000-	12.000	11.474	0.19	28	19
12.000-	13.000	12.569	0.26	54	26
13.000-	14.000	13.518	0.24	78	24
14.000-	15.000	14.404	0.19	97	19
15.000-	16.000	15.261	0.02	99	2
16.000-	17.000	16.261	0.01	100	1
17.000-	18.000	17.500	0.00	100	0
18.000-	19.000	18.500	0.00	100	0
19.000-	20.000	19.500	0.00	100	0

MEASURED FREQUENCY DISTRIBUTION (%)

INT
MID PT

5 10 15 20 25 30 35 40 45 50

0.5
1.5
2.5
3.6
4.5
5.5
6.3
7.3
9.0
9.6
10.5
11.5
12.6
13.5
14.4
15.3
16.3
17.5
18.5
19.5

TRACK LENGTH μ

DA94-100,SSTR/EAST CAPE
AMG

FT94-147
22/10/95
AGE + CF
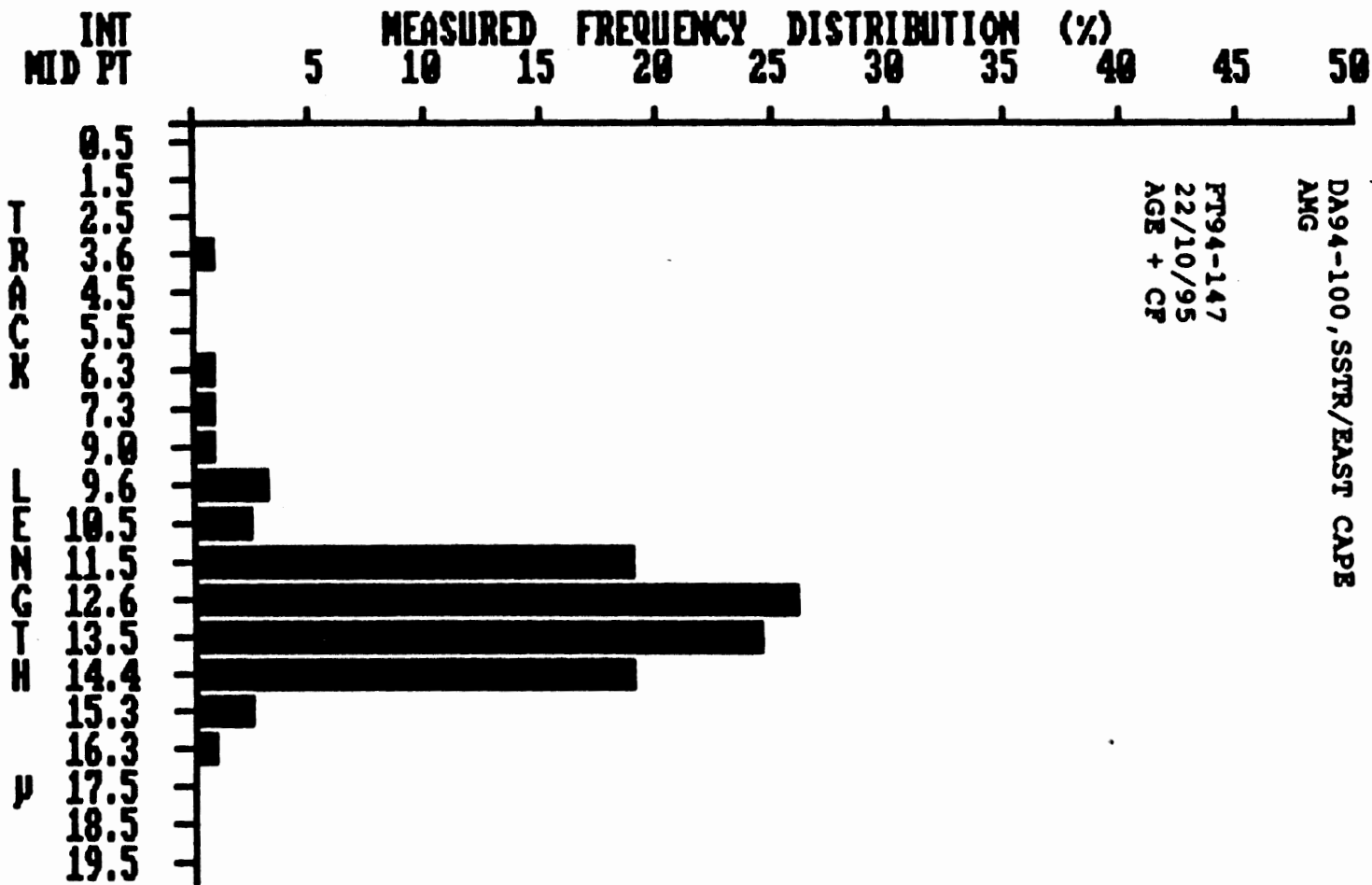
```
SAMPLE LOCATION (OR STD)...DA94-99,SSTR/EAST CAPE
DATE OF ANALYSIS...........22/10/95
LAB IDENTIFICATION CODE....FT94-146
IRRADIATION CODE...........
DISKETTE...................A
DATAFILE...................FT94A146.A1L
MINERAL ANALYZED...........A
ANALYSIS BY................AMG
```

FT   LENGTH   DATA   POINTS   IN   μm

```
14.66   12.87   14.69   11.66   14.96   12.84   11.96   15.25   14.11   14.64
12.60   11.81   13.50   11.29   12.22   12.45   12.19   12.58   14.12   14.05
13.92   14.32   13.14   13.11   12.71   11.60   11.11   13.34   11.11   14.00
13.93   12.04   10.50   11.11   14.29   13.35   14.36   12.17   11.11   13.93
13.52   6.84   13.96   12.00   14.01   13.95   14.44   12.11   10.92   14.57
15.44   11.37   12.61   14.86   14.01   13.52   9.44   10.57   10.92   11.11
11.40   12.75   13.20   12.91   13.45   14.20   13.88   13.30   11.11   13.57
13.25   14.37   14.33   10.91   12.15   13.73   15.08   13.59   12.62   13.85
12.40   10.67   12.96   11.90   14.38
```

SUMMARY   OF   MEASURED   STATISTICS

```
                              85  FT LENGTHs MEASURED
THE MEAN IS                 12.945
THE STD DEV IS               1.444
THE STD ERROR IS             0.158
THE SKEWNESS IS             -0.905
THE KURTOSIS IS              1.321
```

MEASURED   FREQUENCY   TABLE

INTERVAL RANGE FROM	TO	INT. MID. POINT	FREQUENCY VALUE	CUMULATIVE FREQUENCY	%
0.000-	1.000	0.500	0.00	0	0
1.000-	2.000	1.500	0.00	0	0
2.000-	3.000	2.500	0.00	0	0
3.000-	4.000	3.500	0.00	0	0
4.000-	5.000	4.500	0.00	0	0
5.000-	6.000	5.500	0.00	0	0
6.000-	7.000	6.500	0.00	0	0
7.000-	8.000	7.374	0.01	1	1
8.000-	9.000	8.500	0.00	1	0
9.000-	10.000	9.700	0.02	4	2
10.000-	11.000	10.669	0.07	11	7
11.000-	12.000	11.622	0.12	22	12
12.000-	13.000	12.525	0.26	48	26
13.000-	14.000	13.585	0.27	75	27
14.000-	15.000	14.418	0.21	96	21
15.000-	16.000	15.257	0.04	100	4
16.000-	17.000	16.500	0.00	100	0
17.000-	18.000	17.500	0.00	100	0
18.000-	19.000	18.500	0.00	100	0
19.000-	20.000	19.500	0.00	100	0

INT
MID PT

MEASURED FREQUENCY DISTRIBUTION (%)

5 10 15 20 25 30 35 40 45 50

DA94-99,SSTR/EAST CAPE
AMG

FT94-146
22/10/95

T
R
A
C
K

L
E
N
G
T
H

μ

0.5
1.5
2.5
3.5
4.5
5.5
6.5
7.4
8.5
9.7
10.7
11.6
12.5
13.6
14.4
15.3
16.5
17.5
18.5
19.5
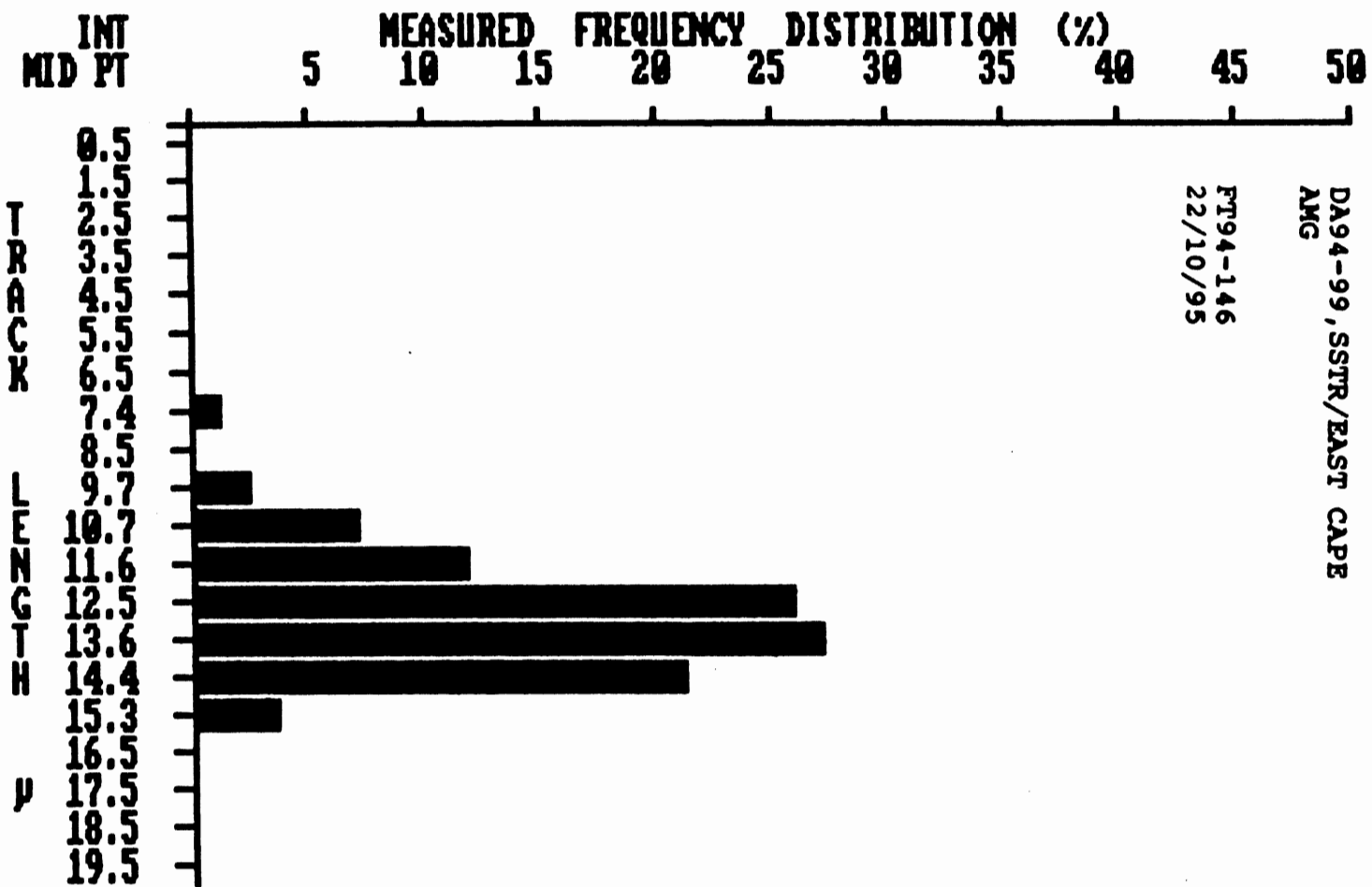
```
SAMPLE LOCATION (OR STD)...DA94-97,SSTR/EAST CAPE
DATE OF ANALYSIS...........15/10/95
LAB IDENTIFICATION CODE....FT94-145
IRRADIATION CODE...........
DISKETTE...................A
DATAFILE...................FT94A145.A1L
MINERAL ANALYZED...........A
ANALYSIS BY................AMG
```

FT LENGTH DATA POINTS IN μm

```
11.40   13.37    9.94   11.05   10.55   14.62   12.75   14.94   11.21   12.78
...      ...      ...    ...     ...     ...     ...     ...     ...     ...
14.16    4.80   12.54   13.78   16.97   13.52   14.17   11.33   13.99   13.34
14.47   12.27   14.07   11.36   11.99   12.54   14.30   11.22   12.45   13.54
11.46   12.58   12.56   14.59           12.20            12.40           10.63
...     ...     ...     ...             ...              ...             ...
10.99   12.49    0.27                   12.40                    14.81   13.97
10.93   11.85   13.53   13.36   12.61   12.93   12.73   13.09   12.52   10.43
11.75   10.73   13.03   15.17
```

SUMMARY OF MEASURED STATISTICS

```
                              94 FT LENGTHs MEASURED
THE MEAN IS                  12.565
THE STD DEV IS                1.727
THE STD ERROR IS              0.179
THE SKEWNESS IS              -0.791
THE KURTOSIS IS               1.741
```

MEASURED FREQUENCY TABLE

INTERVAL RANGE FROM	TO	INT. MID. POINT	FREQUENCY VALUE	CUMULATIVE FREQUENCY	%
0.000-	1.000	0.500	0.00	0	0
1.000-	2.000	1.500	0.00	0	0
2.000-	3.000	2.500	0.00	0	0
3.000-	4.000	3.500	0.00	0	0
4.000-	5.000	4.500	0.00	0	0
5.000-	6.000	5.500	0.00	0	0
6.000-	7.000	6.068	0.01	1	1
7.000-	8.000	7.903	0.01	2	1
8.000-	9.000	8.204	0.02	4	2
9.000-	10.000	9.945	0.01	5	1
10.000-	11.000	10.662	0.11	16	11
11.000-	12.000	11.569	0.18	34	18
12.000-	13.000	12.544	0.23	57	23
13.000-	14.000	13.463	0.23	81	23
14.000-	15.000	14.467	0.15	96	15
15.000-	16.000	15.276	0.03	99	3
16.000-	17.000	16.967	0.01	100	1
17.000-	18.000	17.500	0.00	100	0
18.000-	19.000	18.500	0.00	100	0
19.000-	20.000	19.500	0.00	100	0

MEASURED FREQUENCY DISTRIBUTION (%)

INT
MID PT

DA94-97,SSTR/EAST CAPE
AMG
FT94-145
15/10/95
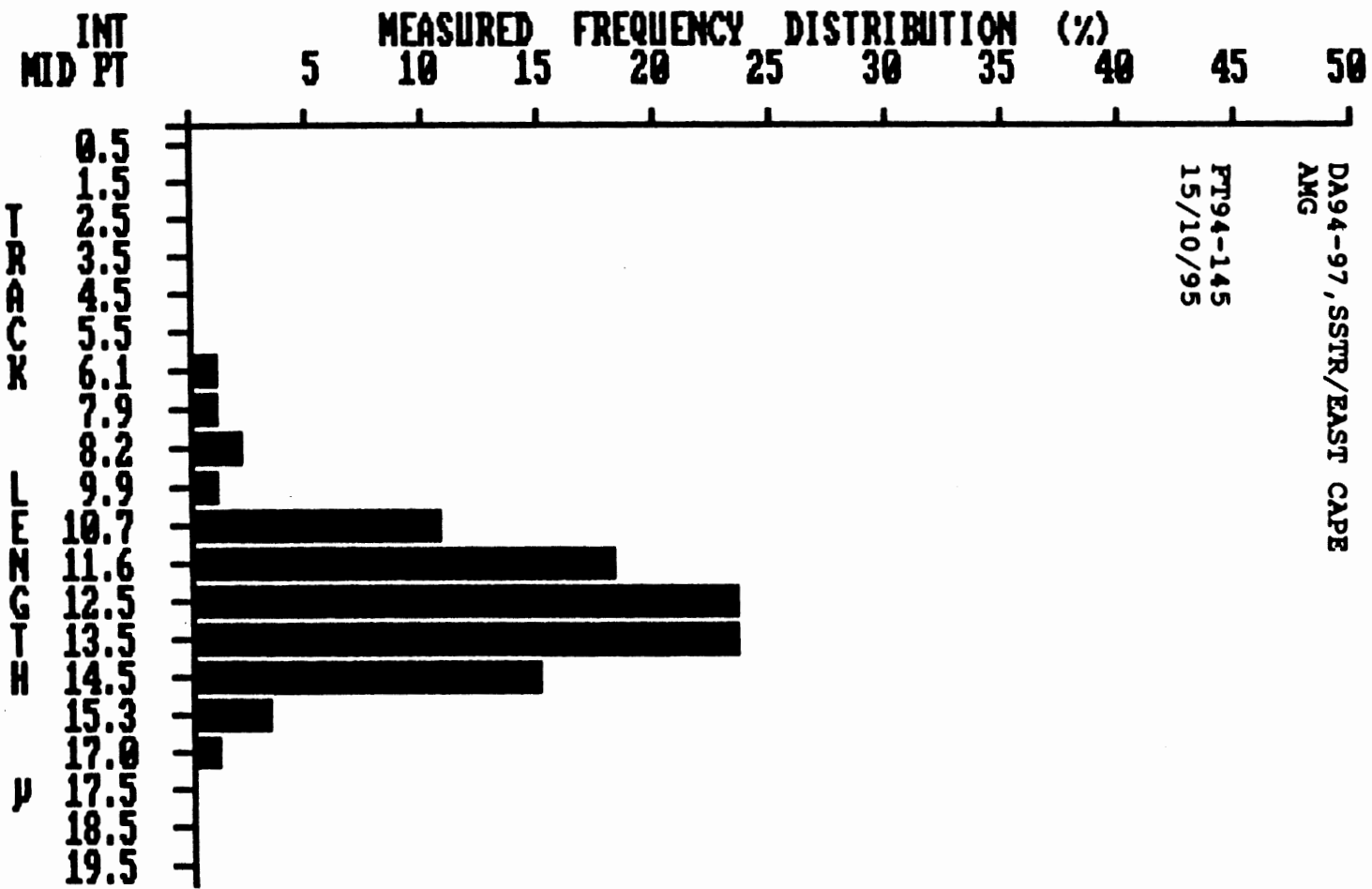
Appendix G

Compositional Data

TABLE G.1

Microprobe Compositional Data of Apatite Separates
From the Sawtooth Range, Axel Heiberg Island

Point	P	Si	S	La	Ce	Y	Nd	Nb	Fe	Mn	Mg	Ca	Na	Sr	F	Cl	O	Total
DUR	18.012	0.095	0.013	0.320	0.583	0.043			0.003		0.083	38.578	0.233		3.390	0.420	38.158	99.910
133 1a	18.320	0.058		0.066	0.187	0.021			0.089	0.007	0.062	39.193	0.074		3.290	0.182	37.290	98.530
133 1b	18.331	0.057		0.105	0.216	0.077			0.086		0.087	38.925			3.312	0.148	38.244	99.440
133 2c	9.950	0.183	0.670	0.057	0.127	0.000			0.147		0.109	20.188			0.893	0.707	17.276	50.310
133 2d	18.722	0.078		0.265	0.308	0.303			0.174		0.201	39.106	0.017		4.181	0.112	39.576	103.030
133 3e	18.447	0.010		0.182	0.199	0.315			0.010			39.018	0.098		5.246	0.032	46.227	109.630
133 3f	18.765	0.023		0.221	0.293	0.327			0.068		0.019	39.584	0.059		3.705	0.045	37.992	100.890
133 4g	18.545	0.017		0.267	0.365	0.340			0.161		0.122	38.904	0.027		4.264	0.209	40.297	103.470
133 4h	18.365	0.048		0.258	0.390	0.341			0.162		0.115	38.716	0.108		4.356	0.120	40.648	103.580
133 5i	18.695	0.067		0.300	0.314	0.258			0.058		0.013	39.630	0.092		2.899	0.000	40.208	102.370
133 5j	18.743	0.000		0.259	0.222	0.283			0.000		0.038	39.762			3.006	0.025	41.405	103.680
133 6k	18.405	0.047		0.383	0.580	0.415			0.064		0.053	38.850	0.064		4.678	0.251	40.469	104.030
133 6l	18.419	0.028		0.419	0.697	0.405			0.130		0.054	38.891	0.108		4.794	0.212	41.261	105.340
134 1a	18.384	0.017		0.017	0.248	0.102			0.096		0.042	38.939	0.094		3.626	0.095	38.732	100.130
134 1b	18.374	0.053		0.000	0.124	0.042			0.123		0.100	39.114			3.559	0.119	38.488	100.040
134 2c	18.701	0.031		0.054	0.142	0.074			0.197		0.103	39.132	0.041		3.351	0.115	38.785	100.600
134 2d	18.206	0.114		0.097	0.285	0.083			0.208		0.065	38.823			3.434	0.072	38.502	99.820
134 3e	18.347	0.068		0.161	0.434	0.109			0.068		0.013	38.989	0.056		3.157	0.370	39.386	101.020
134 3f	18.379	0.096		0.087	0.433	0.073			0.004		0.057	39.048	0.043		2.869	0.224	38.012	99.220
134 4h	18.451	0.141		0.073	0.290	0.074			0.021		0.047	39.212	0.031		3.659	0.168	38.894	100.960
134 4i	18.212	0.186		0.031	0.246	0.059			0.003		0.031	38.750	0.039		3.524	0.170	36.844	97.990
134 5j	18.460	0.024		0.004	0.111	0.080			0.027			39.325	0.000		3.228	0.000	38.894	100.100
134 5k	18.520	0.000		0.049	0.053				0.043		0.014	39.379	0.005		3.505	0.048	38.921	100.330
134 5l	18.481	0.017		0.023	0.034	0.045			0.016	0.022	0.051	39.208	0.106		3.153	0.041	37.492	98.480
134 6m	18.505	0.031		0.124	0.478	0.102			0.040		0.052	38.725	0.154		3.484	0.121	37.918	99.610
134 6n	17.996	0.028		0.241	0.571	0.057			0.140		0.035	37.277	0.227		2.843	0.192	34.776	94.320
134 7o	18.593	0.066		0.000	0.100				0.131		0.097	39.095	0.074		3.252	0.086	37.613	99.030
134 7p	18.655	0.047		0.048	0.153	0.034			0.158		0.099	38.967	0.033		3.575	0.049	39.288	100.900
135 1a	18.104	0.132		0.011	0.086	0.028			0.031			39.130	0.175		3.480	0.066	34.735	95.910
135 1b	18.612	0.010		0.040	0.151	0.114						39.792	0.060		4.595	0.005	39.401	102.660
135 2c	18.820			0.020	0.106	0.150						39.290	0.089		3.438	0.035	40.511	102.310
135 2d	18.594	0.012		0.028	0.110	0.129					0.016	39.104	0.008		3.540	0.091	40.012	101.580
135 3e	18.400		0.003		0.098	0.216			0.040		0.027	39.558	0.093		3.765	0.055	40.218	102.250
135 3f	18.713			0.029	0.109	0.233			0.006		0.017	39.294	0.054		3.961	0.000	41.660	103.970
135 4g	18.389			0.021	0.085	0.238			0.070			38.968	0.036		3.385	0.047	39.467	100.530

TABLE G.1

Microprobe Compositional Data of Apatite Separates
From the Sawtooth Range, Axel Heiberg Island

Point	P	Si	S	La	Ce	Y	Nd	Nb	Fe	Mn	Mg	Ca	Na	Sr	F	Cl	O	Total
135 4h	18.607			0.016	0.107	0.217			0.009		0.009	39.295	0.078		3.499	0.012	39.767	101.490
135 5i	18.820			0.051	0.080	0.166			0.044		0.025	39.520	0.042		4.108	0.023	39.985	102.680
135 5j	18.670			0.034	0.108	0.157			0.070			39.426	0.061		4.088	0.040	39.588	102.040
135 6k	18.367	0.068		0.051	0.195	0.230			0.058		0.056	39.125	0.029		3.397	0.034	39.399	100.780
135 6l	18.491	0.026		0.042	0.174	0.188			0.042		0.077	39.348	0.102		3.671	0.028	40.237	102.290
135 7m	18.021	0.100		0.049	0.213	0.345			0.069		0.018	38.872	0.000		3.074	0.087	39.113	99.820
135 7n	18.488	0.118		0.046	0.165	0.228			0.019	0.017	0.091	38.918	0.075		2.866	0.052	38.795	99.670
135 8o	18.060	0.084	0.028	0.405	0.650	0.163				0.000	0.096	38.692	0.192		3.966	0.377	39.954	102.640
135 8p	18.087	0.119	0.009	0.365	0.645	0.164			0.002		0.057	38.723	0.182		4.067	0.399	39.490	102.240
136 1a	18.500	0.081		0.047	0.166	0.058			0.216		0.224	38.942	0.055		2.850	0.116	39.326	100.480
136 1b	18.255	0.063		0.006	0.158	0.083			0.178		0.177	38.832	0.061		2.940	0.153	40.225	101.060
136 2c	18.425	0.043		0.049	0.058	0.039			0.201		0.157	38.878	0.078		2.794	0.076	39.457	99.990
136 2d	18.432	0.026		0.043	0.087	0.061			0.157		0.146	39.001	0.078		2.901	0.057	40.083	100.870
136 3e	18.440	0.093		0.012	0.187	0.063			0.224		0.155	38.767	0.000		3.109	0.121	39.218	100.380
136 4f	18.317	0.027		0.006	0.170	0.062			0.242		0.137	38.949	0.000		3.107	0.143	39.849	100.980
DUR	17.978	0.129	0.120	0.050	0.266	0.463	0.076	0.138	0.046	0.035		38.658	0.162		3.404	0.412	38.211	100.020
139 1a	18.452	0.045			0.014	0.000	0.066	0.011		0.028	0.058	38.987			3.510	0.000	34.251	95.540
139 1b	18.446	0.039			0.021	0.041		0.000	0.016	0.028		38.907			3.454	0.007	34.378	95.380
139 2a	18.448	0.009	0.002		0.019	0.019		0.024		0.041		39.202			2.851	0.291	34.409	95.440
139 2b	18.292	0.032	0.021		0.024	0.169	0.020	0.027	0.040	0.000		39.010	0.039		2.683	0.306	34.770	95.230
139 3a	18.394	0.007				0.017	0.099	0.000	0.003	0.021		39.406	0.050		2.792	0.000	35.676	96.370
139 3b	18.454	0.004		0.013	0.002	0.000		0.014	0.038			39.209	0.049		2.997	0.000	35.737	96.440
DUR	17.937	0.009	0.096	0.096	0.306	0.507	0.026	0.133		0.061		38.211	0.000		3.137	0.000	34.415	95.320
139 4a	18.416	0.015		0.024	0.023	0.048		0.000		0.045		39.040	0.094		2.856	0.000	34.821	95.260
139 4b	18.618	0.076				0.000		0.008	0.036	0.003	0.011	39.350	0.070		2.808	0.008	34.227	95.130
139 4c	18.579	0.048			0.019	0.047		0.019	0.040	0.000		39.348	0.075		2.811	0.000	35.042	95.900
139 5a	18.408				0.003	0.044	0.012	0.001		0.057		38.893			2.922	0.021	35.102	95.380
139 5b	18.351	0.001		0.045	0.010			0.012			0.005	38.900	0.070		2.714	0.035	34.552	94.640
139 6a	18.607	0.069			0.021	0.016		0.011	0.027		0.014	39.506	0.000		3.328	0.095	36.271	97.810
139 6b	18.671					0.014			0.045	0.061	0.026	39.561	0.070		3.211	0.122	35.146	96.830
139 8a	18.403	0.014		0.014			0.101	0.005	0.087			38.963	0.043		2.887	0.046	34.729	95.250
139 8b	18.544				0.033		0.082	0.004	0.038	0.050		39.248			3.246	0.056	37.314	98.610
139 9a	18.021				0.022			0.085	0.036	0.007		38.962	0.008		2.639	0.156	38.135	98.220
139 9b	18.143		0.127			0.160	0.067	0.080	0.008	0.035		39.066	0.002		2.722	0.163	35.983	96.510
139 9c	18.095	0.055	0.124	0.028	0.171	0.094	0.079	0.013	0.048			38.937			2.722	0.165	36.104	96.490

TABLE G.1

Microprobe Compositional Data of Apatite Separates
From the Sawtooth Range, Axel Heiberg Island

Point	P	Si	S	La	Ce	Y	Nd	Nb	Fe	Mn	Mg	Ca	Na	Sr	F	Cl	O	Total
DUR	18.402	0.134		0.405	0.585	0.059	0.124					38.938	0.184		3.436	0.438	38.437	101.142
143 2a	16.896		0.139			0.100			0.105		0.073	37.383	0.686		2.031		43.181	100.594
143 3a	18.694					0.061						39.841	0.105		2.787		41.434	103.001
143 4b	14.903		0.159			1.510						34.132	0.666		1.141		40.873	92.105
DUR	18.132	0.117		0.300	0.527	0.074	0.164					38.879	0.167		3.197	0.418	38.145	100.198
143 5	16.788					0.144			0.186			38.136	0.107		3.067		38.464	97.487
143 6	18.809					0.117						40.081	0.156		1.186		42.600	102.949
DUR	17.890	0.118		0.343	0.587	0.090	0.153					38.782			2.989	0.459	38.383	100.103
FT94-145 1A	17.905	0.202	0.418	0.324	0.436	0.022	0.099	0.300		0.017		38.910		3.090	0.142	0.030	40.832	102.660
FT94-145 1B	18.404	0.055		0.380	0.496	0.018	0.107	0.060		0.053		39.110		3.310	0.106	0.072	40.375	102.290
FT94-145 2A	18.577	0.095		0.281	0.609	0.042	0.195	0.107		0.061		39.728		2.806	0.212	0.031	40.253	102.900
FT94-145 2B	18.417	0.053		0.152	0.430	0.057	0.174	0.081		0.054		39.030		2.770	0.177	0.038	39.902	101.110
FT94-145 3A	18.534	0.012		0.109	0.068	0.021	0.002	0.081		0.022		39.655		2.754	0.068		39.743	100.860
FT94-145 3B	18.272	0.116		0.067	0.256	0.144	0.048	0.024		0.036		39.139		2.732	0.048	0.031	40.278	100.990
FT94-145 4A	18.650	0.020		0.147	0.455	0.116	0.105	0.175		0.028		39.250	0.260	1.540			40.685	101.380
FT94-145 4B	16.759	0.049		0.081	0.326	0.031	0.063	0.181		0.007		37.613	0.101	0.692	0.021	0.105	16.689	72.540
FT94-145 4C	18.377	0.104		0.125	0.433	0.112	0.150	0.131		0.013		39.240	0.221	2.108	0.033		40.663	101.660
FT94-145 5A	18.937			0.042	0.055	0.016	0.008			0.012		40.245		1.476	0.042	0.053	40.288	100.950
FT94-145 7A	18.694			0.074	0.096	0.223	0.030	0.098		0.034		39.800		3.286		0.077	39.926	102.100
FT94-145 7B	18.751				0.002	0.202		0.105		0.018		40.027		2.651	0.038	0.053	39.124	100.860
FT94-153 1A	18.360			0.031	0.115	0.188	0.075	0.204	0.156	0.043		38.654		3.410	0.013	0.104	39.218	100.480
FT94-153 1B	18.237	0.034		0.074	0.162	0.235	0.081	0.348	0.243	0.031		38.304		2.982	0.059	0.064	37.097	97.750
FT94-153 2A	18.609			0.032	0.059	0.027		0.143		0.017		39.500		1.556	0.059	0.027	40.829	100.700
FT94-153 2B	18.701				0.021	0.029		0.122		0.046		39.893		1.294	0.044	0.081	39.745	99.750
FT94-153 3A	18.530				0.037		0.003	0.010		0.022		39.672		2.068	0.099	0.039	40.848	101.220
FT94-153 3B	18.380			0.066	0.022		0.031	0.062		0.011		39.708		1.927	0.116	0.032	39.353	99.480
FT94-153 4B	18.847			0.001	0.032			0.047		0.035		40.052		2.142	0.035	0.005	40.552	101.590
FT94-153 4C	18.642			0.003	0.030		0.002	0.023		0.044		40.071		2.280	0.033	0.050	40.850	101.840
FT94-153 5A	18.543	0.015			0.031	0.011	0.034					39.061		1.369	0.901	0.067	41.225	101.100
FT94-153 5B	18.633	0.022		0.018	0.137		0.006	0.020				39.185		1.485	0.890	0.028	41.201	101.530
FT94-153 6A	17.866	0.246		0.219	0.505	0.036	0.080	0.156				37.408	0.652	1.556	0.037	0.006	40.832	99.520
FT94-153 6C	18.043	0.245		0.254	0.799	0.029	0.191	0.136				38.159	0.596	2.060	0.021	0.001	40.670	101.150
FT94-153 6D	18.072	0.157		0.220	0.556	0.051	0.090	0.022		0.017		38.500	0.563	1.950	0.007		40.980	101.140
FT94-154 1B	18.443	0.002		0.053	0.190	0.363	0.071	0.088		0.039		38.600		3.601	0.029	0.063	41.051	102.320
FT94-154 1C	18.401	0.067		0.072	0.145	0.371	0.059	0.111	0.012	0.071		38.634		3.947	0.017	0.072	40.294	102.100

TABLE G.1

Microprobe Compositional Data of Apatite Separates
From the Sawtooth Range, Axel Heiberg Island

Point	P	Si	S	La	Ce	Y	Nd	Nb	Fe	Mn	Mg	Ca	Na	Sr	F	Cl	O	Total
DUR	18.095	0.140	0.003	0.499	0.764	0.046	0.165	0.234		0.028		38.598		3.346	0.487	0.013	38.481	100.850
FT94-154 2A	18.831	0.031			0.038	0.109	0.030	0.036		0.039		40.489		1.692		0.043	40.524	101.640
FT94-154 2B	18.729			0.054	0.219	0.248	0.047	0.074		0.050		39.883		1.873	0.064		40.683	101.750
FT94-154 3A	18.291			0.075	0.037	0.037	0.014	0.031		0.015		39.087		2.827		0.064	39.211	99.490
FT94-154 3B	18.569			0.021	0.002	0.015		0.005		0.036		39.773		3.013	0.009	0.030	39.416	100.770
FT94-154 4A	18.712	0.031		0.098	0.257	0.053	0.018	0.036		0.032		40.058		2.752	0.004		39.587	101.520
FT94-154 4B	18.473				0.054	0.017	0.008	0.073		0.002		40.012		3.093			39.913	101.490
FT94-154 5A	18.622			0.089	0.040	0.041		0.082		0.000		39.383		3.033		0.001	40.445	101.610
FT94-154 5B	18.608			0.051	0.105	0.042	0.015	0.039		0.003		39.637		4.844	0.001		40.598	103.830
FT94-154 6A	17.729	0.254	0.124	0.278	0.695	0.231	0.263	0.048				38.766		3.215		0.231	38.440	100.230
FT94-154 6B	17.976	0.220		0.150	0.563	0.213	0.177					39.262		3.107	0.006	0.008	38.381	100.050
FT94-154 7A	18.611			0.079	0.276	0.032	0.081	0.119		0.012		39.167	0.921	1.982	0.074	0.044	41.029	102.340
FT94-154 7B	18.395	0.001		0.113	0.144	0.039	0.096	0.167		0.040		38.672	0.776	1.514	0.061	0.019	40.112	100.050
DUR	18.037	0.144		0.405	0.644	0.095	0.162					38.844	0.195	3.248	0.415		37.946	100.259
DUR	18.060	0.112		0.307	0.606		0.162					39.055	0.145	3.493	0.428		38.037	100.463
AX-21 1A	50.000	18.652	0.044		0.024	0.163	0.044	0.192		0.172		38.885	0.002	2.446	0.097	0.029	40.093	100.740
AX21-1B	51.000	18.627	0.019		0.085	0.063		0.185		0.257		39.223	0.124	2.170	0.105	0.019	39.925	100.700
AX21-2A	52.000	18.415	0.088		0.079	0.180	0.085	0.128	0.011	0.027		39.208	0.087	2.206	0.013	0.085	40.317	100.790
AX21-2B	53.000	18.446	0.066		0.085	0.230	0.058	0.141	0.070			39.149	0.078	2.044	0.094	0.047	41.027	101.390
AX21-3A	54.000	18.399	0.085		0.040	0.318	0.072	0.109	0.065			39.367	0.065	2.272	0.045	0.095	40.783	101.500
AX21-3B	55.000	18.316	0.150		0.090	0.354	0.089	0.108	0.084	0.013		38.727	0.065	2.263	0.114	0.093	39.645	99.950
AX21-4A	57.000	18.782	0.002		0.002	0.108	0.020	0.196		0.250		39.334	0.022	1.441	0.063	0.022	40.926	101.100
AX21-4B	58.000	18.814	0.015			0.042		0.223	0.063	0.190		39.485		1.270	0.029		40.648	100.630
AX21-4C	59.000	18.784	0.021		0.044	0.095	0.046	0.165	0.071	0.238		39.303	0.030	1.434	0.080	0.020	41.695	101.840
AX20-1A	60.000	15.449	0.285			0.651	0.112	0.226		0.036		33.263	0.331	3.897	0.074	0.174	35.794	90.260
AX20-1B	61.000	17.872			0.068	0.426	0.191	0.038		0.046		38.659	0.225	3.090	0.003	0.180	38.956	99.600
AX20-1C	62.000	18.556			0.266	0.861	0.126	0.105		0.013		38.482	0.253	2.831	0.076	0.248	39.424	101.230
AX20-1D	63.000	18.265	0.041		0.311	0.781	0.113	0.104		0.048		38.476	0.226	2.593	0.077	0.311	38.941	100.200
AX20-2A	64.000	18.695	0.067		0.147	0.331	0.110	0.235	0.174	0.142		39.161	0.177	1.534	0.053	0.083	40.385	101.240
AX20-2B	65.000	18.775	0.055		0.087	0.332	0.073	0.411	0.155	0.077		39.221	0.108	1.403	0.055	0.094	40.185	100.920
DUR	66.000	18.115	0.141		0.395	0.668	0.092	0.027		0.041		39.047	0.116	2.940	0.462	0.215	39.180	101.370

TABLE G.2

Microprobe REE Data of Apatite Separates
Chondrite normalization factor from Evansens et al (1978)
From the Sawtooth Range, Axel Heiberg Island

Sample	LA	Ce	Nd	Y
DUR	8711.17	6086.73		203.81
133 1a	1798.37	1954.02		100.48
133 1b	2858.31	2257.05		367.62
133 2c	1558.58	1322.88		
133 2d	7209.81	3222.57		1444.76
133 3e	4945.50	2077.32		1501.43
133 3f	6032.70	3065.83		1557.14
133 4g	7277.93	3808.78		1617.62
133 4h	7035.42	4070.01		1622.38
133 5i	8166.21	3285.27		1228.57
133 5j	7051.77	2316.61		1346.67
133 6k	10446.87	6063.74		1977.14
133 6l	11422.34	7286.31		1926.19
134 1a	455.04	2587.25		486.67
134 1b		1292.58		199.52
134 2c	1468.66	1485.89		350.95
134 2d	2645.78	2979.10		395.24
134 3e	4395.10	4533.96		519.05
134 3f	2373.30	4523.51		346.67
134 4h	1991.83	3033.44		352.38
134 4i	836.51	2566.35		280.48
134 5j	103.54	1161.96		380.00
134 5k	1332.43	552.77		
134 5l	632.15	359.46		213.81
134 6m	3373.30	4994.78		484.76
134 6n	6574.93	5961.34		269.52
134 7o		1047.02		
134 7p	1302.45	1597.70		162.86
DUR	8711.17	6086.73		203.81
135 1a	299.73	899.69		134.29
135 1b	1092.64	1573.67		541.90
135 2c	539.51	1102.40		712.38
135 2d	765.67	1144.20		613.33
135 3e		1027.17		1029.52
135 3f	792.92	1141.07		1110.95
135 4g	574.93	884.01		1131.43
135 4h	446.87	1119.12		1032.86
135 5i	1386.92	836.99		790.95
135 5j	915.53	1132.71		748.10
135 6k	1392.37	2034.48		1094.76
135 6l	1152.59	1819.23		893.33
135 7m	1340.60	2221.53		1644.29
135 7n	1258.86	1728.32		1083.33
135 8o	11024.52	6791.01		775.24

TABLE G.2

Microprobe REE Data of Apatite Separates
Chondrite normalization factor from Evansens et al (1978)
From the Sawtooth Range, Axel Heiberg Island

Sample	LA	Ce	Nd	Y
135 8p	9931.88	6734.59		779.52
136 1a	1280.65	1729.36		274.29
136 1b	163.49	1650.99		393.81
136 2c	1321.53	600.84		186.67
136 2d	1171.66	907.00		291.43
136 3e	318.80	1952.98		297.62
136 4f	149.86	1776.38		296.19
DUR	8711.17	6086.73		203.81
DUR	7258.86	4842.22	1068.92	659.05
139 1a	373.30		932.49	52.38
139 1b	566.76	428.42		
139 2a	506.81	201.67		113.81
139 2b	662.13	1769.07	274.26	128.57
139 3a		181.82	1395.22	
139 3b	49.05			64.29
DUR	8335.15	5299.90	362.87	633.33
139 4a	623.98	500.52		
139 4b				38.57
139 4c	517.71	485.89		89.52
139 5a	92.64	455.59	173.00	4.29
139 5b	280.65		253.16	56.19
139 6a	569.48	164.05		50.95
139 6b		149.43		
139 8a			1414.91	24.29
139 8b	888.28		1158.93	18.10
139 9a	604.90			404.29
139 9b		1670.85	939.52	380.95
139 9c	765.67	1787.88	1323.49	376.19
DUR	11035.42	6729.36	2278.48	452.38
143 2a				476.19
143 3a				290.48
143 4b				7190.48
DUR	8174.39	5506.79	2306.61	352.38
143 5				685.71
143 6				557.14
DUR	9346.05	6133.75	2151.90	428.57
DUR	13588.56	7984.33	2326.30	218.10
FT94-145 1A	8831.06	4550.68	1393.81	105.71
FT94-145 1B	10348.77	5177.64	1497.89	86.19
FT94-145 2A	7645.78	6363.64	2741.21	201.43
FT94-145 2B	4136.24	4493.21	2448.66	272.86
FT94-145 3A	2956.40	714.73	23.91	97.62
FT94-145 3B	1814.71	2676.07	680.73	686.67
FT94-145 4A	4013.62	4753.40	1476.79	552.86

TABLE G.2

Microprobe REE Data of Apatite Separates
Chondrite normalization factor from Evansens et al (1978)
From the Sawtooth Range, Axel Heiberg Island

Sample	LA	Ce	Nd	Y
FT94-145 4B	2201.63	3402.30	884.67	149.52
FT94-145 4C	3405.99	4523.51	2102.67	535.24
FT94-145 5A	1155.31	576.80	113.92	78.10
FT94-145 7A	2016.35	998.96	427.57	1060.95
FT94-145 7B		15.67		962.38
DUR	13588.56	7984.33	2326.30	218.10
FT94-153 1A	844.69	1201.67	1054.85	892.86
FT94-153 1B	2016.35	1690.70	1140.65	1119.05
FT94-153 2A	863.76	616.51		130.00
FT94-153 2B		220.48		136.67
FT94-153 3A		385.58	45.01	
FT94-153 3B	1787.47	229.89	437.41	
FT94-153 4B	32.70	331.24		
FT94-153 4C	73.57	314.52	30.94	
FT94-153 5A		320.79	478.20	52.38
FT94-153 5B	487.74	1432.60	78.76	
FT94-153 6A	5953.68	5280.04	1125.18	172.86
FT94-153 6C	6918.26	8346.92	2689.17	137.14
FT94 153 6D	5989.10	5811.91	1264.42	244.76
FT94-154 1B	1452.32	1984.33	997.19	1730.00
FT94-154 1C	1950.95	1514.11	822.78	1768.57
DUR	13588.56	7984.33	2326.30	218.10
FT94-154 2A		394.98	414.91	516.67
FT94-154 2B	1479.56	2289.45	655.41	1182.86
FT94-154 3A	2029.97	390.80	192.69	174.76
FT94-154 3B	569.48	16.72		70.00
FT94-154 4A	2678.47	2685.48	248.95	252.38
FT94-154 4B		567.40	118.14	82.38
FT94-154 5A	2427.79	416.93		194.29
FT94-154 5B	1386.92	1096.13	212.38	200.95
FT94-154 6A	7564.03	7259.14	3701.83	1098.57
FT94-154 6B	4073.57	5877.74	2490.86	1012.86
FT94-154 7A	2152.59	2886.10	1133.61	154.29
FT94-154 7B	3073.57	1503.66	1343.18	185.71
DUR	8365.12	6332.29	2278.48	
DUR	11035.42	6112.85	1744.02	280.95
AX20-1	976.69	6983.15	656.25	2456.30
AX20_2	387.09	2868.77	2036.48	1921.50
AX21_1	179.19	977.45	1186.92	464.10
AX21_2	269.28	1773.25	847.35	1493.10
AX21_3	215.00	2905.54	683.55	1694.70
AX21_4	97.24	668.07	1161.09	649.60
DURANGO	1301.85	5780.80	171.36	1921.50
DURANGO	1504.80	6213.94	71.51	1105.65

FT94-143
With Didingo Mandary

FT94-145
With Durango standard

FT94-15
with Durango standard

FT94-139
with Durango standard

AX-20 & AX-21
with Durango standard